AN INVESTIGATION OF SHORT RANGE

ELECTROMAGNETIC WAVE COMMUNICATION

FOR UNDERWATER ENVIRONMENTAL MONITORING

UTILISING A SENSOR NETWORK PLATFORM

AHMED ABDALLAH ABDOU

A THESIS SUBMITTED IN PARTIAL FULFILMENT OF THE

REQUIREMENTS OF LIVERPOOL JOHN MOORES UNIVERSITY

FOR THE DEGREE OF DOCTOR OF PHILOSOPHY

July 2014

Ahmed Abdallah Abdou

Acknowledgments

Ahmed Abdallah Abdou

To the President of the Republic of Djibouti, the First Lady, all members of his Government and the People of Djibouti, Yemen and Somalia

To my family Alrassouly & Almozati, my father and my mother, my brother and sisters, my wife, my son Sajed, my daughter, my other children that will come and grandchildren …

Ahmed Abdallah Abdou

Abstract

Current state of the art water communications systems rely on optical and acoustic propagation. But these have underperformed in many applications. Wireless Sensor Network (WSN) using radio communication underwater is state of the art. The frequency of operation and the antenna are the big challenges that if unlocked, will present many advantages. The aim of this research is to investigate short range electromagnetic wave communication for underwater environmental monitoring utilising a sensor network platform. Theoretical study and preliminary experiments have confirmed that ISM (industrial, scientific and medical) band at 433MHz was suitable for potable and freshwater communication. Traditional antennas have been constructed, tested and modelled in a High Frequency Simulator Structure (HFSS) but were found unsuitable for use underwater. A 433MHz bowtie antenna was modelled in HFSS and shown to perform well in both air and potable water without any matching circuit. The antenna was prototyped on a printed circuit board, waterproofed and tested successfully in a tank. Furthermore to eliminate RF crosstalk, a battery powered wireless transmitter that generated a carrier signal at 433MHz, was used successfully in the laboratory tank, and during experiments that were repeated in freshwater in Liverpool Stanley Canal. This range, in excess of 5m, was large enough to combine the bowtie antenna with off the shelf, low power transceivers operating at the 433MHz, and specific sensors to form a WSN for potable and freshwater applications. The contribution to knowledge is the experimental demonstration of reliable communication at 433MHz using a broadband antenna which unlocks the potential of underwater WSN applications, including applications in water quality measurement, using radio communication.

Ahmed Abdallah Abdou

Contents

Ahmed Abdallah Abdou

Ahmed Abdallah Abdou

Ahmed Abdallah Abdou

Ahmed Abdallah Abdou

Ahmed Abdallah Abdou

Ahmed Abdallah Abdou

Ahmed Abdallah Abdou

List of figures:

Ahmed Abdallah Abdou

Ahmed Abdallah Abdou

14

Ahmed Abdallah Abdou

Ahmed Abdallah Abdou

Ahmed Abdallah Abdou

17

Ahmed Abdallah Abdou

Ahmed Abdallah Abdou

19

Ahmed Abdallah Abdou

Ahmed Abdallah Abdou

List of tables:

Ahmed Abdallah Abdou

22

Ahmed Abdallah Abdou

Chapter 1. Research background

1.1. Introduction

People need water to survive. It is important that communities, industry, agriculture and the environment get a sustained supply of high quality water. Water pollution occurs from different sources and increases with population. The severity of the damage pushes international communities and national authorities to enforce laws and regulations. Environmental agencies and industry currently apply traditional methods for assessing water's health.

1.2. Properties of water

In water, there are many important properties to be taken into account. A change in these parameters may indicate a change in the quality of the water. These parameters include temperature, pH, conductivity, turbidity, dissolved oxygen and suspended solids.

- Temperature exerts a major influence on biological activity and growth. Temperature governs the kinds of organisms that can live in rivers and lakes. Water temperature can affect the ability of water to hold oxygen as well as the ability of organisms to resist certain pollutants. It is also important because of its influence on water chemistry. Portable water thermometers include thermocouples and infrared.

- pH is a measure of how acidic or alkaline water is. The range goes from 0 to 14, with 7 being neutral. When pH is less than 7 it indicates acidity, whereas a pH of greater than 7 indicates a base. pH is a measure of the relative amount of free hydrogen and

hydroxyl ions in the water. Water that has more free hydrogen ions is acidic, whereas water that has more free hydroxyl ions is basic. Pollution can change water's pH, which in turn can harm animals and plants living in the water. There are large model pH metres for use in labs and small portable models for field use. An estimate of pH can be given by using Litmus paper which is a strip of paper with colour change indicating a rough estimation.

- Conductivity is a measure of the ability to conduct an electrical current. It is highly dependent on the amount of dissolved solids (such as salt) in the water. In seawater, conductivity is ≈4S/m [1] whereas for freshwater it is 100 times lower ≈0.05S/m [2]. Measured with a conductivity meter, the specific conductance is an important water-quality measurement because it gives a reliable indication of the amount of dissolved material in the water. Total Dissolved Solids (TDS) metres measure the quantity of solids in water in parts per thousands (ppt). It has been discovered experimentally that there is an approximate relationship between conductivity and TDS [3]. The conversion from S/m to ppt can be done by multiplying by 5 in water with a high proportion of sodium chloride and by a factor of 6.7 for most other waters. Therefore, the TDS of a 4S/m conductive seawater can be calculated as 20ppt whereas for 0.05S/m conductive freshwater is 0.335ppt.

- Turbidity is a measure of suspended matter in water. High concentrations of particulate matter affect light penetration and habitat quality. In streams, increased sedimentation and siltation can occur, which can result in harm to habitat areas for fish and other aquatic life. Particles also provide attachment places for other pollutants, notably metals and bacteria. For this reason, turbidity readings can be used as an indicator of potential pollution in a water body. Turbidity is measured in nephelometric turbidity units (NTU) with a turbidity sensor by shining a light into the water and reading how much light is reflected back to the sensor.

- Suspended solids are solids whose sizes exceed 1mm. These include sand, silt, rust, plant fibres and algae. They are an indicator of possible bacterial or hazardous contamination. Total suspended solids are the mass of solids that can be separated from the water by filtration.

- Dissolved Oxygen (DO) refers to the volume of oxygen present in water and it is a basic indicator of ecosystem health. A small amount of oxygen, up to about ten molecules of oxygen per million of water, is dissolved in water. This dissolved oxygen is breathed by fish and zooplankton and is needed by them to survive. Bacteria in water can consume oxygen as organic matter decays. Thus, excess of organic material in lakes and rivers can cause eutrophic conditions, which is an oxygen-deficient situation that can cause a water body "to die". DO can be measured using electrodes (electrochemical sensors) and optodes (optical sensors).

1.3. Impacts on water courses

One of the main concerns with water is the quality and refers to the pollution of water. Water pollution is the contamination of natural water bodies by chemical, physical, radioactive or pathogenic microbial substances. Water pollution affects drinking water, rivers, lakes and oceans all over the world. This consequently harms human health and the natural environment.

1.3.1. Water pollution types

Water pollution can come from a number of different sources as displayed in Figure 1. Point source and nonpoint source pollution can be distinguished [4]. The former refers to pollution coming from a single source such as an oil spill. The second refers to pollution coming from many sources such as agricultural runoff.

Ahmed Abdallah Abdou
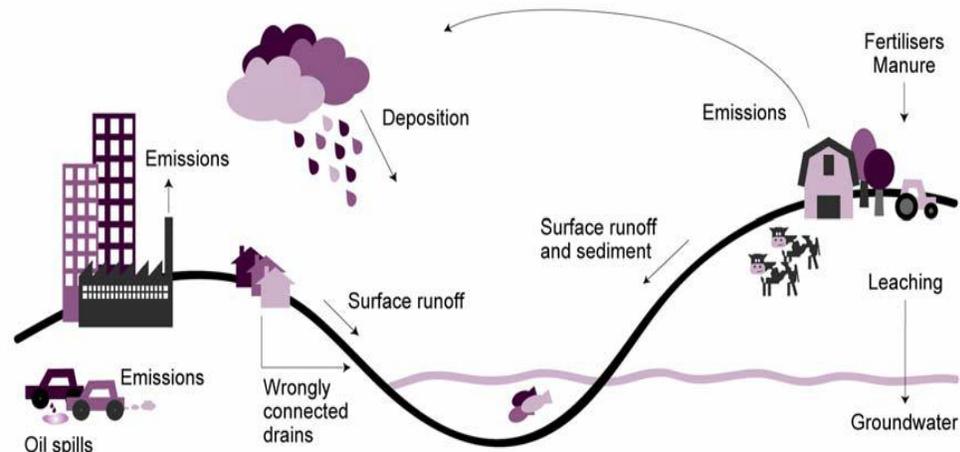
Figure 1 Common sources of pollution [5]

Most of these pollution types directly affect the area surrounding the source. However sometimes the pollution may come from hundreds miles away from the source, such as nuclear waste and is called trans-boundary pollution. There are many types of water pollution as listed below:

- Surface water pollution is the pollution of natural water resources which are found on the exterior of the earth's crust including oceans, rivers, and lakes.

- Groundwater pollution is the pollution of the water found underground in soil or under rock structures called aquifers. Groundwater pollution is often caused by pesticide contamination from the soil.

- Microbiological water pollution is a natural form of pollution caused by microorganisms that live in water such as bacteria, viruses and protozoa and may cause fish, land animals and humans to become ill.

Ahmed Abdallah Abdou

- Oxygen depletion caused by an excess of biodegradable substances increasing the number of microorganisms that use all the oxygen available in water. This results in death of aerobic microorganisms and an increase of anaerobic microorganisms. Harmful toxins such as ammonia and sulphides are released by the anaerobic microorganisms and are harmful to people, animals and the environment.

- Excess of nutrients found in wastewater and fertilizers ending up in water can cause excess of weed and algae growth. Aquatic organisms living in the surrounding marine life could be left without oxygen as the algae use it up. Drinking water and clogged filters can also be contaminated.

- Chemical water pollution is the runoff of the chemicals from industrial and agricultural work into the water. Industrial chemicals include metals and solvents which can pollute rivers and lakes. These chemical are poisonous to many forms of aquatic life. Agricultural chemicals or pesticides used in farming can cause water pollution and be poisonous to the aquatic life. Another form of chemical pollutant is the petroleum contamination through oil spills from ships.

- Suspended matter from pollutants' molecules not dissolving in water can also cause water pollution. Suspended particles settle and cause a thick silt to form at the bottom which could be harmful to marine life that lives on the floor of rivers or lakes.

Ahmed Abdallah Abdou

1.3.2. Causes and damage of water pollution

The causes of water pollution are multiple and their consequences are harmful to humans and animals. Damage could be immediate or after long term exposure. The causes and consequences of water pollution include:

- Sewage and wastewater produced by domestics households, industrial and agricultural practices can cause pollution of lakes and rivers. Sewage in developed countries is carried away from the home quickly and hygienically through sewage pipes. However if chemicals and pharmaceutical substances are flushed down the toilet, sewage can cause problems. When people are ill; sewage often carries harmful viruses and bacteria into the environment causing health problems. In developing countries sewage disposal is a major problem and untreated sewage water can contaminate the environment and cause diarrhoea or typhoid which are the primary cause of infant mortality.

- Industrial water pollution is when industry produces pollutants that are harmful to people and the environment, as many industrial facilities use freshwater to carry away waste from the plant and into rivers, lakes and oceans. These pollutants could be asbestos, lead mercury, nitrates, phosphates, sulphur, oil and petrochemicals. Some of these pollutants may have a mild effect; others can be serious and may result in immune suppression, reproductive failure or acute poisoning.

- Oil pollution can be caused by oil spills, routine shipping, run-offs and dumping in oceans. Although an oil spill may be a localised problem, it has severe effects on

Ahmed Abdallah Abdou

the local marine wildlife such as fish, birds and sea otters. As oil cannot dissolve in water, it forms a thick mud which suffocates fish and stops birds from flying as it gets caught on their feathers. It also blocks light from photosynthetic aquatic plants.

- Atmospheric deposition is the pollution caused by air pollution. When it rains, droplets are polluted with gases such as carbon dioxide, sulphur dioxide and nitrogen oxide forming acid rain. Acid rain pollutes, and may harm, rivers, lakes and aquatic life.

- Dumping of litter in aquatic environments causes problems. For example a six pack ring packaging can trap marine animals and may cause their death. Different items take different time to degrade in water. Cardboard can take 2 weeks to degrade whereas foam and plastic packaging may take up to 50 and 400 years respectively.

- Nuclear waste can be produced in industrial, medical and scientific processes that use radioactive material. Mining and refining of uranium and thorium can form marine nuclear waste. Nuclear waste has damaging effects and is harmful to marine habitats

- Leakages of petroleum into the surrounding soil and groundwater from old underground steel storage tanks which have corroded over time. This contamination can affect drinking water and cause health problems.

- Global warming increasing water temperature can disrupt many marine habitats and result in the death of many aquatic organisms. Coral reef bleaching is an example of water temperature rise making the coral reef expels the microorganisms

Ahmed Abdallah Abdou

on which it is dependent. Other corals may be contaminated and this may affect the marine life that depends on them.

- Eutrophication refers to when the environment is supplemented with nutrients that may cause problems such as algal blooms in marine environment. The excess of nutrients may come from nearby farming water run-off containing fertilizers. This causes rapid growth of phytoplankton resulting in algal bloom. Other than depleting the oxygen in the water, algae may also block sunlight from photosynthetic underwater plants.

1.4. Legislation

There are many laws that protect the world's oceans, rivers, lakes and ground water from unnecessary water pollution. Each continent and country may differ in which laws they enforce but they aim to have the same overall positive influence.

At the international level, legislation regarding water pollution focuses more on marine pollution but also regulates transboundary watercourses and international lakes.

- A number of conventions were signed at an international level to prohibit dumping of waste and other hazardous materials at sea. These date back to 1954 with the International Convention for the Prevention of Pollution of the Sea by Oil [6]. Along with others, these laws have been enforced to regulate oil spillages from ships and other vessels.

30

- Other international laws deals with transboundary watercourses and international lakes like the Convention on the Protection and use of Transboundary Watercourses and International Lakes 1992 [7] and their amendments.

The European Community set out water pollution as a priority matter at its first action programme on the environment in 1973. Since then, a number of European directives have been introduced to reduce and control pollution in European waters. There are also lots of European laws to control and prevent pollution of rivers, lakes, ground waters, estuaries and coastal areas and include:

- The urban waste water directive which aims to protect surface inland waters and coastal waters from pollution by regulating the collection and treatment of urban waste water. [8]

- The nitrate from agricultural sources directive which aims to protect waters against pollution caused by nitrates especially from agricultural sources such as fertilisers. This will enable marine and freshwaters to be protected from eutrophication. [9]

- The drinking water directive which aims to establish strict standards regarding the quality of drinking water. The directive provides parameters and analysis methods; these standards must be met to ensure safe drinking water. [10]

- The Water Framework Directive WFD (2000/60/EC) within the European Community, which became part of the United Kingdom law in 2003, came into force to protect and enhance the quality of surface freshwater (including lakes, streams and rivers), groundwater, estuaries, coastal waters [11]. The overall objectives of the WFD are to

Ahmed Abdallah Abdou

provide a sufficient supply of good quality surface and ground water to provide for sustainable, balanced and equitable water use throughout the member states. Also to significantly reduce pollution in both ground and surface waters that has continued to show an overall reduction in quality over the past decades even though legislation has been put in place to protect them. Finally to protect the marine environment by reducing the concentration of pollutants to near background values for naturally occurring substances and to zero for man-made synthetic substances [12].

- The Environmental Liability Directive 2004/35/EC establishes a framework based on "the polluter pays" principle to prevent and remedy environmental damage [13]. This applies to marine pollution incidents like oil spills if they damage protected habitats or species, or coastal waters.

- The bathing water directive aims to keep good standards in the quality of bathing water in freshwater and coastal water areas [14].

- The Marine Strategy Framework Directive 2008/56/EC aims to achieve good environmental status in Europe's seas by 2020. It requires member states to assess the state of their seas, set standards and introduce a programme of measures for achieving good environmental status [15].

In England and Wales, a range of national laws consolidate existing water pollution laws and others implement the international and European laws. Some of the laws are listed below and aim to:

Ahmed Abdallah Abdou

- Consolidate existing laws to regulate water quality and prevent pollution of water in the Water Resources Act 1991. This has been amended in 2009 as in [16].

- Consolidate existing laws related to regulation of water and sewerage industries in the Water Industry Act 1991 [17].

- Implement the European environment liability directive in England and Wales. These national 2009 SI 2009/153 and SI 2009/995 regulations respectively for England and Wales refer to the environmental damage (Prevention and Remediation) and hold the operator responsible; in the case of imminent threat of environmental damage or actual environmental damage the operator is to take immediate steps to prevent damage or further damage and to notify the authority [18].

- Introduce a new framework for managing the demands placed on the sea, improving marine conservation and opening up access for the public to the English coast as stated in the marine and coastal access act 2009 [19].

- Implement the European marine strategy regulations under 2010, SI 2010/1627 regulation for the achievements of good environmental status seas.

- Implement the European water quality standards

- Give effect to the European water framework directive in the water environment regulation focusing to achieve good chemical and ecological status of inland and coastal waters by 2015.

Authorities are required to set and achieve certain water quality standards. The Environment Agency in England and Wales has taken the lead to carry out a set of approaches and meet certain goals in order to contribute to the future of water health with regards to the Water

Ahmed Abdallah Abdou

Framework Directive WFD (2000/60/EC). To achieve this directive, the Environment Agency has responsibilities cited in [20] including:

- Analysing the characteristics of the 11 River Basin Districts in England and Wales and assessing the impact of human activity on the water bodies within these districts.

- Monitoring the status of water bodies against the objectives set for them.

- Preparing, reviewing and keeping an up to date register of protected areas for each River Basin District.

- Preparing and consulting on the River Basin Management Plans Taking the lead in drawing up and carrying out Program of Measures.

In each River Basin District in England and Wales, liaison panels made up of individuals from water companies, ports, business and industry, the Consumer Council for Water, agriculture, other industry sectors specific to the district and environmental regulators, have been created.

1.5. Recent governmental engagement

The Natural Choice White Paper published in June 2011 in [21] on the Natural Environment emphasizes the importance of valuing nature and the benefits it offers. The paper acknowledges that rivers, lakes, groundwater, estuaries, wetlands and river corridors provide vital ecosystem services and public benefit. But only 27% of river and lakes are fully functioning ecosystems. Under EU law, England is legally required to improve this figure by 2017. The department is keen to change water bodies in England to be in excellent health, with reduced pollution (nutrients, sediments, chemical and bacteria) by 2050. Along the way, the

Ahmed Abdallah Abdou

aim is to increase the proportion of water bodies in Good Ecological Status (GES) from 26% to 32% by 2015, then get the majority of bodies to GES as soon as possible and get as many of the water bodies as possible to GES by 2027.

The U.K. government is also committed to achieve good environmental status across England's marine area, working in partnership with those who use, enjoy and derive their income from the marine environment. The Government has set the strategic policy framework through the UK Marine Policy Statement, adopted in March 2011.

In December 2011, another White Paper named Water for Life was published in [22] by the Department for Environment Food and Rural Affairs (DEFRA). This makes clear that damage done to water ecosystems has to be stopped and reversed, so they can continue to provide essential services to people and the natural environment. It is cited that damage to rivers and other water bodies comes from pollution and over abstraction. They acknowledge an improvement in tackling pollution classified as point sources pollution such as discharges from sewage treatment works and industrial processes. However tackling diffuse pollution coming from many pollution sources such as run-off from roads and farmland, and detergents and other toxic materials people put down drains, is still a problem.

A strategy to identify and address the most significant diffuse sources of water pollution from non-agricultural sources is projected. The government is committed to protect water ecosystems to achieve good ecological status through a river basin planning approach under the EU Water Framework Directive.

Ahmed Abdallah Abdou

A consultation ran from November 2012 to February 2013 to inform and influence development of the strategy for the management on urban diffuse water pollution in England and a report was published in [23] by DEFRA.

Through a series of questions to be answered, views were sought to tackle the problem. A summary of the answers to the consultation is published in [24].

The actions undertaken by the government to improve water quality are cited in [25] and include:

- Planning for better water: the government is working with partners across the U.K. to plan for better water quality and protect sensitive local areas such as bathing water.

- Managing catchments: ten catchment-level partnerships are established to develop and implement plans for creating and maintaining healthy water bodies.

- Reducing agricultural pollution: the government is working closely with farmers to reduce pollution from farms affecting rivers and water bodies.

- Controlling urban pollution: the government is working closely with the Environment Agency to understand urban pollution better, as sources may be numerous.

- Controlling chemical pollution: chemical pollutants are monitored and reduced in open water and other water bodies to protect the environment.

- Managing waste water, sludge and septic tanks: working to make sure pollutants from waste water, sludge and septic tanks are reduced and controlled.

Ahmed Abdallah Abdou

A Public Policy Exchange symposium will be held in London in September 2014 to give opportunity for local authorities, central government including non-departmental public bodies, water companies, businesses, the environmental sector, regulators, civil society groups, third sector organisations and other key stakeholders to discuss how we can help to protect and improve water quality for ourselves and generations to come.

However to meet European and international standards, the Government, Environment Agency, water companies and other partners are currently relying on periodic and single point measurement methods to monitor water bodies.

1.6. Current monitoring methods

1.6.1. Water sampling

The revised European Community Directive [26] that relates to the quality of water for human consumption adopted at the end of 1998, has required new water quality regulations to be drawn in the United Kingdom. Regulations and developments in sampling and analytical techniques required revision. This has resulted in a series of booklets being published under the name The Microbiology of Drinking Water, and provides general advice and guidance on many microbiological aspects connected with potable water supplies, as well as giving details of methods. In the first part [27] of the booklet named Methods for the Examination of Waters and Associated Materials, which contains details of the practices and procedures that should be adopted for taking samples for microbiological analysis, it is stated that the results of a laboratory examination of any single water sample are representative only of the water at the time and at that particular point at which the sample is taken. Furthermore satisfactory results

Ahmed Abdallah Abdou

from single samples do not justify an assumption that the water is safe to drink at all times and that contamination is often irregular and may not be revealed by the examination of a single sample. In the second part [28] it is reported that whenever a sample is taken for analysis it should be recognised, irrespective of the volume of water sampled, this volume represents only a very small fraction of the water being sampled. Along with the sampling procedures come other important requisitions for sample handling techniques, preservation and transportation of the samples. Furthermore, if fluctuations occur then accuracy of the sampling reduces and the only way of increasing sampling accuracy is by increasing the sampling frequency which will incur further cost.

1.6.2. Sensor technology

Traditional water sampling procedures incur a high cost in engaging a full cycle of separate actions from preparing the procedure, trough collecting, storing and analysing the samples present many disadvantages. An alternative for this standard water sampling procedure is to use sensor technologies. A sensor is used for an element which produces a signal relating to the quantity being measured. Sensors can be analogue or digital depending on the nature of their outputs. A sensor is said to be analogue if its output can change over a continuous range to represent the measured parameter. If the sensor gives outputs which are digital in nature, i.e. a sequence of on/off signals which can be interpreted as a number whose value is related to the size of the variable being measured, the sensor is called digital. Handheld water quality sensors are available to purchase in [29] and [30] for single parameter or multi-parameter monitoring. Such units are sometimes called probes and their price can go up to £1000 for a dissolved oxygen sensor [31]. Other than the high cost of these probes, the geographical

38

monitoring area is limited to the probe (single point measurement) and the readings are stored in-situ for manual periodic retrieval.

1.6.3. Real time technologies

Real time technologies involve sending the data sampled automatically by adding telemetry to the monitoring sensor system. Such systems will allow fast responses and actions. These systems are integrated in floating buoys and are commercialised in [32]. One of these modules has been used to monitor the water quality in the Dubai creek, UAE [33]. The buoy is moored to a heavy anchor and is able to take readings from the multi-parameter sensor to monitor temperature, pH, salinity, dissolved oxygen concentration and Chlorophyll A. The buoy is equipped with a cell phone modem which communicates readings to the base station computer in Dubai municipality. Another application using floating buoy system was installed in 2000 in Wales' Cardiff Bay [34]. The system was then upgraded in 2008 to automatically publish live data to a dedicated website. The cost of these systems and their maintenance is high and they do not provide geographical coverage.

Although the challenges in water environment are becoming more alarming, industrial and environmental bodies have kept relying on traditional in-situ and periodic methods in assessing water health. As technology is evolving, it is providing solutions to many problems. Only some of environmental agencies and water industries in developed countries have made use of technology with the revolution of sensors technology and real time systems. In countries with financial resource shortage, the cost of these systems makes it almost impossible to acquire them. Therefore globally there has been a huge need for scientists and

Ahmed Abdallah Abdou

technologists to find new and cheap alternatives capable of replacing conventional and costly ways for assessing water environment in real time.

1.7. Design specification

If a WSN requires a large number of nodes, then the overall cost can be minimised by using off-the-shelf transceivers. Commercial transceivers are only available in the ISM bands. To design an underwater WSN for water quality monitoring using electromagnetic propagation in one of the ISM bands requires the following:

- A range of at least 3 metres.
- A sufficient bandwidth to convey all the sensor data from a large number of distributed nodes, as well as overheads such as handshaking and encryption. It is envisioned that 256kbps would be sufficient data rate that would also provide some necessary redundancy.
- The antennas need to be insensitive to possible changes in the permittivity of water, of a manageable size and cheap to manufacture. With this in mind it was decided to limit the maximum antenna dimension to 250mm.
- As the sensors are liable to move in flowing water, the orientation of the antennas cannot be guaranteed; therefore an omnidirectional antenna will be used.
- To maximise battery lifetime, the transmitted power will be limited to +6dBm.

1.8. Research aims and objectives

To achieve the aim of this research, several objectives have to be met which include:

- Investigate the feasibility of RF underwater communications using the unlicensed ISM bands

Ahmed Abdallah Abdou

- Test the feasibility of using commercially over air wireless transceivers in water

- Design, simulate and test an antenna to operate efficiently underwater

- Investigate the feasibility of forming a wireless sensor network to operate in water.

1.9. Thesis overview

In order to achieve the aim and meet the objectives of this research, the thesis is structured in chapters. The first chapter has discussed the importance of water, the problems faced in many water environments and the current methods used to assess water's health.

In the second chapter, a literature review will describe and evaluate state of the art technologies used underwater. This will lead to highlighting a need to investigate electromagnetic (radio and microwave) communication underwater utilising a sensor network platform.

In chapter 3, the theory of electromagnetic wave propagation in air and in water will be studied thoroughly and verified with preliminary experiments. This will predict the behaviour of the electromagnetic wave in water so that a useful frequency band is located within the spectrum.

In Chapter 4, as antennas are another crucial element in underwater radio and microwave communication along with frequency of operation, a set of traditional antennas will be investigated. These antennas will be made for the 433MHz ISM band and tested in water. Also a modelling stage in High Frequency Structure Simulator will permit to predict and analyse the behaviour of the antennas with regards to the change of medium (air and water). A study

Ahmed Abdallah Abdou

on antenna parameters will lead to assessing the suitability of using traditional narrowband antennas in underwater communication systems.

In chapter 5, a technique of using a broadband antenna will be revealed and applied to accommodate change of properties in air designed antenna when used in water. A potential broadband Bowtie antenna will be modelled in air then in water using HFSS to validate the technique. The antenna will be designed on Easily Applicable Graphical Layout Editor (EAGLE) which will then be loaded on the computer numerical control routing machine to produce the antenna on a printed circuit board. The antenna will be tested in air and in a tank with potable water and the return loss results will be then compared to the results of the modelling.

Chapter 6 will involve the setup of a complete wire free transmitter. A setup consisting of batteries powered electronics will generate a carrier signal operating in the ISM band at 433MHz. The electronics and the batteries of the transmitter will be waterproofed to undergo underwater tests. In the laboratory, the carrier signal will be transmitted in air and its strength will be measured by the receiver which consists of another waterproofed antenna connected to a spectrum analyser. Then the experiment will be repeated in potable water in a tank. A comparison for air and water will be given. Other tests will include the antenna's radiation pattern in air and in water.

In chapter 7, the transceivers will be subjected to real world applications. Therefore a robust plastic container will be designed in SolidWorks and prototyped to house the electronics, the batteries and the antennas. The tests will take place in the freshwater Stanley canal in

Ahmed Abdallah Abdou

Liverpool, United Kingdom. Tests will include reflection coefficient, horizontal transmission and radiation pattern.

In chapter 8, further modelling of the Bowtie antenna in water will be done to see if the antenna can be optimised by changing its dimension. Two cases will be presented. The first case will be the reality that we are restricted on the size of the antenna board because of the PCB levelling board. The second case is that the length of the board could be increased. The available bandwidth and the lower frequency will be monitored in each case.

Chapter 2. Literature review of current state of the art water communication

2.1. Introduction

Underwater communication is of great interest to military, industry and scientific communities. This growing interest has extended the range of underwater applications and has pushed researchers to find new and cheap alternatives. To reduce cost, provide geographical coverage and offer real time information for taking reactive remedial action as appropriate, sensors must be able to communicate even while submerged. Investigation on the current state of the art water communication technologies shows a diversity of techniques is used. These include underwater wired networks, wireless point to point communications and wireless sensor networks with the last two using acoustic and optical propagation commonly. Each of these has its advantages and disadvantages. However the growing fast application ranges in water along with the development of WSN technology and their availability in markets at low prices have recently triggered interest of the use of WSN in water.

2.2. Underwater Wired Network technology

Wired Networks have been used underwater to monitor pipelines as explained in [35]. The wired network allows measurement of many sensors including vibration, temperature, flow rate, pressure in the vicinity of the pipes as in Figure 2. These sensors are electrically powered by the wired network which also serves as their communication link. While power may

Ahmed Abdallah Abdou

constitute a challenge for wireless (RF) technology in underwater pipelines, there has been the possibility to use pipeline flow energy [36]. The electric power can be generated using turbines embedded through the pipeline. Other sources of power can be externally provided by gas-based power generators or third party generators. While wired networks provide many advantages in underwater pipelines including power sourcing and ease of installation over wireless RF technology, some reliability issues are reported [37]. Damage occurring to the wires of the network may completely or partially affect the communication network. Also an outage of power will mean that some of the nodes may not be able to communicate. Furthermore, the physical visibility of the wire may render the network vulnerable to unauthorised people cutting some of the network wires. Reliability and security issues in wired networks are making the pipeline industry look for other types of technology.
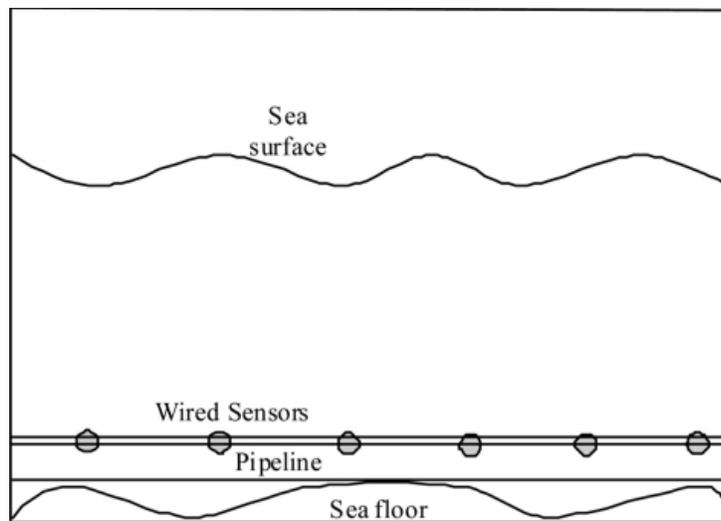
Figure 2 Underwater wired sensor network [35]

Ahmed Abdallah Abdou

2.3. Underwater wireless communication point to point

Underwater communication systems have been used in a broad range of applications including submarine and surface vessels, coastal surveillance, real-time control of unmanned underwater vehicles (UUV), diver to diver communication, automated underwater vehicles (AUV), oil and gas exploration and environmental research etc. There are three main types of communications systems and these use acoustic, optical or electromagnetic (radio & microwave) propagation.

2.3.1. Acoustic propagation

Underwater acoustic communication is a technique of sending and receiving messages below water [38]. There are several ways of employing such communication but the most common is using hydrophones or acoustic transducers as in Figure 3.
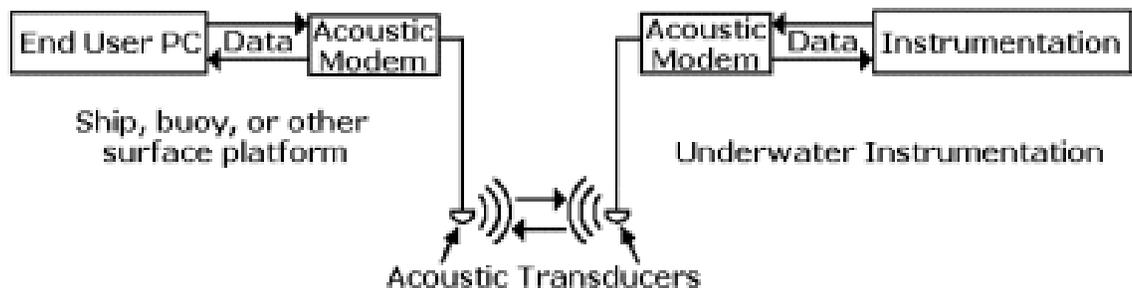
Figure 3 Underwater acoustic communication [40]

A hydrophone is a microphone designed to be used underwater for recording or listening to underwater sound. A commercial hydrophone is displayed in Figure 4. Most hydrophones are based on a piezoelectric transducer that generates electricity when subjected to a pressure change. Such piezoelectric materials or transducers can convert a sound signal into an

46

Ahmed Abdallah Abdou

electrical signal or vice versa since sound is a pressure wave. Multiple hydrophones can be arranged in an array like in Figure 5 so that it will add the signals from the desired direction while subtracting signals from other directions.

Figure 4 Commercial acoustic transducer or hydrophone [39]
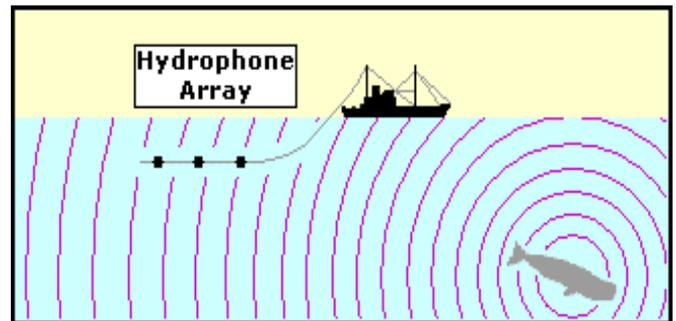
Figure 5 Array of hydrophones towed from a ship to pick up sounds in the water and help locate the animals that are producing the sounds [40]

Acoustic monitoring is also used to determine whether or not a sound source is affecting the behaviour of marine animals [40]. For example, dolphins and beluga whales have been found to shift the frequency of their clicks to avoid noise in the normal frequency range of their echolocation [41]. This indicates that noise may be affecting the animals by reducing the efficiency of their echolocation.

47

Ahmed Abdallah Abdou

2.3.1.1. *Attenuation of acoustic waves*

Attenuation, or path loss that occurs in an underwater acoustic channel over a distance l for a signal of frequency f is defined in [42] by:

$$A(l, f) = A_0 l^k a(f)^l$$

(1)

Where A_0 is a unit-normalising constant, k is the spreading factor, and $a(f)$ is the absorption coefficient. The acoustic path loss is expressed in dB by:

$$10 \log_{10} \frac{A(l, f)}{A_0} = k \times 10 \log l + l \times 10 \log a\,(f)$$

(2)

The first term in the above summation represents the spreading loss and the second term represents the absorption loss. The spreading factor k describes the geometry of propagation which are k = 2 for spherical spreading, k = 1 for cylindrical spreading and k = 1.5 for the so-called practical spreading. The absorption coefficient can be expressed empirically, using the Thorp's formula which gives a(f) in dB/km for f in kHz as in [43] by:

$$10 \log a(f) = 0.11 \times \frac{f^2}{1 + f^2} + 44 \times \frac{f^2}{4100 + f^2} + 2.75 \times 10^{-4} f^2 + 0.003$$

(3)

This formula is generally valid for frequencies above a few hundred Hz. For lower frequencies, the following formula may be used:

48

Ahmed Abdallah Abdou

$$10 \log a(f) = 0.002 + 0.11 \times \frac{f^2}{1 + f^2} + 0.011 f^2$$

(4)

The absorption coefficient is displayed in Figure 6. It increases rapidly with frequency, thus imposing a limit on the maximum usable frequency for an acoustic link of a given distance. For a 1MHz signal, the absorption coefficient is approximately 320dB/km compared to a 100 kHz signal with 40dB/km of absorption coefficient.
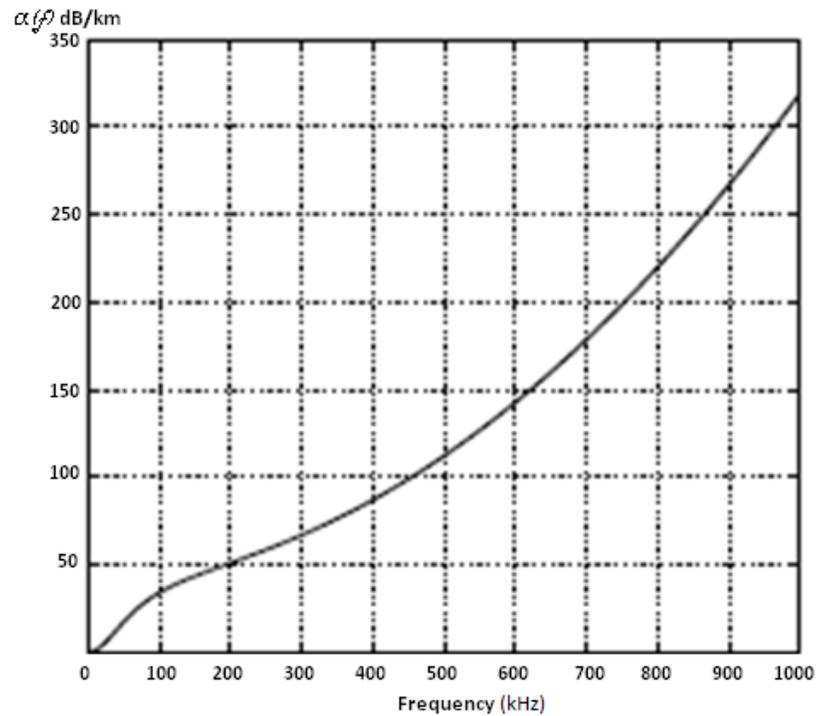
Figure 6 Absorption coefficient, a(f)[dB/km] [42]

The path loss represents the attenuation on a single unobstructed propagation path. If a signal of frequency f and power P is transmitted over this path then the received signal power is

49

Ahmed Abdallah Abdou

$P/A(l, f)$. When there are multiple propagation paths, each of length l_p, $p = 0 \dots P - 1$, the channel transfer function is described by:

$$H(l, f) = \sum_{p=0}^{P-1} \Gamma_p / \sqrt{A(l_p, f)} \, e^{-j2\pi f \tau_p}$$

$$(5)$$

where $l = l_0$ is the distance between the transmitter and receiver, Γ_p represents the additional losses incurred on the pth path (e.g. reflection loss), and $\tau_p = l_p/c$ is the delay with c=1500m/s defined as the nominal speed of sound underwater.

2.3.1.2. Noise

Another important factor in an underwater channel with acoustic propagation is the noise. In the ocean, the ambient noise can be modelled using four sources: turbulence, shipping, waves and thermal noise. Details of the empirical formula are given in [44] and it models the four noise components by their power spectral density (p.s.d). The overall p.s.d of the ambient noise is the sum of all four noise components and an approximation is given as follows:

$$10logN(f) = 50 - 18logf$$

$$(6)$$

In the plot of the empirical model and the approximation of ambient noise p.s.d in [42], one can see that noise level is high at low frequencies then decays at the higher end of the acoustic spectrum.

Recalling that the acoustic path loss is frequency dependent, it then imposes a bandwidth limitation on the underwater communication system, such that a greater bandwidth is available for a shorter transmission distance. This has pushed underwater point to point acoustic researchers towards a network of acoustic modems.

Although many underwater communication systems prefer acoustic as a method of underwater wireless transmission, they present some disadvantages. Underwater acoustics suffer from low velocity; the operating frequencies limit the bandwidth and therefore the data rate is reduced. In deep water, acoustic signals only propagate well with very low frequency signal carriers, which reduce the signal bandwidth and transmission rates, thus extending communication time, which shortens battery life. In shallow water underwater acoustic attenuation is unfeasibly high [45]. Underwater acoustics suffer from multipath propagation and poor performance due to turbidity and ambient noise and has a negative impact on the marine life [46].

2.3.2. Optical communication

Underwater optical communication is a technique for transmitting and receiving light in a water medium. Underwater optical communication has been studied by other research groups in the past. The traditional way was to use Infrared communication (IR) as in [47] where an underwater analogue communication system was reported. It uses infrared light to transmit crayfish neuronal activity information from live crayfish in a small aquarium of 30cm width $\times$ 40cm depth $\times$ 15cm height. The maximum distance at which the transmitted signal could be received was tested in a larger aquarium and found to be 50 cm. Then the use of visible light

Ahmed Abdallah Abdou

generated by Light Emitting Diodes (LEDs) and Lasers became popular considering the minimum absorption wavelength window of the water [48]. LED based systems are the most common types of underwater optical systems because they have been demonstrated for low-cost, low-power, and compact systems [49]. With the aim of surveying underwater habitats, optical communication systems were developed in [50]. The AquaOptical system depicted in Figure 7 is claimed to achieve a data rate of 1.2Mbit/sec at distances up to 30m in clear water. In water with visibility estimated at 3m, it claims achieving communication at data rates of 0.6Mbit/sec at distances up to 9m. Although these are considered to be low cost, turbidity has a big influence on its reliability.

Figure 7 The transmitter and receiver of AquaOptical [50]

However laser-based systems have been demonstrated for extended ranges, high data rates and low latencies [51]. The Neptune Underwater Communications displayed in Figure 8 from

Ahmed Abdallah Abdou

Saphotonics is a commercial product consisting of a flexible laser transmitter. Its modulation capability is based on water conditions and link distance. They claim a data rate up to 250 Mbps at distances up to 200 metres, depending on water turbidity. However if that is to be used in a low visibility water or in the case of disturbed sediment at seabed, this would make the laser fail to operate.
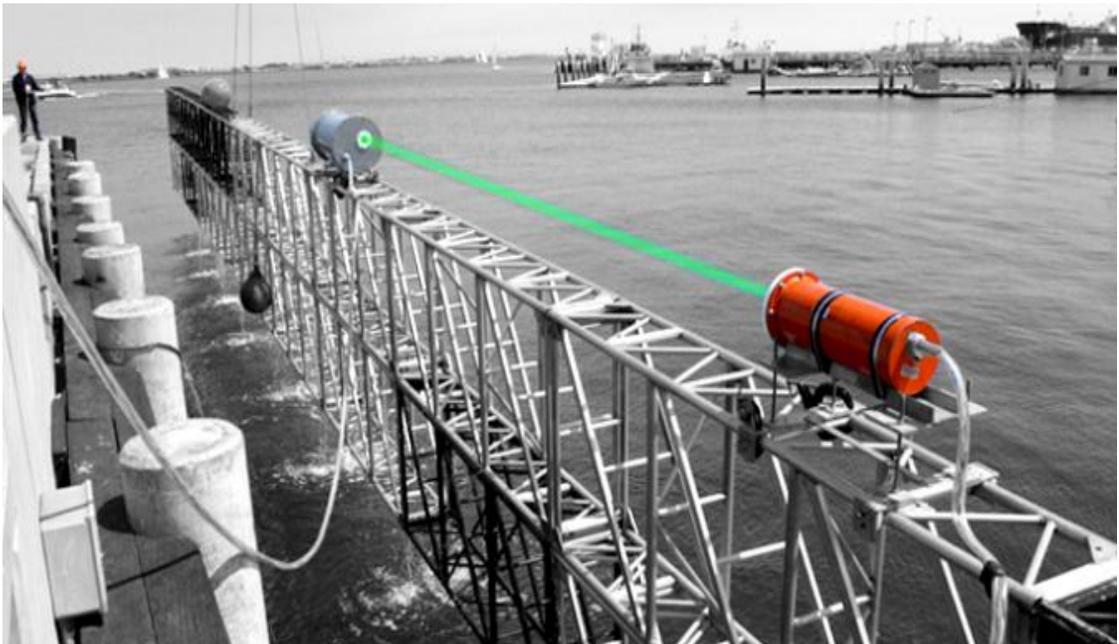
Figure 8 Neptune Underwater Communications with laser communication getting tested in

San Diego Harbour [52]

For high speed optical communication, waveguide modulated optical lasers have been proposed in [53]. They demonstrated optical communication at 1Gbit/s through a short distance of 2m. The device is however directional, very bulky and expensive due to the difficulty in modulating green lasers at high speed.

Ahmed Abdallah Abdou

2.3.2.1.   Attenuation of optical waves

In optical communication, the two major causes of attenuation of light are absorption and scattering. Absorption refers to the conversion of the electromagnetic energy into another form of energy such as heat or chemical. Scattering is when the electromagnetic radiation is redirected away from its original path. These two processes are wavelength dependant and are represented by:

$$c(\lambda) = a(\lambda) + b(\lambda)$$

(7)

Where a and b are absorption and scattering measured in m^{-1}, and λ is the vacuum wavelength of light, in nm.

The attenuation of an optical signal for a distance d is formulated in Beer's law using the attenuation coefficient as:

$$I = I_0 e^{-c(\lambda)d}$$

(8)

With regards to attenuation coefficient variation with wavelength and chlorophyll concentration, it is reported [54] that the ideal wavelength of a vertical optical wireless communication link for each of the profiles represented by varying surface chlorophyll concentration, is extremely dependent on the expected length of the link, especially in places of high surface chlorophyll. Therefore the selection of an appropriate wavelength for a communication system depends significantly on the expected orientation and location of the link. This may limit the use of the underwater communication system to specific applications.

Ahmed Abdallah Abdou

The refractive index of the ocean water also changes with depth and potentially can lead to a long distance communication link being diverged away from the receiver.

Simulation work carried out in Matlab and published in [55] shows the effects of four types of water including pure sea water, clean ocean water, coastal ocean water and turbid harbour water on the underwater optical wireless communication system with a wavelength of 405nm and 650nm for a distance of 10m. In the scattering results both wavelengths have similar high scattering behaviour in the turbid water. Furthermore, the total attenuation results demonstrate higher attenuation levels on both wavelengths for turbid water compared to the rest which present a lower attenuation level.

2.3.2.2. Noise

In free space optical communication devices, background optical noise is a limitation [56]. Sources of noise include solar light, sunlight reflected by the moon at night which can be a problem in shallow water, and also artificial light sources. In underwater at depth up to 10 metres, the main source of noise is solar light [57].

Optical communications underwater have the potential to achieve much higher data transfer rates than an acoustic communication system at significantly lower power consumption, simpler computational complexity, and smaller packaging, unfortunately its use is limited due to turbidity and environmental background noise, conditions that vary widely across different oceans and other bodies of water [58]. Other drawbacks of optical communication include optical scattering caused by suspended particles and planktons, high levels of ambient light in

Ahmed Abdallah Abdou

the upper part of the water column, multipath propagation and beam spreading, drive researchers to look for alternative technologies.

2.3.3. Electromagnetic (RF and Microwave) communication

Radio and Microwave propagation underwater is a good alternative in situations where traditional acoustic and optical communications fail to operate. This includes congested and noisy underwater environments like ports and harbours, in shallow water and in water with a high turbidity level. With a high speed of propagation up to around 3×10^7 m/s, EM propagation offers many advantages including propagation velocity, bandwidth, data rate and better transmission in crossing boundaries (air, water, seabed and ice). EM wave propagation is clearly faster than acoustic and this has important advantages for command latency and networking protocols where signals get exchanged between nodes and sinks. It is perfect for noisy environments where acoustic signals will be highly affected. Furthermore as far as we know it has no effects on marine life whereas acoustic is becoming an issue for marine mammals.

Research on electromagnetic propagation underwater has been going on since the World War I for US navy submarines in the extreme low frequency range [59]. This work on seawater has been followed by many others who have significantly contributed. Besides, research and experiments conducted in Liverpool John Moores University have claimed that transmission of 5MHz frequency is feasible in seawater up to 90m at a high data rate of 500kbps that allows duplex video and data streams [60]. In [61], propagation at frequencies of 6 MHz and 10.7MHz in a reflective metal tank were possible. Recently a review [62] on EM propagation

Ahmed Abdallah Abdou

underwater has been conducted and predicted its usefulness in wireless communication at high frequencies for high data rates which could be used in many applications. Furthermore, the authors carry out an experimental study in potable water with off-the-shelf transceivers operating at 2.4GHz Industrial Scientific and Medical (ISM) band, resulting in a successful communication range of 200mm [63]. To increase the range they suggested that the lower ISM frequency 433MHz could be used and a different antenna that is specially designed for water communication should be sought.

Leading from theoretical and experimental seawater investigations published in [1] and in [60], Wireless For Subsea is one of the companies that currently sell wireless RF underwater systems [64]. They claimed in 2006 that underwater radio modem S1510 (Figure 9) transmits up to 3 metres in seawater with 0.6W of power at 40bps data rate. They also claim that Seatooth S200 (Figure 10) transmits up to 30 metres through seawater at 16W of power. However the data rate is 100bps due to the low frequency of operation. Their latest claim includes Seatooth S300 (Figure 11) transmitting up to 7 metres in seawater at a data rate of 156kbps. Although the power transmitted is high and the antennas used are conventional loops that require matching, there is no published evidence which support their claims.

Figure 9 Underwater radio S1510 transmitter and receiver [64]

57

Ahmed Abdallah Abdou

Figure 10 Underwater radio modem Seatooth S200 [64]

Figure 11 Underwater radio modem Seatooth S300 [64]

2.4. Wireless Sensor Networks in water

In the past decade, production of sensor nodes has soared due to the demand of different sensor nodes applications. These include large power hungry devices from Sensoria e.g. the Sensoria WINS NG 2.0 [65], which are used when power is not an issue, as well as the System on Chip (SoC) classified devices referred to as "motes". Motes are designed to be both small and low power. There are many families of motes including µAmp, BT node, Firefly and Berkeley's range of Mica motes. Each of them has its own characteristics and aims.

Ahmed Abdallah Abdou

In Liverpool John Moores University, researchers have been working on WSN applications including spot welding monitoring in the automotive industry and asset tracking in the airline and gas industry [66]. They have also used WSN in an environmental application for monitoring car exhaust pollution [67]. Other WSN researchers have mainly focused on how to make motes smaller, cheaper and lower powered. A few have tried to use WSN in unusual places for EM propagation such as soil properties in underground monitoring [68]. The fast growing application range in water along with the development of WSN technology and its availability in markets have recently triggered interest of the use of WSN in water.

2.4.1. Underwater WSN using Acoustic communication

A miniature acoustic communication subsystem for underwater wireless sensor networks called CORAL has been prototyped using a low power modem [69]. The system is tested in a tank and 200mm of communication range is achieved with a transducer operating at 1.7 kHz. This operating frequency limits the data rate. In water the bandwidth reported of 3.8 kHz is relatively small and therefore limits the usefulness of the modem.

In [70], the design and implementation of an omni-directional underwater acoustic micro-modem based on a low power micro-controller. The system is tested in a tank, pond and river. The modem has been able to transmit wirelessly up to 70m with a data rate of 0.2kbps in the river. The data rate is more than a thousand times less than can be achieved with a 256kbps radio transceiver. This is due to the low frequency used which is one of the main drawbacks of acoustic communication. Most importantly, the 4.5W energy used to power the system is not compatible with the low power requirement in Wireless Sensor Networks.

Ahmed Abdallah Abdou

2.4.2. Underwater WSN using Optical communication

A network is built around twenty underwater sensor nodes called Aquaflecks, for data collection by an autonomous underwater vehicle [71]. Each node has a custom board for optical communications that drives a high power LED and a sensitive matched photodiode. The LED emits light in a 30 degree cone and supports a maximum data rate of 320kbits/s at a maximum range of 2m. Although the transmission rate is high, the nodes need to be within the 30degree cone range for hard docking to allow short range communication in low turbidity water environment. To overcome these challenges, the authors integrate acoustic communication to cover a longer range of 20 metres with a low data rate of 50 bits/s.

Additional research on underwater wireless sensor networks based on optical communication between two nodes is described in [72]. Challenges and results are also presented in the paper. During the experimental tests in a tank, a transmission over 1.8 metres was achieved at 100 Kbps. However beyond 1.9 metres the bit error rate increased and made the transmission impossible although the tests were performed in water with high visibility. Optical systems were found to be impractical in high turbidity. Optical signals suffer from optical scattering and are rapidly absorbed in water. Also the level of ambient light in the upper part of the water is another adverse factor in using optical communication.

In [73] an underwater optical link is proposed for communication between sensors on a swimmer during a training session. The system uses LED and an optical detector at 520nm. The effects of bubbles are studied and experimented in a still pool, still spa water and bubble spa water. The authors conclude that the path is still thought to be viable in the context of a

Ahmed Abdallah Abdou

sensor network for swimmers for distances greater than 1 metre. As the relative movement between the arm and the head is very large, the beamwidth of the transmitter and receiver must be very large. The swimmer is located at the water–air interface. This can provide an additional problem associated with changing ambient noise and changing surface reflection conditions. During free-style swimming, the side of the goggles closest to the extended arm with the wrist sensor is commonly in the water when the wrist is in air and vice versa. Also one of objectives of the sensors is to communicate and collaborate as a network platform to send information to the coach at poolside to provide direct feedback to the swimmer. For this reason, a communications system that functions in both air and water is highly desirable. Furthermore the high level of ambient light in the upper part of the water column and multipath propagation would not make optical communication a viable solution.

2.4.3. State of the art proposed system: Underwater WSN using Electromagnetic (RF and Microwave) communication

There are very limited trials of Wireless Sensor Networks in water using radio and microwave propagation [74]. However, recently some groups including ourselves have shown interest in investigating this technology. In [75], the authors publish their simulation work at 2.4GHz ISM frequency band. The simulations are only run in air and the results are used to discuss as if it was water. No evidence of simulations in water is presented. Moreover, the 2.4GHz is a highly attenuated band in water and tests performed in published paper [63] achieved reliable small communication range up to 200mm.

Ahmed Abdallah Abdou

Additional research is based on the 2.4GHz ISM band [76]. The tests are performed with transceivers and conventional antennas, and the maximum achieved communication range is 170mm. Both transceivers are connected to a laptop located outside the water via a serial cable. The experimental setup used to make their measurements increases chances of signal spreading out of the water through the cables. Furthermore, the separation distance is small and does not seem feasible to build a wireless sensor network for geographical coverage.

2.4.3.1. Research overview

Current state of the art wireless sensor nodes rely on optical and acoustic propagation in water. However these have underperformed in many applications. Radio and microwave propagations underwater have many advantages but the communication range is affected by the attenuation due to the conductivity and polar nature of water. However, of the ISM bands, 433MHz offers equilibrium between attenuation and data rate. As wireless nodes using electromagnetic (radio and microwave) communication became cheaper and smaller, it becomes viable to set a network of many nodes operating at 433MHz ISM band to cover a large area. The nodes could organise themselves into a wireless sensor network, reconfigure routes as radio link quality changes and cooperate in routing data packets to a base station (multi-hop communication) as demonstrated in Figure 12. The sensor network deployed underwater could monitor physical variables such as water temperature and pressure as well as variables such as conductivity, turbidity and certain pollutants. The network could track release of pollutants flowing into water from land. It could monitor and model the behaviour of underwater ecosystems. The network could be used to identify or monitor in real time deliberate pollution or even potential terrorist attack to water reservoirs that could contaminate

Ahmed Abdallah Abdou

water supply and endanger public health. A map of the water reservoir with areas of contamination could be generated for the authorities to take immediate action like stopping the supply of contaminated water from getting to the public.
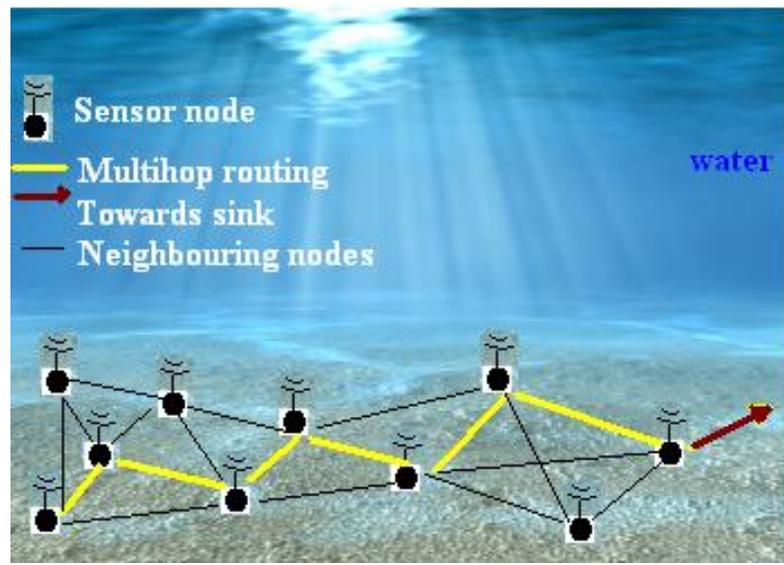
Figure 12 Underwater multi hop Wireless Sensor Network

The sensor node could comprise five components as in [77]: controller, memory, sensors and actuators, communication device and power supply. The controller will process all the relevant data, and is capable of executing codes. The memory will store programs and intermediate data and usually different types of memory are used for programs and data. The sensors and actuators are the actual interface to the physical world; these devices can observe or control physical parameters of the water environment. The communication device allows nodes to send and receive information over a wireless channel. The power supply, usually in the form of batteries, is necessary to provide energy. All of these are shown in Figure 13.

Ahmed Abdallah Abdou
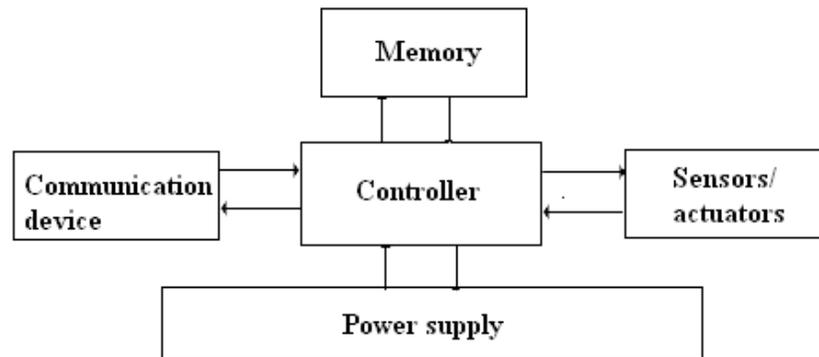
Figure 13 Main sensor node hardware components [77]

2.5. Summary

State of the art water communication has been investigated. To provide geographical coverage and reduce cost, a breakthrough in underwater communication is to use a wireless sensor network. In many applications, acoustic and optical traditional ways of communicating underwater between sensors nodes have underperformed and have been found unreliable. This has triggered interest in alternatives including the underwater WSN using the radio and microwave communication we are proposing. Therefore, electromagnetic propagation is studied in the next chapter to understand the subject and to investigate a useful technology in many underwater applications where acoustic and optical would fail to operate.

Ahmed Abdallah Abdou

Chapter 3. Electromagnetic (EM) wave propagation

3.1. Introduction

In this chapter the theory of electromagnetic wave propagation in air and in water will be studied and compared with experimental results. At first, the important work of James Maxwell's equations which have been verified in optics, microwaves, antennas, communications, radar and many sensing applications, in unifying the existing laws of electricity and magnetism of the previous great scientists onto the well-known Maxwell model will be explained. This will lead onto an elaboration on how an electromagnetic wave propagates. An overview of the electromagnetic spectrum will be given, to show how it is typically divided into frequency bands. This includes the radio and microwave band that the Industrial Scientific and Medical band is part of. Then the theory of electromagnetic wave propagation underwater will be revised. For this the permittivity of water will be thoroughly studied, along with the effects of permittivity and salinity of water. Then a modification of the attenuation model will be presented to take into account the losses due to the polar nature of water. This will predict the behaviour of the electromagnetic wave in water to locate theoretically a useful frequency band to communicate at. A set of experiments will follow using an off the shelf transceiver operating at 2.4GHz ISM to verify the theory and to show the capability of this frequency in water. Finally the impact of the antenna on the underwater communication will be experimented on.

Ahmed Abdallah Abdou

3.2. Maxwell equations

James Clerk Maxwell, a Scottish mathematical physicist of the 19th century united the known laws of electricity and magnetism to form a set of equations known as the Maxwell's equations [78]. The equations existed in incomplete forms as a result of the work of Faraday, Ampere, Gauss and Poisson. The electromagnetostatic model is modified to show mutual dependence between the electric field vectors E and D and the magnetic field vectors B and H for time varying conditions.

$$\nabla \times E = -\frac{\partial B}{\partial t}$$

(9)

$$\nabla \times H = J + \frac{\partial D}{\partial t}$$

(10)

$$\nabla \cdot D = \rho$$

(11)

$$\nabla \cdot B = 0$$

(12)

Equation (9) is a differential equation with a curl operator $\nabla \times$ which is a measure of field rotation. It is the Faraday's law of electromagnetic induction. It states that a time varying magnetic flux generates an electric field with rotation. In the equations, E represents the electric field in volt per meter (V/m) and B is the magnetic flux density in Tesla (T).

Equation (10) is also a differential equation with the curl operator $\nabla \times$ which is a measure of field rotation. It is a modified version of the Ampere's circuital law. The modification which is

66

Ahmed Abdallah Abdou

the additional term $\frac{\partial \mathbf{D}}{\partial t}$ called the displacement current density is one of the major contributions by Maxwell. This modification allows for the coupling between the magnetic field and the time varying electric flux. It points out that a current or a time varying electric flux (also known as displacement current) generates magnetic field with rotation. In the equations, H is the magnetic field in amperes per metre (A/m) and J is the electric current density in amperes per square metre (A/m^2).

Equation (11) is a differential equation with the divergence operator $\nabla \cdot$ which is a measure of the total flux radiating from a point. It is the consequence of Gauss's law of induction. It implies that the divergence of the electric flux D at a point is proportional to the positive charge density ρ present at the point.

Equation (12) is the differential equation with the divergence operator $\nabla \cdot$ which is a measure of the total flux radiating from a point. It is the consequence of Gauss's law of magnetism. It indicates that the divergence of magnetic flux B at any point is equal to zero.

3.3. Electromagnetic waves propagation

Maxwell's equations predicted that electromagnetic waves can break away from the electric currents that generate them and propagate independently through empty space with the electric and magnetic field components of the wave constantly regenerating each other. The charge and current densities ρ, J can be thought as sources of the electromagnetic fields. In wave propagation problems, these densities are localised in space. Therefore the generated electric and magnetic fields are radiated away from the sources and can propagate to large distances to

Ahmed Abdallah Abdou

a receiving antenna. Away from the sources, which is the source free regions of space, there are no free charges, ρ and J are equal to 0. Figure 14 describes the electric and magnetic fields in source free regions.
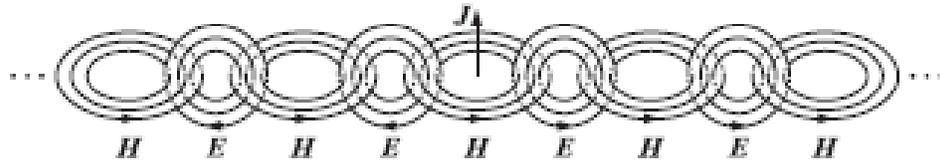
Figure 14 Source-free electric and magnetic fields [79]

In [79] , the author describes Figure 14 with relation to Maxwell's model that a time-varying current J on a linear antenna generates a circulating and time-varying magnetic field H, which through Faraday's law generates a circulating electric field E, which through Ampere's law generates a magnetic field, and so on.

As an electromagnetic wave propagates away from the transmitting antenna, it takes on a spherical wavefront. By the time it reaches a distant receiving antenna, the wavefront has a very large radius of curvature and is essentially a plane wave. The E and H vectors (electric and magnetic fields, measured respectively in volts/m and amperes/m) both lie in the plane of the wavefront, they are transverse to the direction of propagation as shown in Figure 15. The fields are in phase with each other, they rise and fall together in space and time.

Ahmed Abdallah Abdou
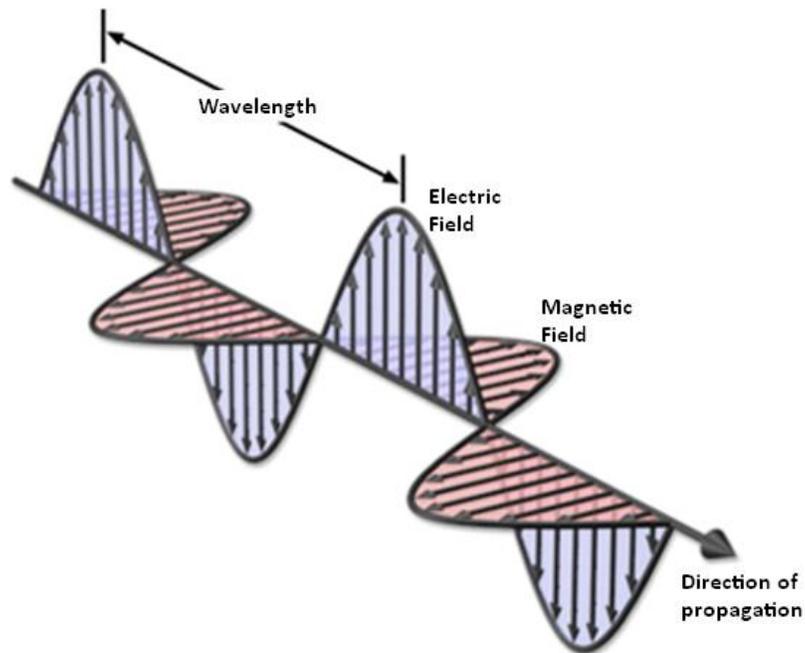
Figure 15 Transverse electromagnetic (TEM) wave

Maxwell's prediction lead to the velocity of these waves to be $\dfrac{1}{\sqrt{\varepsilon_0 \mu_0}}$ where the constants ε_0 and μ_0 in free space are respectively 8.854×10^{-12} Farad/metre and $4\pi \times 10^{-7}$ Henry/metre. This resulted in the experimentally-known speed of light c = 3×10^8 m/sec which revealed the electromagnetic nature of light.

Hertz conducted a series of experiments in the 1880s in which he generated and detected electromagnetic waves with wavelengths very long compared to light. Then Guglielmo Marconi was able to send a radio wave across the Atlantic Ocean in the 1900s. Since then, the importance of Maxwell's equations have been verified in optics, microwaves, antennas, communications, radar and many sensing applications.

Ahmed Abdallah Abdou

3.4. Electromagnetic spectrum

The electromagnetic spectrum is considered as the entire range of electromagnetic radiation ranging from the longest electric and radio waves through visible light to x-rays and the shortest gamma and cosmic waves (Figure 16). These waves have different frequencies and wavelengths but all travel at the same speed. Part of the spectrum includes the frequencies used for radio communications. The boundaries of the radio spectrum are usually considered to range from 9 kHz (9000 cycles per second) to 3000 GHz (3000 thousand million cycles per second). Another part of the spectrum is the visible light with boundaries being the red and violet with respective wavelength of 700nm and 350nm.
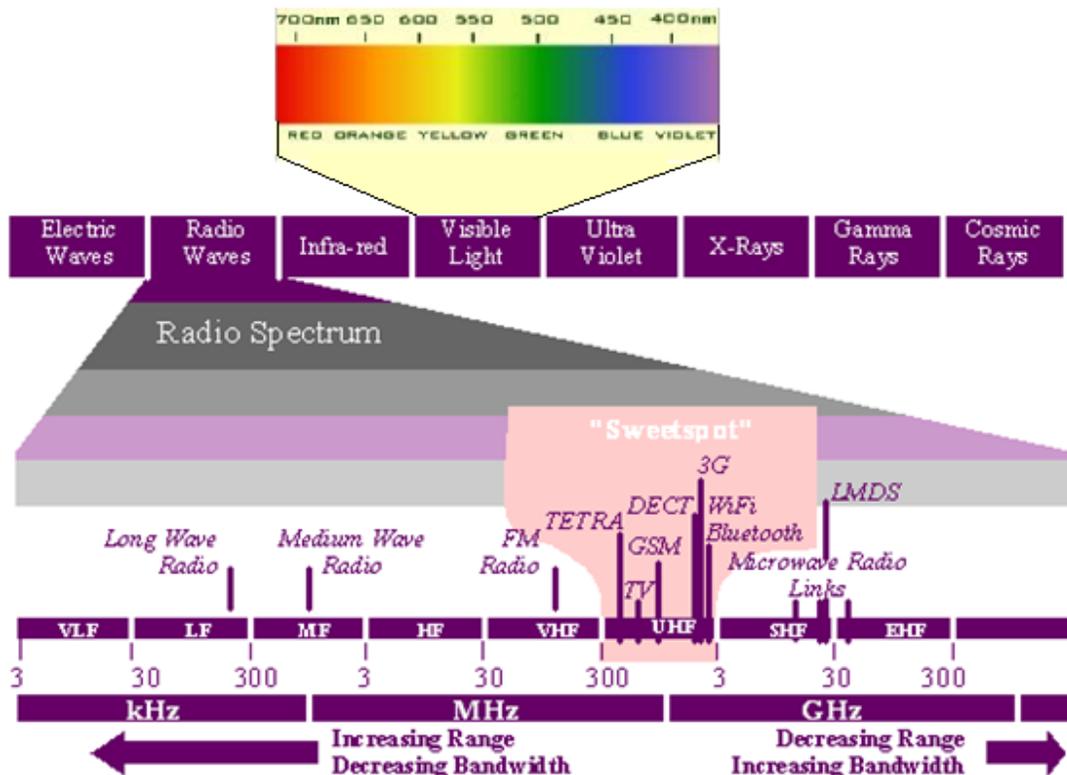
Figure 16 Electromagnetic spectrum [80]

Ahmed Abdallah Abdou

Although the whole spectrum is infinite, the useful spectrum is limited and some frequency bands, such as the UHF, are already very congested. Normally, significant licence fees have to be paid to use the spectrum, although there are some licence-free bands. The most well-known ones are the Industrial, Science and Medical (ISM) bands allocated by the International Telecommunication Union (ITU) as in Table 1. These bands are allocated in regions displayed in Figure 17. The 433 MHz and 2.45 GHz are just two examples.

Table 1 Radio and microwave frequency bands allocated for Industrial Scientific and Medical (ISM) applications by the International Telecommunication Union (ITU) [81]

Frequency band	Central frequency	Wavelength	World regions covered
6.765 – 6.795 MHz	6.78 MHz	44.2 m	Under consideration
13.553 – 13.567 MHz	13.56 MHz	22.1 m	R1, R2, R3
26.957 – 27.283 MHz	27.120 MHz	11.1 m	R1, R2, R3
40.66 – 40.70 MHz	40.68 MHz	7.4 m	R1, R2, R3
433.05 – 434.79 MHz	433.92 MHz	0.69 m	R1
902 – 915 MHz	915 MHz	0.33 m	R1, R2, R3
2400 – 2500 MHz	2450 MHz	0.12 m	R1, R2, R3
5725 – 5875 MHz	5800 MHz	0.05 m	R1, R2, R3
24 – 24.25 GHz	24.125 GHz	1.24 cm	R1, R2, R3
61 – 61.5 GHz	61.25 GHz	0.49 cm	Under consideration

Ahmed Abdallah Abdou

122 – 123 GHz	122.5 GHz	0.24 cm	Under consideration
244 – 246 GHz	245 GHz	0.12 cm	Under consideration
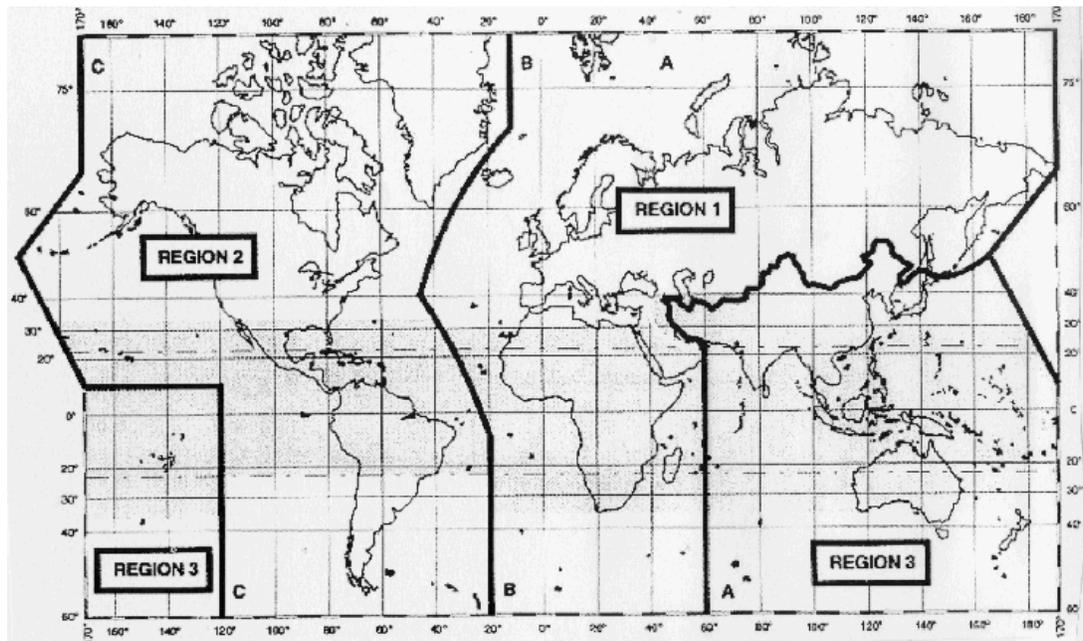
Figure 17 Frequency band regions allocated by ITU [81]

Ahmed Abdallah Abdou

3.5. Electromagnetic wave propagation underwater

3.5.1. Permittivity of water

A lossy dielectric is defined in [82] as a medium in which an EM wave loses power as it propagates. It has a conductivity σ≠0 in comparison to a lossless dielectric which has conductivity σ=0.

The permittivity of a material is the characteristic which describes how it affects any electric field set up in it. When the material is lossy, the relative permittivity is a complex quantity [83] given by:

$$\varepsilon_r = \varepsilon'_r - j\varepsilon''_r \tag{13}$$

The real part is related to the energy stored within the medium. Because water is a polar molecule and rotates when exposed to an alternating electric field, the imaginary part is then associated to the dissipation of the energy due to collisions during that rotation.

At 433MHz, the relative complex permittivity of water is $80.17 - j1.92$ [84].

However as it is not explained which type of water it is referred to, a precise knowledge of the relative complex permittivity of water also known as complex dielectric constant ε_r is therefore essential.

The primary work on complex dielectric constant was attributed to P. Debye in 1929. He initiated a model (Debye model) with a single relaxation wavelength to calculate the permittivity of water [85] as follows:

73

(14)

$$\varepsilon = \frac{\varepsilon_S - \varepsilon_\infty}{1 + (j\omega\tau)^{1-\alpha}} + \varepsilon_\infty - j\frac{\sigma}{\omega\varepsilon_0}$$

With

$j = \sqrt{-1}$

$\omega = 2\pi f$, the angular frequency with f in Hz

ε_s, the static (zero frequency) dielectric constant

ε_∞, the dielectric constant at infinite frequencies

ε_0, the vacuum electric permittivity $= 8.854 \times 10^{-12}$ in farads/metre

τ, the relaxation time in seconds

α, the empirical parameter that describes the distribution of relaxation times

σ, the ionic conductivity in siemens/metre

However in further work [86] and [87], the authors confirmed that the Debye model was unreliable because certain parameters including the static permittivity, the relaxation time and the conductivity are dependant on the temperature and salinity of the water and must be included in the model.

In [88], the authors came up with an improved model which fits the dielectric constant with a single Debye relaxation law for frequencies up to 10GHz. It takes into account parameters

Ahmed Abdallah Abdou

including static permittivity, relaxation time, and conductivity which are dependent on the temperature and salinity of the water.

Further work in [89] and [90] have shown that the Klein-Swift model was getting inaccurate as frequencies increases.

Meissner and Wentz [91] introduced a model with a double Debye relaxation wavelength that they considered necessary to provide an accurate fit for the dielectric constant over a wider frequency range than the single Debye model. This model takes into account the salinity and temperature contrary to the Debye model.

$$\varepsilon(T,S) = \frac{\varepsilon_S(T,S) - \varepsilon_1(T,S)}{1 + i\frac{v}{v1}(T,S)} + \frac{\varepsilon_1(T,S) - \varepsilon_\infty(T,S)}{1 + i\frac{v}{v2}(T,S)} + \varepsilon_\infty(T,S) - i\frac{\sigma(T,S)}{(2\pi\varepsilon_0).v}$$

(15)

With

$i = \sqrt{-1}$

v, the radiation frequency in GHz

$\varepsilon_s(T,S)$, the static (zero frequency) dielectric constant

ε_∞, the dielectric constant at infinite frequencies

ε_1, the intermediate frequency dielectric constant

ε_0, the vacuum electric permittivity $= 8.854 \times 10^{-12}$ in farads/metre

Ahmed Abdallah Abdou

$v_1(T,S)$ and $v_2(T,S)$, the first and second Debye relaxation frequencies

T, the temperature in ^{o}C

S, the salinity in ppt (parts per thousand)

σ, the conductivity in siemens/metre

3.5.1.1.   Salinity effects on permittivity

The complex permittivity is dependent on the frequency, salinity and temperature as formulated in the Meissner and Wentz model in equation (15). To predict the behaviour of the permittivity of different types of water with regards to the frequency, the temperature is maintained at a fixed value. This temperature is 20°C and is one of the measurements of the canal water taken during a visit in summer to the Stanley canal in Liverpool, UK. The second measurement is the conductivity of the water recorded at 0.0606 S/m and converted as in section 1.2 to a salinity of 0.335ppt for use in the model where S is in ppt.

Using the Meissner and Wentz model, the permittivity of water with different salinity concentrations S in ppt is calculated at a temperature of 20°C. A concentration of salinity S=0ppt is used to refer to distilled water as in [92]. A concentration of salinity S=0.0871ppt is used to refer to potable water from converting 0.013S/m which is the measured conductivity of the water running from the laboratory tap. To refer to freshwater, a concentration of salinity S=0.335ppt is used from the conversion of the measured 0.0606 S/m of the Stanley canal water. To refer to seawater, the measured value of 4S/m in [1] is converted to a concentration of salinity S=20ppt and is also within the range of salinity concentration "20ppt ≤ S ≥ 40ppt"

Ahmed Abdallah Abdou

used to refer to seawater in [91]. Although the model is valid for a wide range of frequencies including below 1MHz, we focus on the spectrum between 1MHz and 100GHz. Real ε and imaginary ε permittivity are calculated using the Meissner and Wentz model for the referred types of distilled, potable, fresh and seawater and represented respectively in Figure 18, Figure 19, Figure 20 and Figure 21.
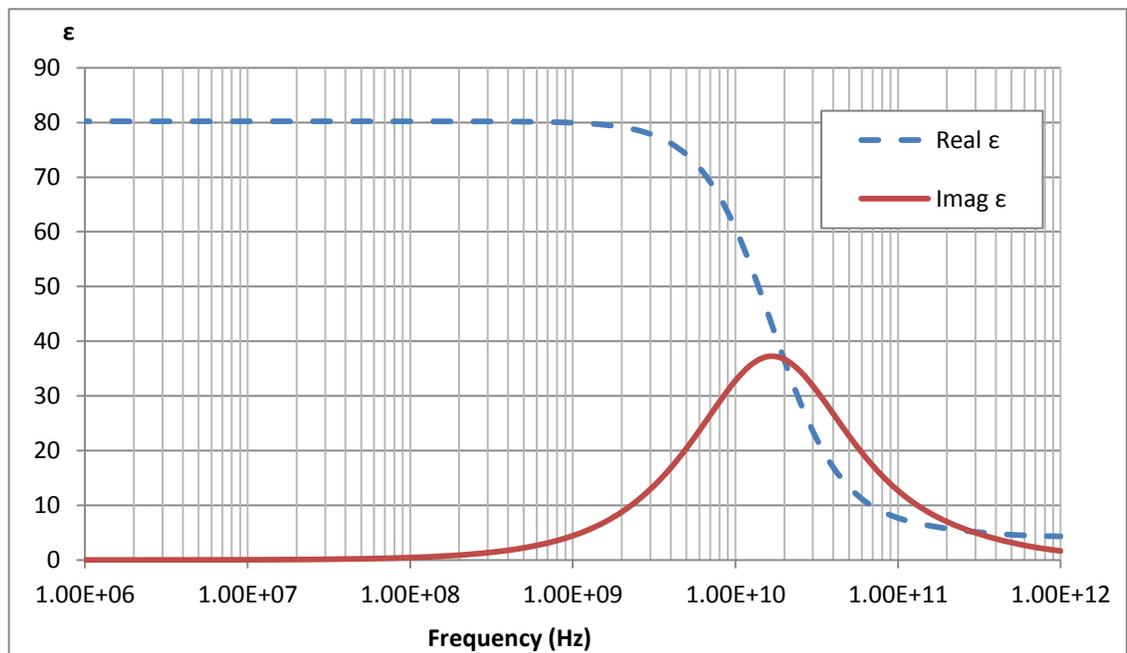
Figure 18 Permittivity of water with S=0ppt referred to as distilled water at T=20°C

Ahmed Abdallah Abdou
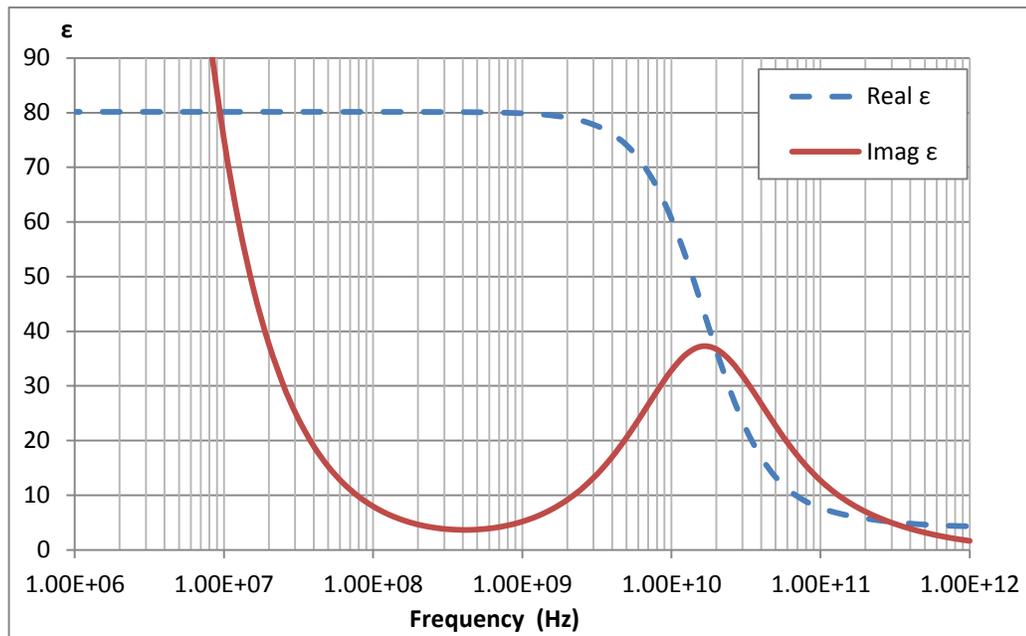
Figure 19 Permittivity of water with S=0.0871ppt referred to as potable water T=20°C
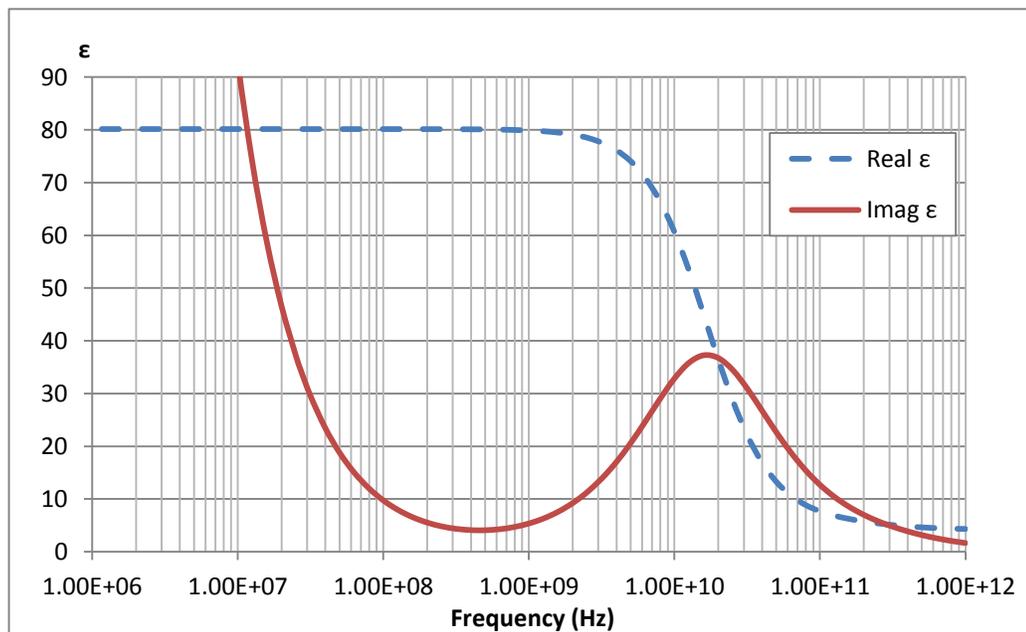
Figure 20 Permittivity of water with S=0.335 referred to as freshwater canal at T=20°C

Ahmed Abdallah Abdou
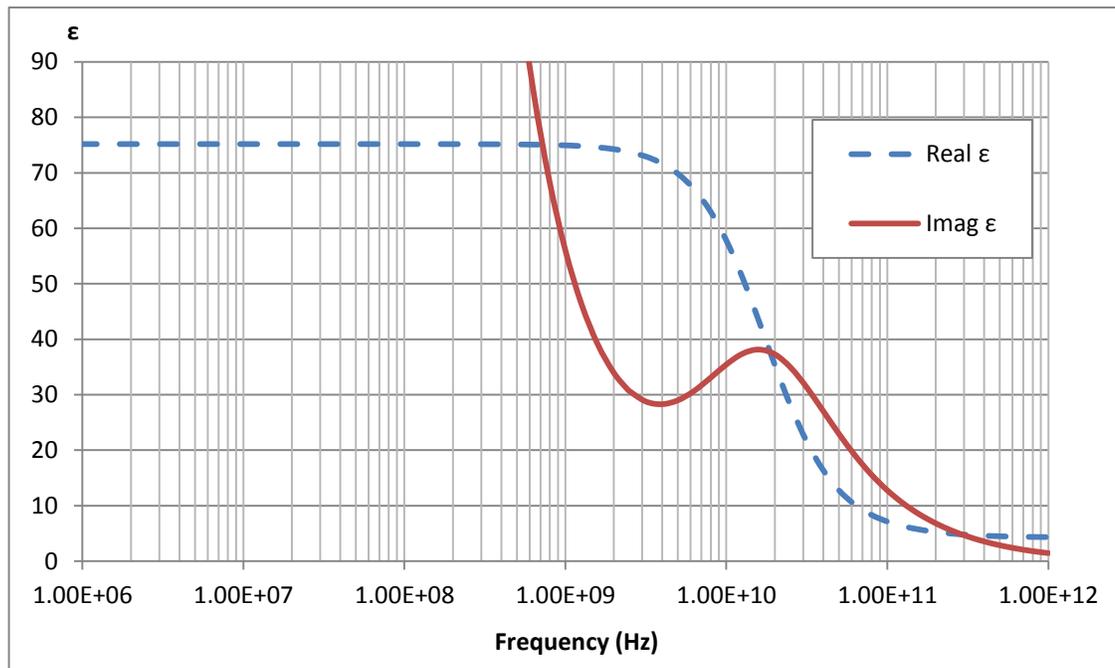
Figure 21 Permittivity of water with S=20ppt referred to as seawater at T=20°C

In all cases the dielectric polarisation orientation is happening at 20GHz. This corresponds to the first Debye relaxation as stated in [91]. This is also the region in Figure 19 where water will be best heated up and by consequence the 2.45GHz frequency of operation is not the only option available for microwave oven design. However this frequency proved to be both effective and relatively cheap to achieve.

The real parts of the complex dielectric permittivity are related to the energy stored within the medium. This value is approximately 80 for all cases except in seawater where it approximates to 75, remains static up to 2GHz, and then drops at relaxation time. The salinity concentration does not have a big impact on the real part permittivity. This means that saline water has slightly less energy storage capability than pure water.

79

The imaginary parts of the complex dielectric permittivity are related to the dissipation of energy due to collision during the rotation of the water polar molecule when exposed to an alternating electric field. For pure water at the low end frequency of our spectrum these values are near zero due to the absence of salinity. Then from the GHz, they start rising up to a maximum, with a corresponding fall of the real parts, to meet at the first Debye relaxation frequency (20GHz). In the presence of salinity, these values are now very large at the low frequency end of the spectrum, and then drop for the 400-500MHz region where it reaches a minimum. This happens in potable water but also in canal freshwater. We predict that within this region (400-500MHz) lies the best frequency to operate in the potable and freshwater canal environment.

In seawater these values are even bigger at the low frequency end of the spectrum, and then drop at the 2-4GHz region where it reaches a minimum which is approximately 10 times bigger than the previous case.

3.5.1.2. Temperature effects on permittivity

Other than frequency and salinity, the complex permittivity is also dependent on temperature as formulated in the Meissner and Wentz model. Here, a prediction of the behaviour of the permittivity with regards to the frequency for each type of water body will be given when its temperature changes. The permittivity of each type of water body is calculated at varying temperature from 0^oC to 30^oC in increments of 15^oC.

80

Ahmed Abdallah Abdou
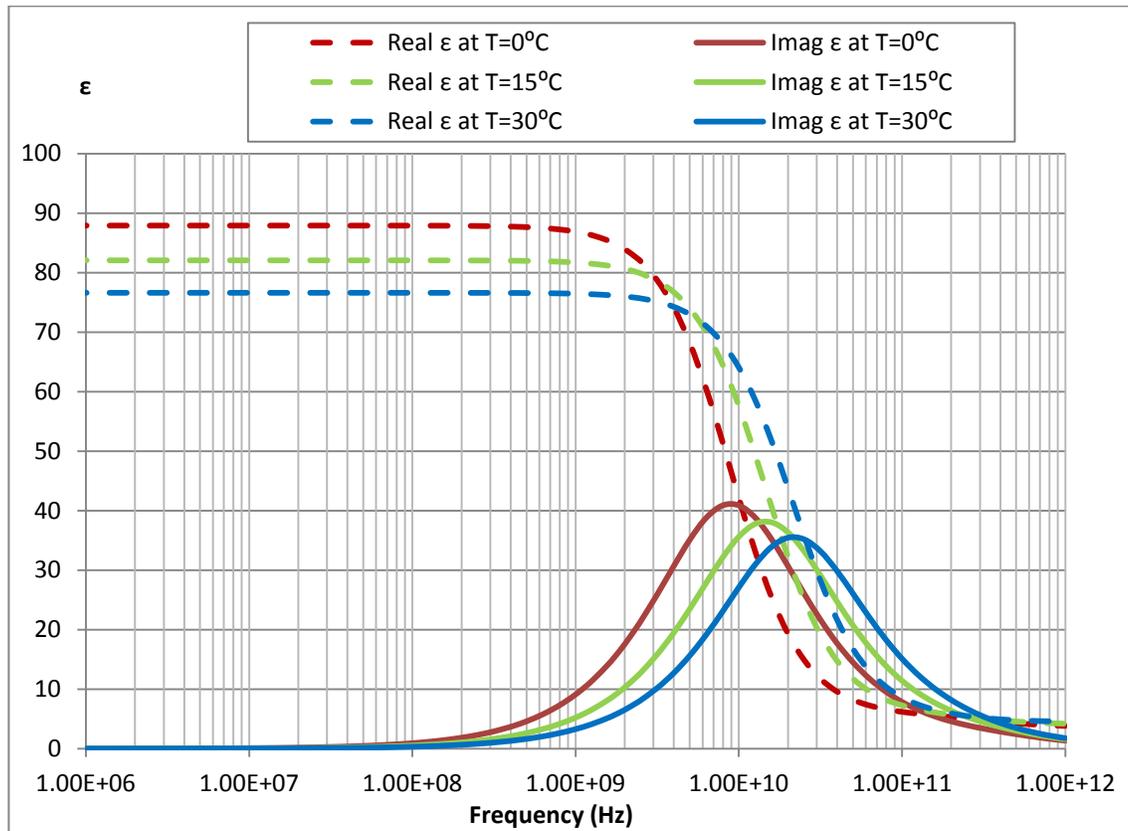
Figure 22 Effect of temperature on the real and imaginary parts of the permittivity of water with salinity concentration S=0ppt referred to as distilled water

In Figure 22, the increase of temperature produces a proportional decrease of the real part of the permittivity for frequencies up to 1GHz. The relaxation frequency at $T=0^oC$ is happening at 10GHz and this corresponds to the first Debye relaxation in the Meissner and Wentz model but also the Debye relaxation frequency in the Debye model where temperature and salinity are not taken into account ($T=0^oC$ and S=0ppt). For distilled water, the increase in temperature produces a relevant increase of the relaxation frequency.

Ahmed Abdallah Abdou
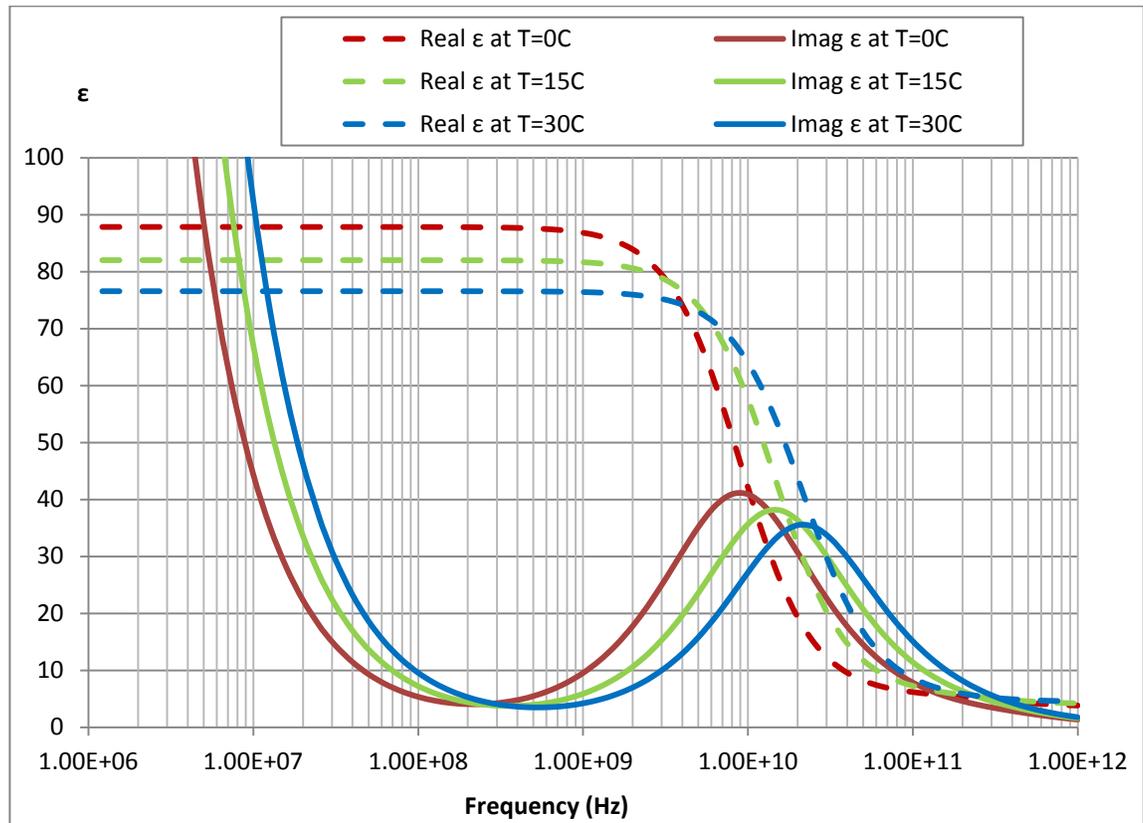
Figure 23 Effect of temperature on the real and imaginary parts of the permittivity of water with salinity concentration S=0.0871ppt referred to as potable water

In Figure 23, the increase of temperature produces a proportional decrease of the real parts permittivity for frequencies up to 1GHz. For the imaginary part permittivity, which is very high compared to that of the real parts because of the salinity effects, a proportional change is visible for the region up 100MHz. This is followed by their minimums shifting in terms of frequency. For referred to as potable water, the increase in temperature also produces a relevant increase of the relaxation frequency. However a region of minimum losses is apparent in the 100MHz to 1GHz region.

Ahmed Abdallah Abdou
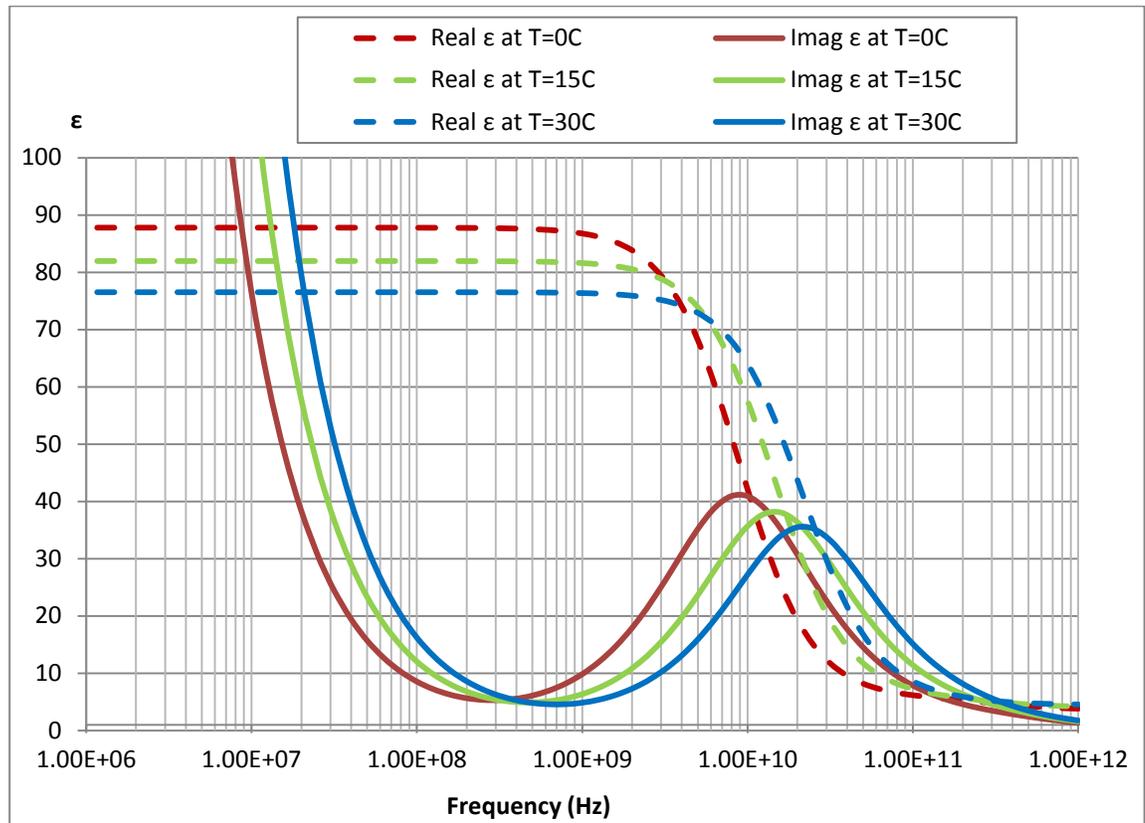
Figure 24 Effect of temperature on the real and imaginary parts of the permittivity of water with salinity concentration S=0.335ppt referred to as canal freshwater

In Figure 24, the increase of temperature produces a proportional decrease of the real parts permittivity for frequencies up to 1GHz. For the imaginary parts permittivity which is very high compared to that of the real parts because of the salinity effects, a proportional change is visible for the region up 100MHz. This is followed by their minimums shifting in terms of frequency. For referred to as canal freshwater, the increase in temperature produces also a relevant increase of the relaxation frequency. This shifts the minimum losses region higher by 50MHz.

Ahmed Abdallah Abdou
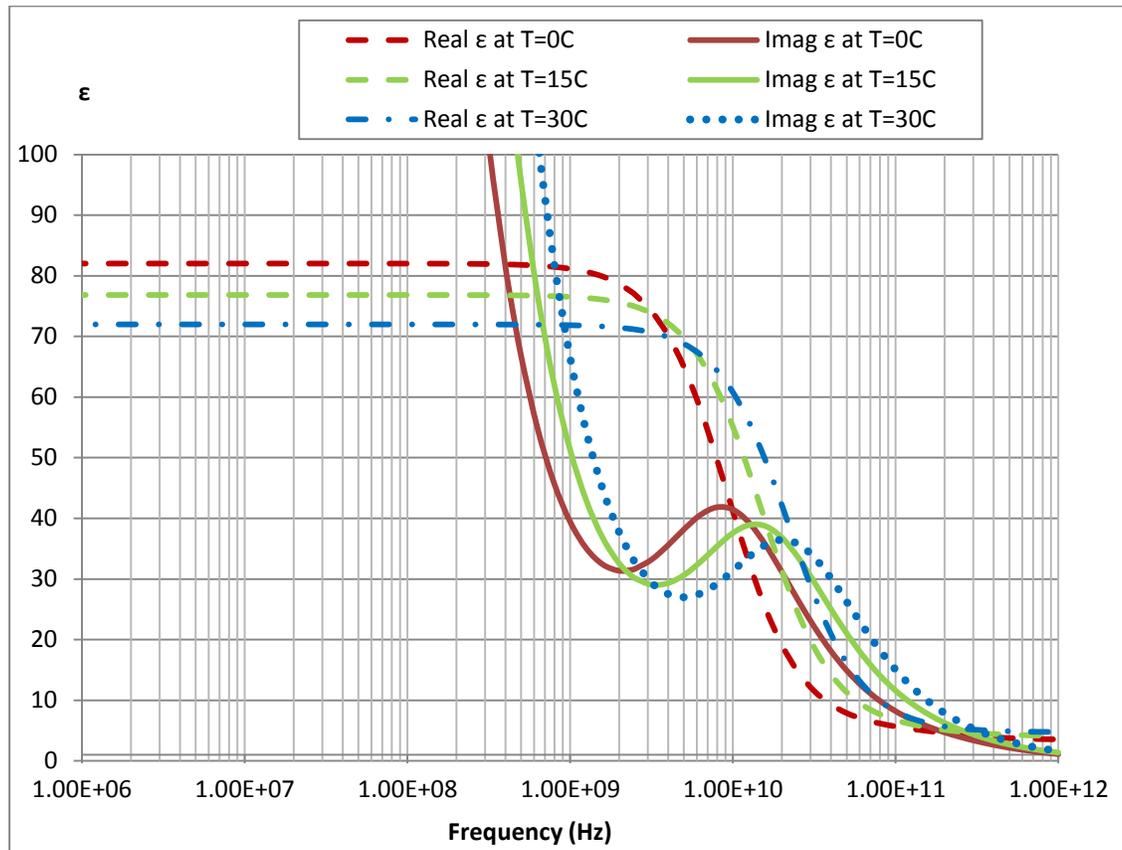
Figure 25 Effect of temperature on the real and imaginary parts of the permittivity of water

with salinity concentration S=20ppt referred to as seawater

In Figure 25, the increase of temperature produces a proportional decrease of the real parts permittivity for frequencies up to 1GHz. For the imaginary parts are very high compared to the real parts because of the conductivity effects, a proportional change is visible for 1GHz region. This is followed by minimums shifting in terms of frequency. These minimums are higher values compared to previous water salinities. For seawater, the increase in temperature also produces a relevant increase of the relaxation frequency. However in this saline water body

Ahmed Abdallah Abdou

the losses are higher than in previous cases and the region is not considered as a minimum region of losses.

For operating frequencies at ISM band (6.7MHz, 433MHz and 2.4GHz) and a temperature of water of T=20°C, Real and Imaginary parts of water permittivity at different concentrations of salinity to refer to different water environments, are calculated using the Meissner and Wentz model and presented in Table 2.

Note that at 433MHz for water with salinity of 0ppt (referred to as distilled) at a temperature of 20°C, the real part of the complex permittivity is 80.17 and the imaginary part is 1.92. This is the permittivity quoted in section 3.5.1 from [84] and validates the model used in equation (15).

Table 2 Real and Imaginary parts of permittivity at ISM frequencies

ISM Frequency	Permittivity of water with S=20ppt (≈seawater), T=20°C		Permittivity of water with S=0.335ppt (≈freshwater), T=20°C		Permittivity of water with S=0.0871ppt (≈tap water), T=20°C		Permittivity of water with S=0ppt (≈distilled water), T=20°C	
	Real	Imaginary	Real	Imaginary	Real	Imaginary	Real	Imaginary
6.7MHz	75.19	7763.98	80.130	159.801	80.196	41.94	80.219	0.03
433MHz	75.15	121.88	80.080	4.393	80.146	2.57	80.170	1.92
2.4GHz	73.88	31.16	78.637	10.885	78.701	10.57	78.723	10.46

Those values are used to calculate the effective conductivity (σeff) and the attenuation (α).

Ahmed Abdallah Abdou

3.5.2. Attenuation of EM wave propagation in water

The complex propagation constant γ describing the behaviour of an EM wave in [78] is defined in equation (16) with a real attenuation constant α in equation (17) and an imaginary phase constant β in equation (18) as follows:

$$\gamma = \alpha + j\beta$$

(16)

$$\alpha = \omega\sqrt{\mu\varepsilon}\sqrt{0.5\sqrt{1+(\sigma/\omega\varepsilon)^2}-1}$$

(17)

$$\beta = \omega\sqrt{\mu\varepsilon}\sqrt{0.5\sqrt{1+(\sigma/\omega\varepsilon)^2}+1}$$

(18)

The attenuation constant determines the rate of decay of a propagating electromagnetic wave and the phase constant determines the rate of phase change. However we focus on attenuation to predict EM wave propagation underwater because it refers to the decrease in the magnitude of a signal as it propagates through a medium. In the case of conducting mediums including water, equation (17) which is the homogeneous Helmholtz equation is modified to include the effective conductivity which is the losses due to the imaginary portion being a measure of the energy lost due to collision during rotation of the polar molecule (water). The modification also includes the energy stored within the medium and is formulated as:

$$\alpha = \omega\sqrt{\mu\varepsilon'}\sqrt{0.5\sqrt{1+(\sigma_{\text{eff}}/\omega\varepsilon')^2}-1}$$

(19)

86

Ahmed Abdallah Abdou

With α, the attenuation in nepers/m

ω, the frequency in radians

μ, the permeability of the medium in N/A^2

ε' , the permittivity of the medium in F/m as $\varepsilon' = \varepsilon_0 \varepsilon'_r$

σ_{eff}, the effective conductivity in S/m as $\sigma_{eff} = \omega \times \varepsilon_0 \varepsilon''_r$

Using the values of real and imaginary parts permittivity from Table 2 in equation (19), attenuation (α) is then calculated for water with different concentrations of salinity (S) including water with salinity S=0ppt to refer to as distilled water, water with salinity S=0.0871ppt to refer to as potable water, water with salinity S=0.335ppt to refer to as freshwater and water with salinity S=20ppt to refer to as seawater for the ISM (Industrial, Scientific and Medical) band. These are presented in Table 3.

Table 3 Attenuations of ISM operating frequencies in water with different salinity concentration

ISM Frequency	Attenuation (dB/m) of water with S=20ppt (≈seawater), T=20°C	Attenuation (dB/m) of water with S=0.335ppt (≈freshwater), T=20°C	Attenuation (dB/m) of water with S=0.0871ppt (≈tapwater), T=20°C	Attenuation (dB/m) of water with S=0ppt (≈distilled water), T=20°C
6.7MHz	75.608	8.563	2.768	0.002
433MHz	459.632	19.335	11.316	8.465
2.4GHz	775.274	267.439	259.588	256.797

A representation of the attenuation (dB/m) in water with different concentrations of salinity referring to different water environments in relation to the frequency (Hz) of operation is displayed in Figure 26.

Ahmed Abdallah Abdou
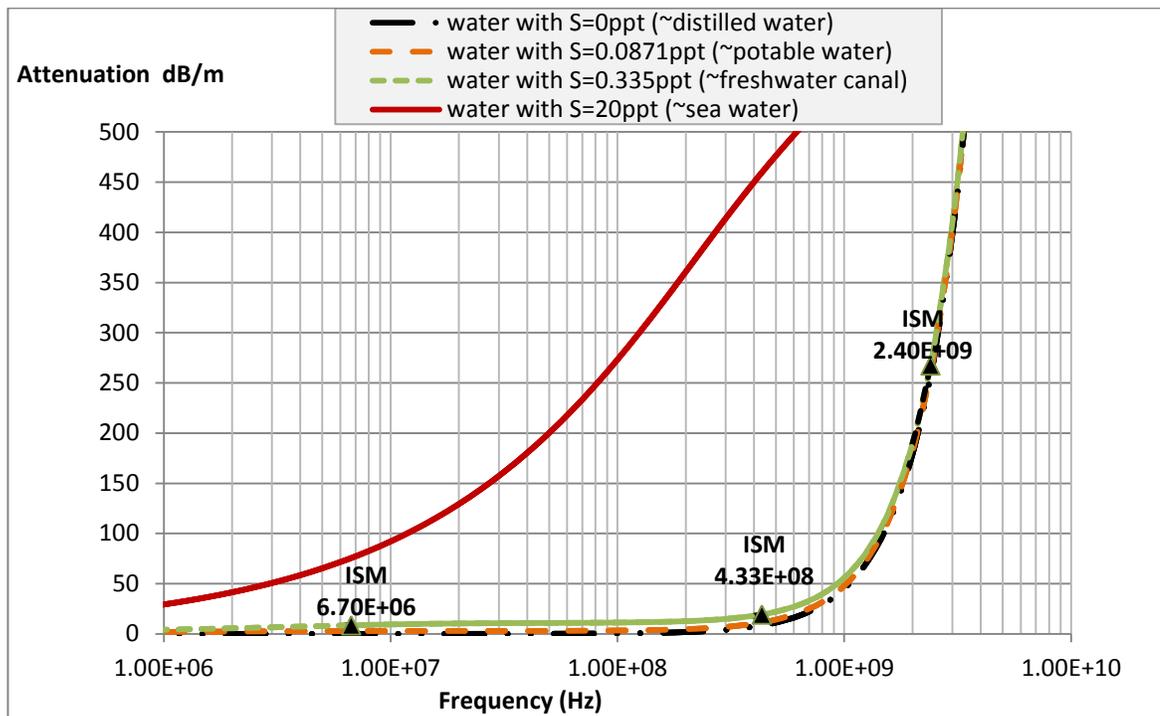
Figure 26 Attenuation (dB/m) in water with different concentrations of salinity S, in relation

to the operating frequency (Hz)

According to Table 3 and Figure 26, attenuation in water with 20ppt of salinity (referred to as seawater) is found to be very large but propagation seems to be feasible in the lowest frequency band (6.7MHz). This theoretical feasible prediction has been practically proved with experiments published in [60]. Propagation of EM waves in seawater [1] was more affected by attenuation in the near field and experiments have shown that insulating the antenna reduced the attenuation.

Attenuation in water with salinity concentration equal to or smaller than 0.335ppt including water referred to as freshwater canal, potable and distilled water is not high in the middle ISM

Ahmed Abdallah Abdou

band at 433MHz. This seems encouraging for building a wireless sensor network using commodity nodes operating at this frequency.

3.6. Experimental verification

3.6.1. Underwater experiments using an off-the-shelf kit at 2.4GHz ISM

Initial investigations concentrated on the most prevalent frequency for commercial WSN transceivers which is 2.4GHz. To validate equation (19) used for predicting the attenuation of radio signals in water, an experiment was set up in a tank of potable water. An off- the-shelf wireless kit operating at 2.4GHz ISM band was used to evaluate the performance.

3.6.1.1. A temperature application in air and in water at a fixed 100mm distance

3.6.1.1.1. Experimental setup

The tank had a length of 690mm, a width of 530mm and a height of 530mm. It was filled with 100 litres of potable water with 0.013S/m of conductivity. The conductivity of the water was measured using a HI33000 conductivity meter. The Ez430-RF2500 wireless kit in Figure 27 contains a USB interface to program the nodes as Access Point or End Point. Once programmed, one board had to be connected to the USB wireless board while the other was fitted to the battery powered board and became a completely isolated wireless set. The boards were based on the MSP430F2274 microcontroller and the CC2500 wireless transceiver operating at 2.4GHz. They were all fitted with temperature sensors. Data such as hub number, temperature, received signal strength indicator (RSSI) and voltage could be exchanged

89

between the two nodes. The kit has a Sensor Monitor application which allows the temperature of the two nodes and their separation distance to be monitored on the computer.
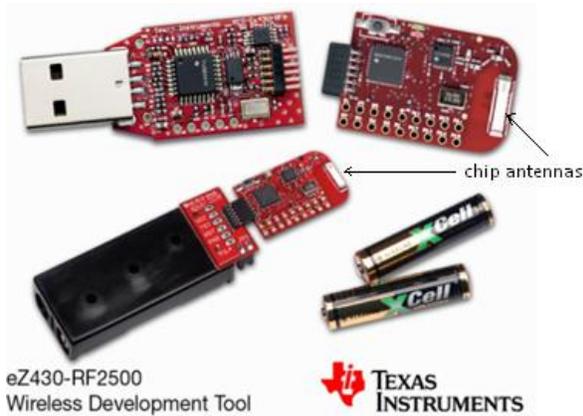
Figure 27 eZ430RF2500 Wireless sensor kit

The kit is designed for transceivers to communicate in air wirelessly using a Surface Mount Device multilayer chip antenna for 2.4GHz with an average gain of 1dBi. More information on the antenna can be found in [93]. At first, the sensor boards were put in air tight waterproof plastic containers of sizes $140\times95\times45$mm and separated by 100mm, in open air on a table as in

Figure 28. Then to determine whether EM wave propagation underwater is practically possible at 2.4GHz, the air-tight enclosures containing the sensors were hung 100mm apart in 375mm water depth in the plastic tank as in Figure 29. The End point is completely isolated and wire free.

Ahmed Abdallah Abdou
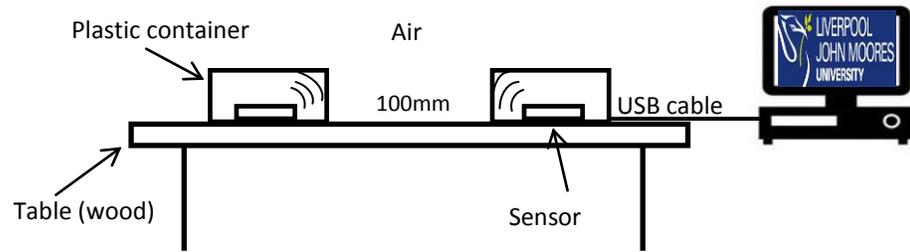
Figure 28 Experimental setup of sensors in containers on table in air
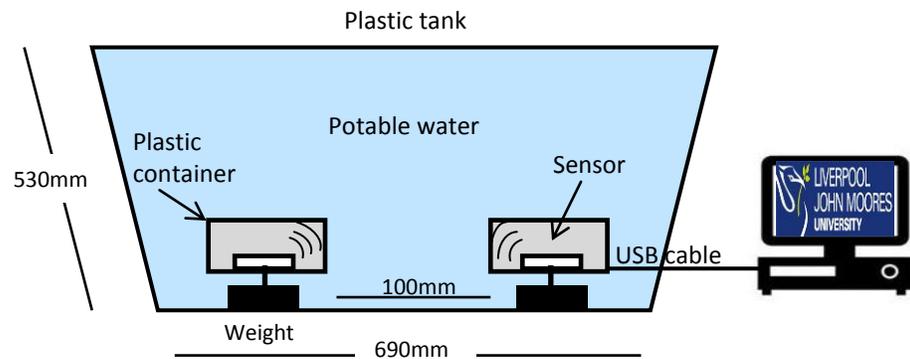
Figure 29 Experimental setup of sensors in containers in a small tank with potable water

These experimental setups and the results obtained are published in [94].

3.6.1.1.2.   Results

Figure 30 displays the hub number, temperature, battery voltage and RSSI of the eZ430-RF2500 communication hyper terminal when the Access Point (HUB0) and the End Point (0001) sensors are both in air. The temperature sensor monitor application screen shot for these sensors is shown in Figure 31.

91

Ahmed Abdallah Abdou

Hub number	Temp (ºC)	Battery voltage (V)	RSSI (%)
0001	23.4	3.0	32
HUB0	28.0	3.6	-
0001	23.4	3.0	32
HUB0	28.0	3.6	-
HUB0	32.5	3.5	-
HUB0	26.3	3.6	-
HUB0	28.4	3.6	-
HUB0	26.7	3.6	-
0001	23.4	3.0	30
HUB0	28.4	3.6	-
HUB0	28.0	3.6	-

Figure 30 Data for sensors in air

Figure 31 Temperature sensor monitor in air

Figure 32 displays the hub number, temperature, battery voltage and RSSI of the eZ430-RF2500 communication hyper terminal when the Access Point (HUB0) and the End Point (0001) sensors are both in water. The temperature sensor monitor application screen shot for these sensors is shown in Figure 33.

Ahmed Abdallah Abdou

Hub number	Temp (ºC)	Battery voltage (V)	RSSI (%)
0001	22.6	3.0	17
HUB0	22.6	3.6	-
HUB0	25.9	3.6	-
0001	22.6	3.0	17
HUB0	25.9	3.6	-
0001	22.6	3.0	17
HUB0	24.7	3.5	-
0001	22.6	3.0	17
HUB0	28.8	3.5	-
0001	22.6	3.0	17
HUB0	25.9	3.6	-

Figure 32 Data for sensors in water
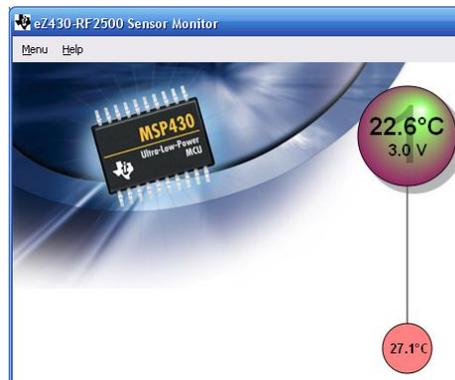
Figure 33 Temperature sensor monitor in water

The RSSI which is recorded and displayed on the Ez430-HyperTerminal has no units. In the

application report [95], the authors define that signal strength as the measured received signal

strength indicator RSSI given by the CC2500 radio. They state that it is output as a percentage

for readability and that the Access Point has always an output of 000%. In the source code

93

Ahmed Abdallah Abdou

[96] and the cc2500 datasheet [97], the relation between RSSI (%) and RSSI (dBm) is formulated as:

$$RSSI\ (\%) = \frac{(RSSI\ (dBm) + 128\ )}{256} \times 100$$

(20)

Using equation (20), the signal strength recorded from the end point nodes is converted into a power level RSSI (dBm) for air and for potable water at 100mm separation distance and displayed in Figure 34 for comparison with the datasheet values.

	Datasheet value (Min)	Tested value (Min)	Sensors in plastic containers in tank of **water**	Sensors in plastic containers in **air**	Tested value (Max)	Datasheet value (Max)
RSSI (dBm)	-104	-99.8	**-84.48**	**-48.64**	-15.36	+1

Figure 34 RSSI (dBm) of eZ430RF2500 Wireless sensor kit in air and in potable water at 100mm separation distance compared to datasheet values

3.6.1.1.3.   Discussion

In the datasheet [97] the maximum RSSI(dBm) of the eZ430RF2500 at 2.4GHz is +1dBm and the minimum RSSI is -104dBm. The maximum and minimum achievable RSSI in open air are given as -99.8dBm and -15.36dBm. In our experiment, when the sensors were put within the closed containers, 100 mm apart in air on a table, the strength value at the end point "0001"

Ahmed Abdallah Abdou

from the access point called "HUB0" is at an average strength value of "31" which is equivalent to -48.64dBm. The temperature of the access point is recorded as 23.4°C. Then when the sensors were put in the air-tight waterproof closed containers and suspended in water depth of 375mm and 100mm apart, the strength value is at 17 which is equivalent to -84.48dBm. This means that there has been a signal drop of 35.84dB due to the change of medium. The temperature at the receiver in water has also dropped to 22.6°C because of the temperature of the water. The theoretical value obtained at 2.4GHz for the potable water attenuation in Table 3 was 259.59dB/m. This means that for the 100mm distance in potable water the signal is expected to attenuate by 26dB. The experimental result has exceeded theoretical prediction by 10dB; this difference can be explained by factors that may include the small number of readings in the underwater experiment. However at such a high frequency of 2.4GHz, the signal drop of 35.84dB due to the change of medium (from air to water) has not affected data communication and was still reliable under water for a fixed range of 100mm.

3.6.1.2. Maximum separation of transceivers in air and in water at 2.4GHz

3.6.1.2.1. Experiment setup

In these experiments, all the equipment in the previous experiment are used but only the small plastic tank of sizes L=690mm, W=530mm and H=530mm is replaced in order to measure the maximum communication range of the transceivers operating at 2.4GHz.The bigger plastic

95

tank is of sizes L=1620mm, W=620mm and H=580mm and filled with potable water of 0.013S/m conductivity as in Figure 35.
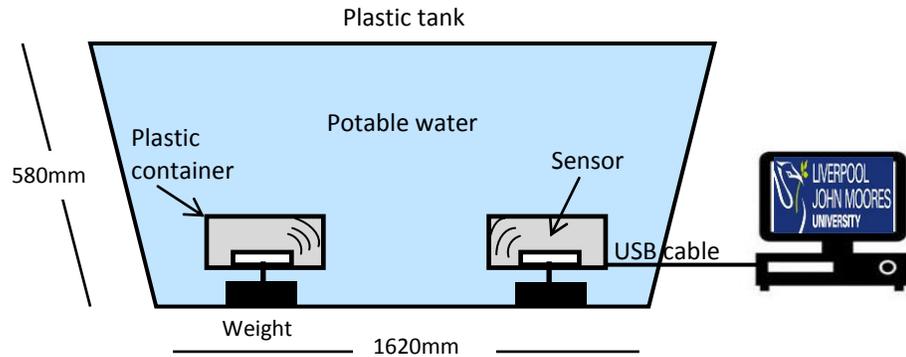
Figure 35 Experimental setup of sensors in containers in a big tank with potable water

In this set of experiments, sensors in air are moved apart with an increment of 100mm up to 1m and the RSSI, also called signal amplitude (dBm), was recorded. Then the sensors within the plastic containers are submerged in the tank of potable water (Figure 35) and the signal strength is recorded every 100mm to find the maximum communication range. The last experiment is repeated but with a lower increment of 20mm in order to take more readings to include the drop of signal amplitude happening within the first 100mm of separation distance of the transceivers.

3.6.1.2.2. Results

Figure 36 graphically represents the signal amplitudes (dBm) of the sensors when moved apart in increments of 100mm up to 1000m in both air and water.

Ahmed Abdallah Abdou
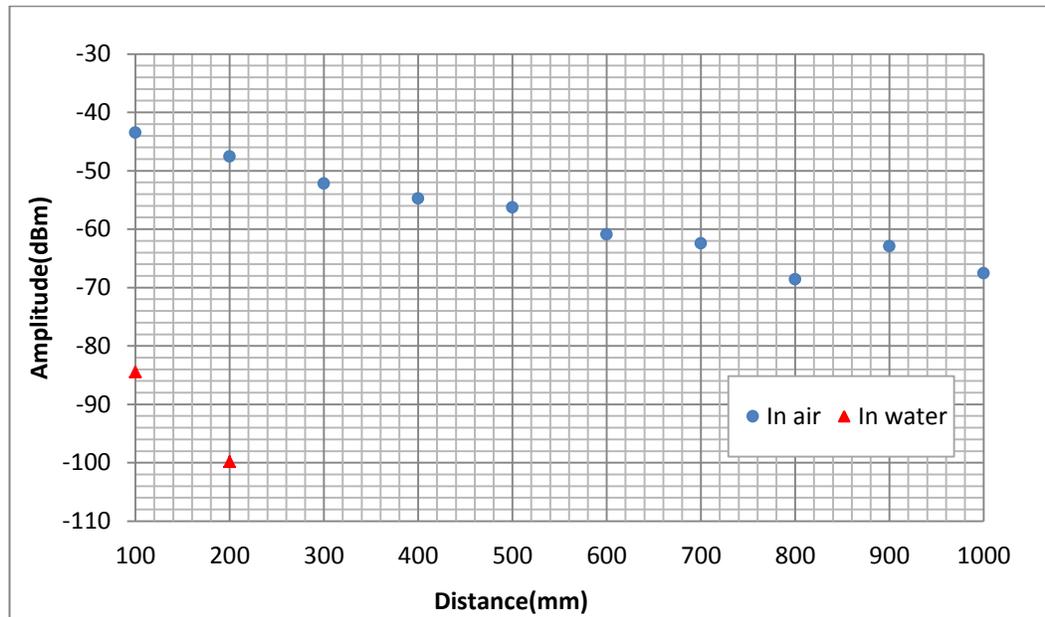
Figure 36 Signal amplitude of eZ430RF2500 (2.4GHz) sensors in air and in water

Figure 37 represents graphically signal amplitudes (dBm) of the sensors when moved apart in 20mm increments up to its maximum communication range in water (200mm).
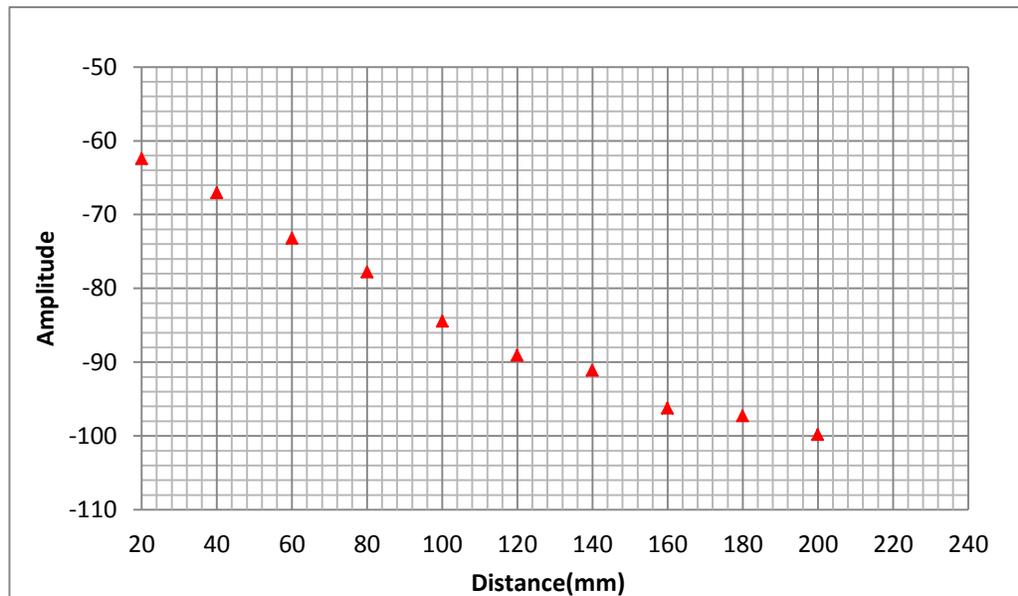
Figure 37 Signal amplitude of eZ430RF2500 (2.4GHz) sensors in water at 20mm increments

97

Ahmed Abdallah Abdou

3.6.1.2.3. Discussion

Figure 36 shows how the signal of the Ez430RF2500 at 2.4GHz travelling in air and in water attenuates with distance. At 100mm separation distance, the signal in air had an amplitude of -43.5dBm, whereas in water, it was significantly lower at -84.5dBm. In air the signal lost 26dB in 1000mm whereas in water it lost 28dB in 100mm as in Figure 37 (from 20mm to 120mm) and could not be detected after 200mm. This experimental value now exceeds the theoretical value of 26dB by 2dB only.

In air, a Near Field Far Field (NFFF) transition region can be seen around 500mm in Figure 36. In water there is no NFFF, and attenuation is almost linear as in Figure 37. These experiments have proven that underwater radio communication is possible at high ISM frequency of 2.4GHz up to a range of 200mm only.

Attenuation at the 433MHz ISM frequency band in potable water is calculated in Table 3 as 11.31dB/m, thus for 100mm communication the loss predicted is 1.13dB which will predict a better margin to increase the communication range.

Furthermore the medium change from air to water produced a drop in the signal which could be explained by the fact that the chip antenna used in the ez430rf2500 kit is poorly matched in water.

Ahmed Abdallah Abdou

3.6.2. Impact of the antenna and the frequency on the underwater communication

3.6.2.1. Experiment setup

The ez430RF2500 wireless sensor kit with its chip antennas used in the previous experiment was replaced. Here a Rohde and Schwarz SMB100A signal generator set at ISM frequencies of 6.7MHz,433MHz and 2.4GHz creates a carrier signal and transmits it in the water at a power of 0dBm as in Figure 39, through a 320mm diameter double loop antenna used in [61] and displayed with frames in Figure 38. The amplitude of this signal was measured using a Hewlett Packard HP8594E spectrum analyser.

Two experiments were performed. The first is to assess the impact of changing the antenna (chip antenna previously used replaced with the double loop antenna with the same output power) in an underwater communication. At 2.4 GHz, signal amplitude was recorded at each increment of 200mm up to 1000mm. Then a frequency sweep of the antenna was done to find its optimum frequency. The second experiment looked at the impact of using lower ISM frequency bands in the transmission stage of an underwater communication system. The amplitude of the received signal for each ISM frequency (6.7MHz, 433MHz and 2.4GHz) is recorded as the antennas were moved in 200mm steps up to 1000mm. Furthermore, losses in three different sizes (1m, 2.4m and 11m) of RG58 cables were measured for the ISM frequencies.

Ahmed Abdallah Abdou
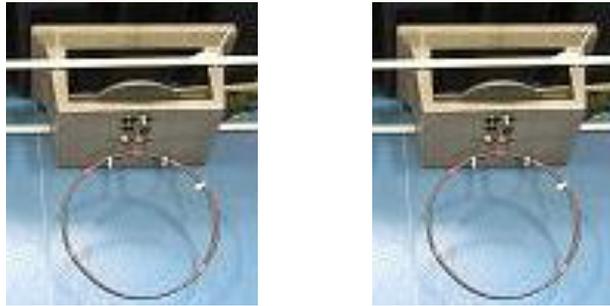
Figure 38 Double loop antennas of 320mm diameter with their frames

Figure 39 Experimental setup at ISM frequencies with double loop antennas

3.6.2.2.   Results

Signal amplitudes (dBm) recorded at increments of 200mm up to 1000mm when using chip antennas and double loop antennas at 2.4 GHz are represented graphically for comparison in Figure 40. Amplitudes (dBm) of the signal received for each ISM frequency (6.7MHz,

Ahmed Abdallah Abdou

433MHz and 2.4GHz) when moving antennas at 200mm steps up to 1000mm are represented in Figure 41. Measured losses for cables (1m, 2.4m and 11m) at ISM frequencies are represented in Figure 42.
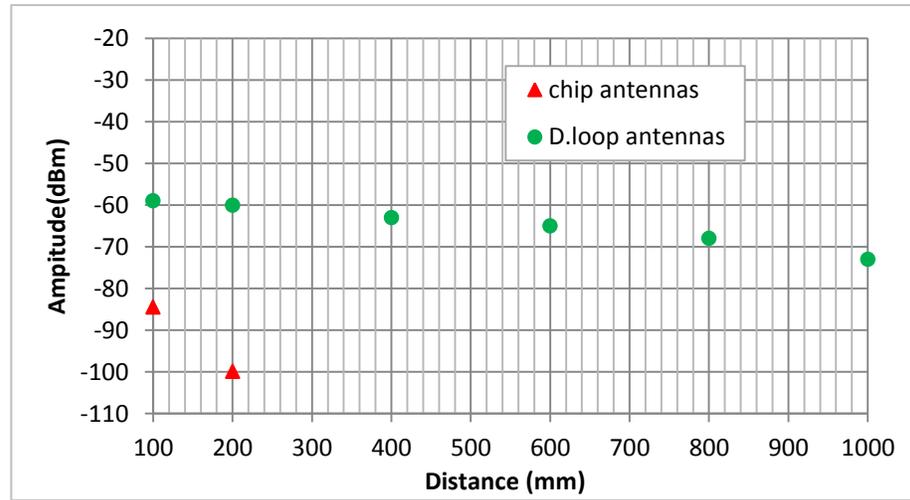
Figure 40 Comparison of chip antennas and double loop antennas at 2.4 GHz underwater
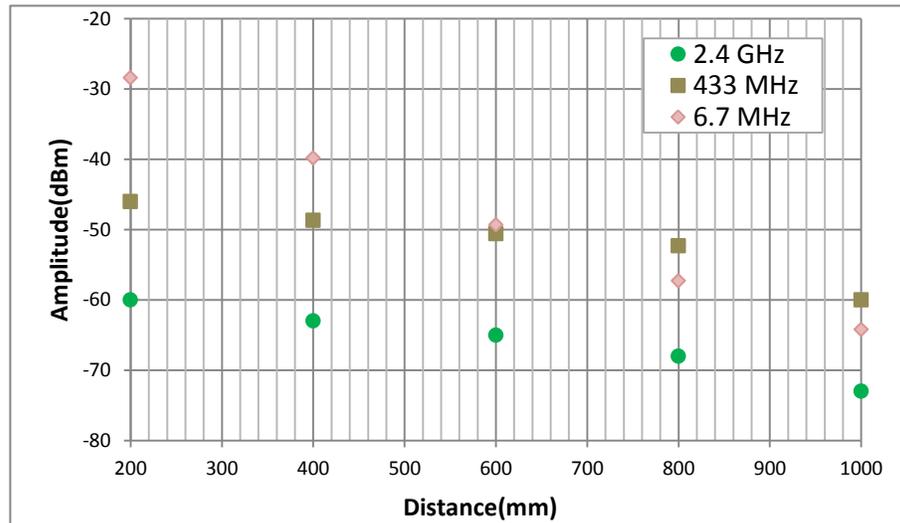
Figure 41 Signal amplitude at ISM frequencies up to 1000mm with 320mm double loop

antenna

101
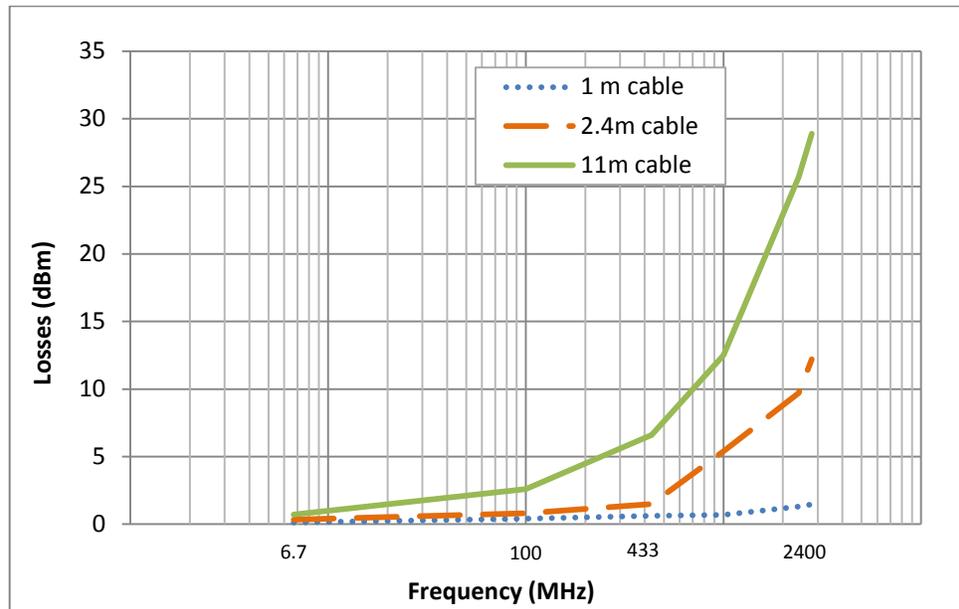
Figure 42 Losses in cables (1m, 2.4m and 11m) at ISM frequencies

3.6.2.3. Discussion

Figure 40 allows the comparison of two types of antennas operating at 2.4GHz in an underwater environment. It can be seen that using the chip antenna with the Ez430RF2500, the signal at 100mm was -84.5dBm and it lost 15.5dB in 100mm, whereas the double loop antennas starts with -59dBm and loses 1dB only. It could be stated that approximately 25dB has been gained in the signal launch by changing the type and size of the antenna. But surprisingly the signal remains strong after 200mm contradicting the theoretically predicted attenuation at 2.4GHz frequency of 25dB in 100mm and the experiment using the wireless transceivers with the chip antennas.

Figure 41 compares the three ISM frequencies when using the double loop antenna. It can be seen that lower ISM frequencies of 433MHz and 6.7MHz show better signal strength at signal

102

Ahmed Abdallah Abdou

launch. However the 6.7MHz curve drops more quickly than the 433MHz. Although the experiments demonstrate that lower ISM frequencies are less prone to signal attenuation in water only at signal launching, the attenuations over distances present some errors. In the experimental setup in Figure 39 the double loop antennas have their RF cable floating in air which may have resulted in crosstalk. Therefore the results obtained with the double loop antenna in water are not purely from the attenuated signal in water at least for the 2.4GHz frequency.

According to Figure 42, losses in RG58 cables used in the experiments increase with their length. Losses in long cables become considerably high at 433MHz and 2.4GHz. Therefore for experiments at such high frequencies, the length of cables must be kept as small as possible.

3.7. Summary

The theoretical model predicted high attenuation in water at the highest ISM band of 2.4GHz. This has been validated in the experiment with the communication being completely lost at 200mm of separation. However this 2.4 GHz ISM band has proved successful for a limited distance. The distance was limited because of factors including the receiver sensitivity at -100dBm whereas some receivers' sensitivity can go down to -122dBm [98] . Most importantly as confirmed in the theory and in the experiments, the 2.4GHz is a highly attenuated frequency band in water. Although it provides many advantages including high data rate and availability in complete kits, it can be used in applications requiring a high data rate for proximity communications i.e. Automated Underwater Vehicles collecting data from an underwater node where acoustic and optical are not viable options. The theoretical calculations predicted that

within the region (400-500MHz) lies the best frequency to operate in the potable and freshwater canal environment. Out of the operating frequencies in the ISM bands, the 433MHz band is less attenuated that the 2.4GHz and gives a better data rate than the 6.7MHz. Experiments have shown that antennas have a huge impact on the transmission and reception stage of the underwater communication system, therefore a study on underwater antennas will be carried out.

Ahmed Abdallah Abdou

Chapter 4. Traditional antennas and water

4.1. Introduction

As antennas are another crucial element in underwater radio and microwave communication, a set of traditional antennas will be investigated in this chapter. The theory required to construct antennas to operate in air or in water will be outlined first. Traditional antennas were made for the 433MHz ISM band and tested in water. The antenna with the best signal amplitudes was then selected to undergo a modelling stage in High Frequency Structure Simulator to analyse the behaviour of the antenna in two different environments (air and water). Important parameters including the return loss, 3D far field radiation pattern and gain, directivity of the antenna from HFSS reports will be presented to assess the suitability of using traditional antennas in underwater communication systems.

4.2. Antenna theory

In free space, wave velocity v (m/s) is related with frequency f (Hz) and wavelength λ (m) in [99] by:

$$v = f\lambda$$

(21)

Dipoles are one of the simplest but most widely used types of antennas. In [99], a linear conductor which, at a given instant has a positive charge at one end and an equal but negative charge at the other end may act as a dipole antenna. As the typical structure of a dipole

105

consists of two metal wires which are normally of equal length l, the dipole length can be determined for a given frequency using equation (21). The half wavelength dipole is the most popular dipole because of the impedance about 73ohms which is well matched with a standard transmission line with impedance 75 ohms or 50 ohms [2].

Another type of popular antenna is the monopole which consists of one metal wire erected on a perfect conducting ground. A monopole is half of the dipole antenna with a perfect conducting ground plane acting as a mirror to generate its image [2]. For a given frequency, the size of a monopole could be determined using equation (21). However, the quarter wavelength is a resonant antenna with an impedance of 37ohms, which matches well the 50 ohms transmission line.

For a loop antenna of diameter d (m), the wavelength equation is given in [99] by:

$$\lambda = \pi d$$

(22)

To decrease the size of loop antennas, multiple loops can be used. Formed with two turns, the double loop antenna used in [61] has its equation written as:

$$\frac{\lambda}{2} = 2\pi d$$

(23)

In free space, the speed of light is about $3 \times 10^8 m/s$ [2], in water the speed is reduced by a factor of $\sqrt{\varepsilon_r \mu_r}$ where μ_r is the relative permeability which is 1 [61]. ε_r is the relative permittivity calculated in Table 2, real parts permittivity values for potable water at 20°C are used for the experiment. Table 4 presents the real parts permittivity, the reduction

106

Ahmed Abdallah Abdou

factor $\sqrt{\varepsilon_r \mu_r}$, the velocity v (m/s) in water and the wavelengths λ (mm) in water and in air at ISM frequencies.

Table 4 Real parts permittivity, reduction factor $\sqrt{\varepsilon_r \mu_r}$, velocity v (m/s) in water, wavelength in water and in air (mm) for ISM frequencies (Hz)

FREQ (Hz)	6.70E+06	4.33E+08	2.40E+09
ε_r (Real)	80.196	80.146	78.701
$\sqrt{\varepsilon_r \mu_r}$	8.955	8.952	8.871
v (m/s) in water	3.350E+07	3.351E+07	3.382E+07
Wavelength in water (mm)	5000	77.4	14.1
Wavelength in air (mm)	44800	693	125

4.3. Construction and tests of traditional antennas in water

4.3.1. Experiment

In order to experiment with antenna behaviour in the water environment, several types and sizes of antennas were built from insulated copper (16 SWG= 1.626mm width) and soldered onto N type connectors. The diameter of the insulated copper was used because it fits neatly into the solder bucket of a standard N type connector. The 433MHz ISM frequency was selected as a compromise between attenuation and data rate, as described in the previous chapter. The wavelength in water is calculated in (Table 4) as about 77mm. Using this value

Ahmed Abdallah Abdou

and equations **(21)(22)(23)**, sizes of conventional antennas could be determined for their construction. One wavelength monopole (77mm) with ground plane, a half wavelength monopole (38.5mm), one wavelength loop (77mm) and one wavelength dipole (77mm) as shown in Figure 43 were built. A large 320mm diameter double loop antenna was available from [61] for comparison. The experimental setup in Figure 44 involves a Rohde and Schwarz SMB100A signal generator for creation of the carrier signal at a frequency of 433MHz and a power of 0dBm for transmission in a plastic tank of potable water ($\sigma = 0.013$ S/m) through an antenna from the ones built. Then through a second antenna with the same specification the signal was received and measured with a Hewlett Packard HP8594E spectrum analyser. An RF transformer was connected to the antennas to achieve maximum power transfer. The amplitude of the signal was recorded at each increment of 200mm up to 1000mm by moving the receiver's antenna. These were repeated for all the antennas constructed.

Figure 43 Antennas built for experiments (from right to left: one wavelength monopole with ground, a half wavelength monopole, one wavelength loop and one wavelength dipole

108

Ahmed Abdallah Abdou
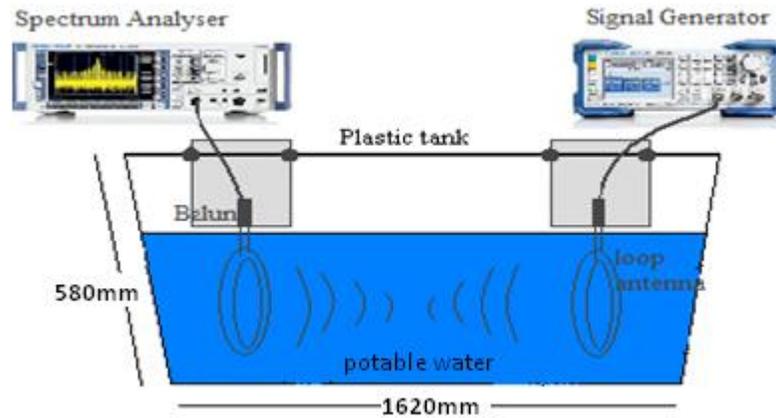
Figure 44 Experimental setup of built antennas

4.3.2. Results

The signal amplitude (dBm) for the different type and size of antennas built for 433MHz ISM frequency, measured every 200mm for a distance of 1 metre in the tank of water are graphically represented in Figure 45.
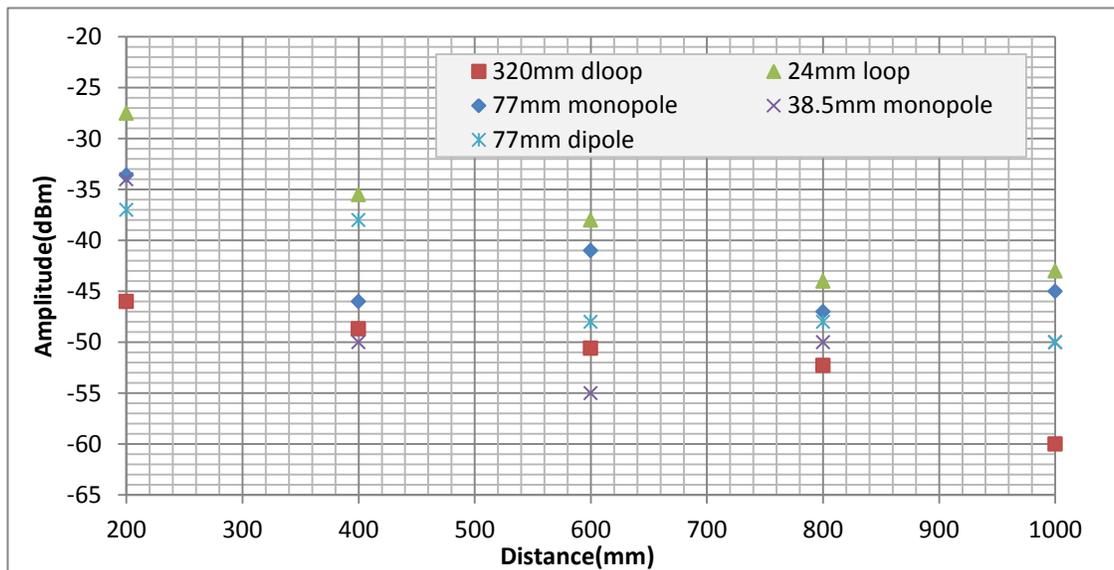
Figure 45 Signal amplitude for different type and size of antennas at ISM 433MHz frequency

for varying distances up to 1m

109

Ahmed Abdallah Abdou

4.3.3. Discussion

In Figure 45, the 23.5mm loop antenna has shown the best signal start at 200mm with amplitude of -27.5dBm compared to other antennas. The second best start is given by the 77mm monopole at -33.6dBm. Then 38.5mm monopole starts with -34dBm followed by the 77mm dipole and 320mm double loop antenna with respectively signal starting at -37dBm and -46dBm. At every 200 mm of separation distance up to 1 metre, the 23.5mm loop antenna had the best signal amplitude. The 77mm monopole had the second best signal amplitude at every 200mm separation distance up to a metre except for at 400mm. Then there is inconsistency over separation distances on which antenna perform better.

4.4. Modelling a traditional loop antenna

From the previous underwater experiments in the tank discussed in section 4.3.3, the loop antenna showed the best signal strength in water over every 200mm separation distance up to a metre. Therefore for further investigations of the antenna, including its behaviour with regard to the change of medium from air to water, the modelling stage of a loop antenna at 433MHz ISM was carried out using High Frequency Structure Simulator.

HFSS is an interactive software package from ANSYS for calculating and simulating in 3D the electromagnetic behaviour of a structure. HFSS is a finite element solver that uses the Finite Element Method. It can be used for antenna structures where it divides the structure into a fine mesh. It then finds the solution to Maxwell equations at each point on the mesh and keeps refining the mesh until the solutions converge. The software has the ability to do post-

Ahmed Abdallah Abdou

processing commands including return loss, input impedance and radiation patterns for analysing the electromagnetic behaviour in detail.

The return loss is defined as a measure of how much power is reflected back (logarithmic scale) from the terminal [2]. Return loss of the loop antennas in water was investigated to find at what frequencies maximum power transfer occurs. Antenna impedance is defined as the ratio of the appropriate components of the electric to magnetic fields at a point [100]. The Smith chart is a graphical demonstrator and can be used to represent the impedance of the antenna and visualize how well matched the impedance of the antenna is in the surrounding environment. The radiation pattern of the antenna is a plot of the radiated power as a function of the angle at a fixed distance, which should be large enough to be considered far field [2]. The radiation pattern can be represented as a 3D plot and can help in determining the directivity of the antenna.

4.4.1. Loop antenna modelling in water

To model the antenna in HFSS the important stages to follow includes the design of the antenna, boundaries and excitations setup, analysis via solution setup and frequency sweep, and results.

At first, a 3D model is designed to represent the antenna. For this a circle of radius 0.6mm is created on the ZX plane and positioned at [12.3mm, 0, 0]. The position of the circle at 12.3mm on the X axis will be the radius of the loop antenna and is found from solving equation (22) for the 77mm wavelength in Table 4. The material of the circle is assigned as Perfect Electric

111

Ahmed Abdallah Abdou

Conductor. The circle is edited and a sweep around Z axis is generated with an angle of -358º

to generate the loop design in Figure 46.
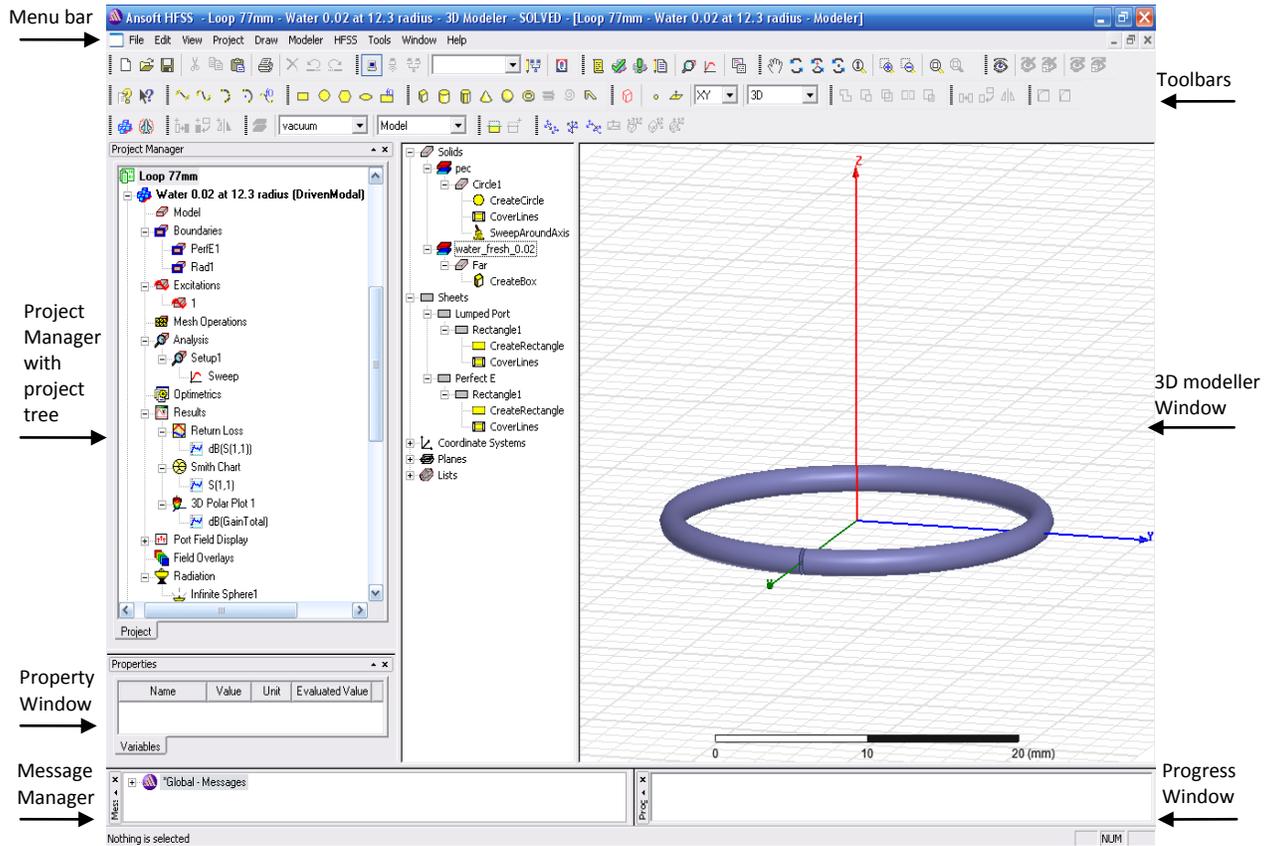
Figure 46 Ansoft HFSS window, panels and 3Dmodel of designed 12.3mm radius loop

antenna

Either lumped port or wave port may be used as excitations for antenna simulations. In [101], antennas with differential feeds should be excited with lumped port. A rectangular sheet is created on the XY plane and its surface is approximated as perfect electric boundary which is then assigned as a lumped port with 50ohms resistance for the excitation of the loop antenna. To imitate the water environment, an absorbing radiation boundary is created so that the

112

system absorbs the wave at the boundary. By preventing reflection, this effectively makes the boundary infinitely far away from the structure. The material of the far field boundary is assigned as water with conductivity of 0.02S/m. The boundary had to be placed at least a quarter wavelength away from the strongly radiating structure of the antenna for the simulation to be reliable [101].

Once the geometry of the loop antenna and its surroundings were designed as in Figure 47 and validated, the analysis parameters had to be defined which involve the solution setup and frequency sweep. For this a solution setup is added where the solution frequency is set at 433MHz. Then a frequency sweep is added and set between 1MHz and GHz and the simulation is run for analysis.
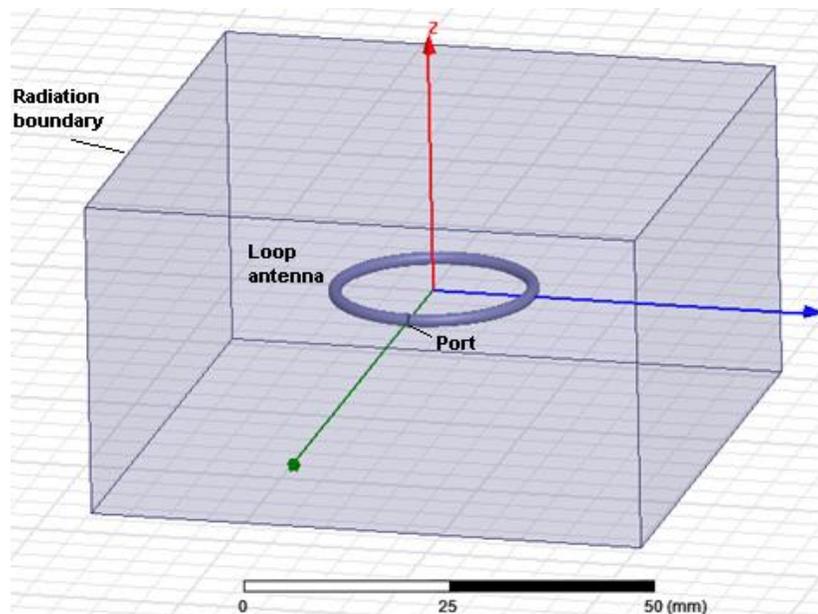
Figure 47 Side-view of the designed 12.3mm radius loop antenna within a radiation boundary

Ahmed Abdallah Abdou

After successful completion of the simulation, reports can be generated. A modal solution data report is created on a rectangular plot to display the magnitude of the Scattering parameter S(1,1) represented as return loss (dB). Another modal solution report is generated on a Smith chart to display the impedance of the antenna in a normalised complex form. A far field report is also created on a 3D polar plot to illustrate the gain of the antenna as a function of angle. This 3D plot is then applied to the model to show the radiation field of the antenna with respect to its position.

4.4.2. Results and discussion for 12.3mm radius loop antenna modelled in water
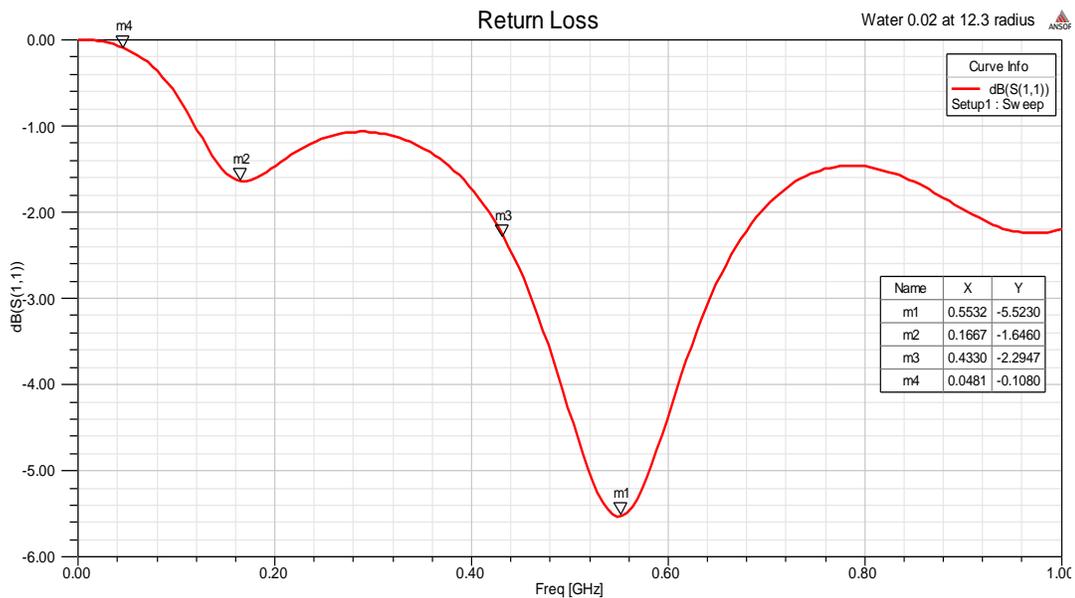
Figure 48 Return loss of the 12.3mm radius loop antenna simulated in water

114

Ahmed Abdallah Abdou

Name	Freq	Ang	Mag	RX
m1	0.5332	-156.1195	0.5394	0.3113 - 0.1918i
m2	0.1667	-12.4022	0.8274	4.6109 - 5.1945i
m3	0.4330	-156.8225	0.7684	0.1364 - 0.2014i
m4	0.0481	148.9189	0.9887	0.0061 + 0.2781i
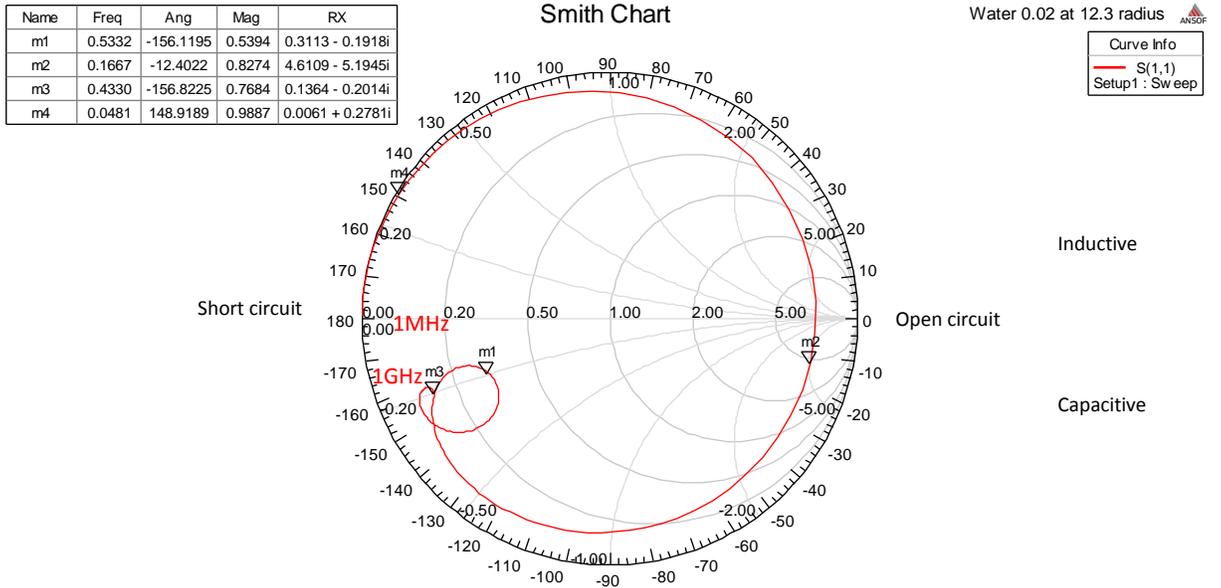
Figure 49 Smith chart of the impedance of the 12.3mm radius loop antenna simulated in
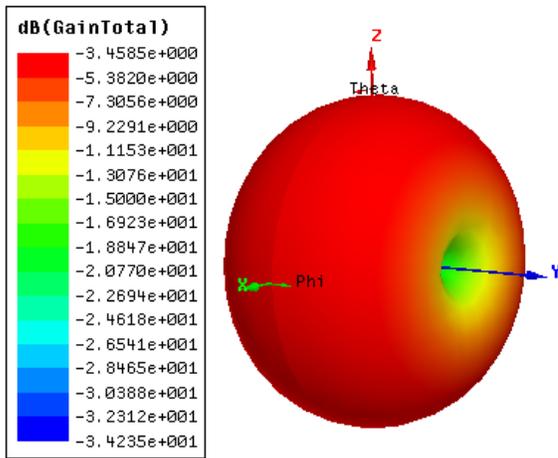
water

Figure 50 3D radiation plot of the gain of the 12.3mm radius loop antenna simulated in water
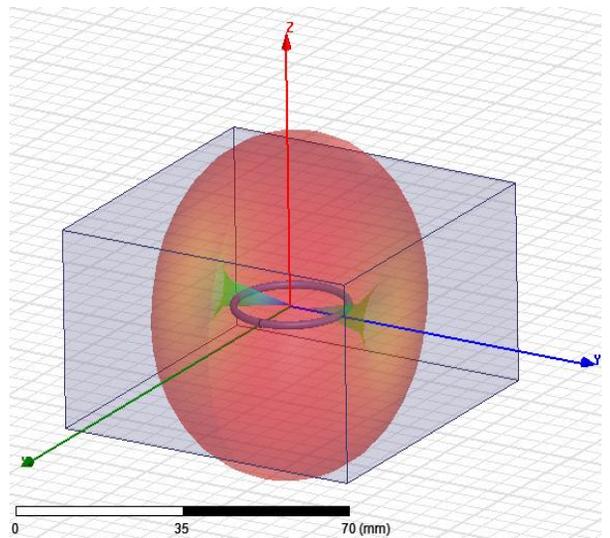
Figure 51 3D radiation field of the 12.3mm radius loop antenna simulated in water with respect to its position

115

Figure 48 shows that the 12.3cm radius loop antenna modelled from theoretical calculation of the wavelength and taking into account the reduction factor in water, resonates a 533MHz with a return loss of 5.5dB which approximates 70% of transmitted power. At the frequency of operation 433MHz, the return loss reads 2.3dB approximating 40% of the power being transmitted. In both cases, a bandwidth cannot be calculated as the return loss does not reach the minimum of 10dB required which approximates 90% of power transmitted. The impedance of the antenna at 533MHz and 433MHz could be calculated from the normalised ones showing in Figure 49 multiplied by 50ohms to give respectively 15.5ohms and 6.5ohms. These figures show that the loop antenna impedance is not matched to the 50ohms required even though at these frequencies the return losses are the best obtained. Figure 50 illustrates that the maximum gain at the far field is -3.46dB and is happening at the ZX plane whereas minimum gain of -20dB occurs on the Y axis. The shape of the loop radiation field as in Figure 51 looks like a doughnut on the ZX plane with some nulls on the Y axis.

4.4.3. Results and discussion for loop antenna radius 16mm modelled in water

The loop antenna with radius 12.3mm resonated at 533MHz. Because the frequency of interest is 433MHz, the modelling in section 4.4.1 is kept unchanged except for the radius which is iterated until resonance occurs at 433MHz. The optimised radius is found at 16mm and the return loss, smith chart and radiation patterns are presented.
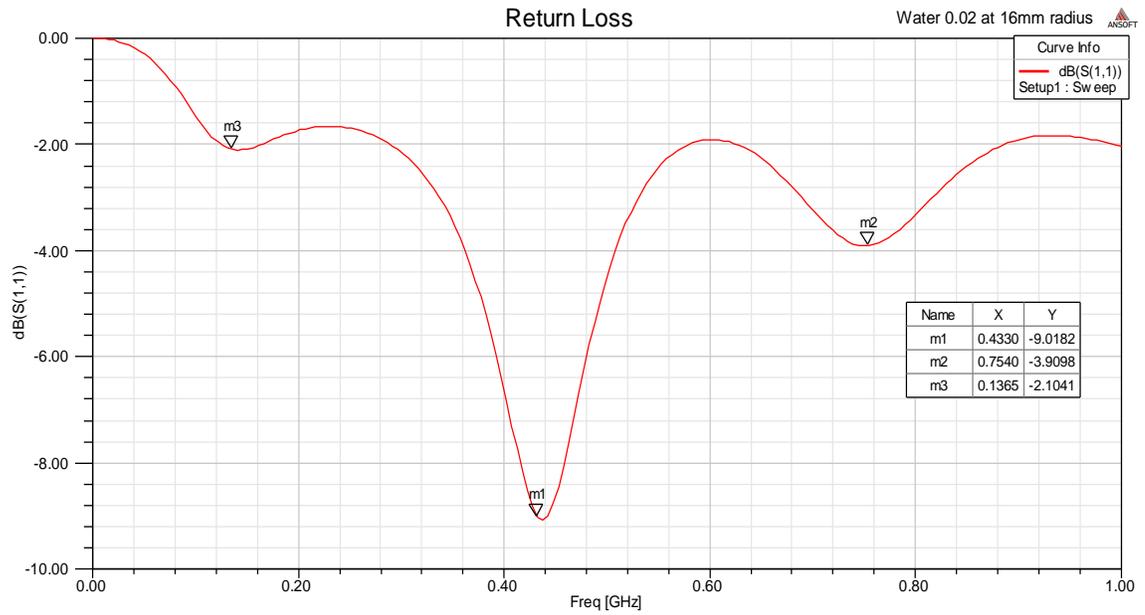
Figure 52 Return loss of the 16mm radius loop antenna simulated in water

Name	Freq	Ang	Mag	RX
m1	0.4330	-149.0725	0.3542	0.5046 - 0.2101i
m2	0.7540	-152.8127	0.6373	0.2338 - 0.2293i
m3	0.1365	-5.0592	0.7874	7.4037 - 2.7063i
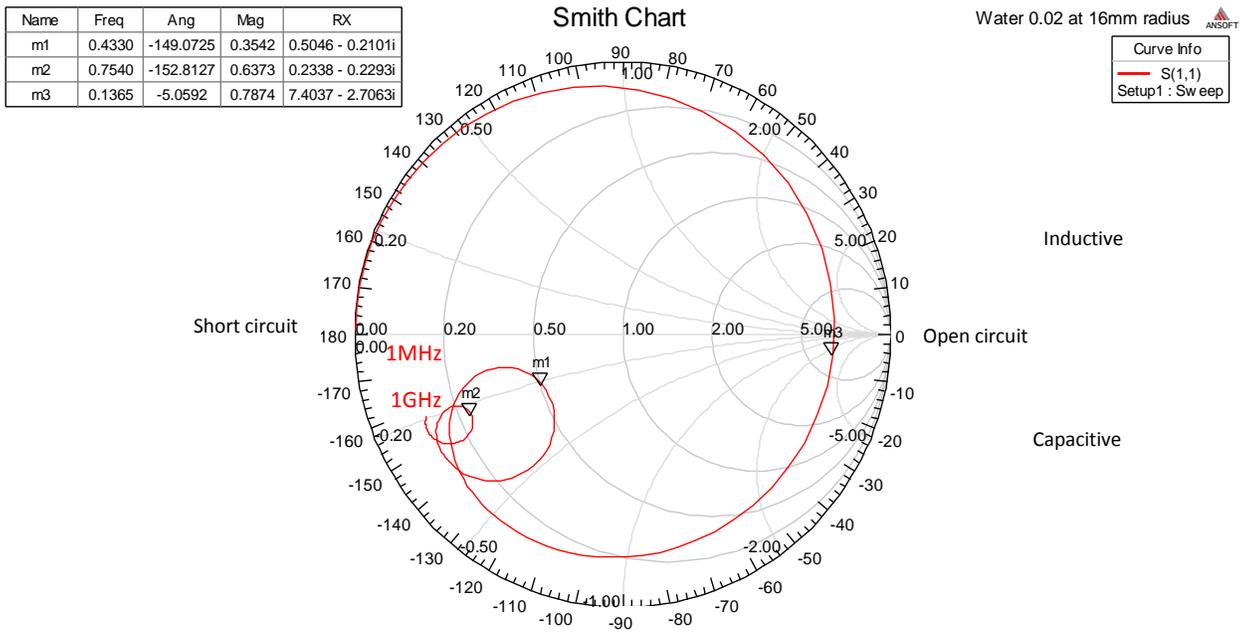
Figure 53 Smith chart of the impedance of the 16mm radius loop antenna simulated in water

Ahmed Abdallah Abdou
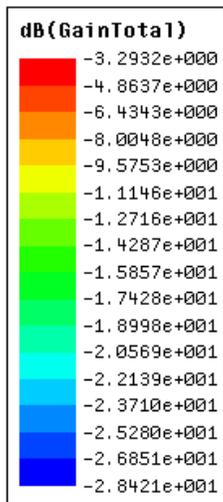
Figure 54 3D radiation plot of the gain of the 16mm radius loop antenna simulated in water
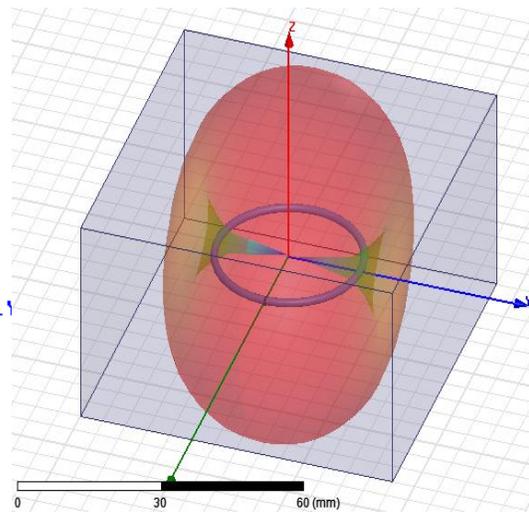
Figure 55 3D radiation field of the 16mm radius loop antenna simulated in water with respect to its position

Figure 52 shows that the return loss does not reach the minimum of 10dB for the bandwidth and its impedance in Figure 53 is 25ohms at 433MHz resonance. The antenna gain in Figure 54 is slightly higher -3.29dB compared to -3.46dB in Figure 50 as the antenna size is 3.5mm bigger. The radiation of the antenna in Figure 55 is still like a doughnut on the ZX plane with some nulls on the Y axis.

4.4.4. Results and discussion of the 12.3mm radius loop antenna modelled in Air

The 12.3mm is modelled in air by changing the radiation boundary material for investigations

118

Ahmed Abdallah Abdou

Name	X	Y
m1	4.2477	-5.3655
m2	8.2430	-3.6980
m3	0.4330	-0.0374
m4	0.0481	-0.0031
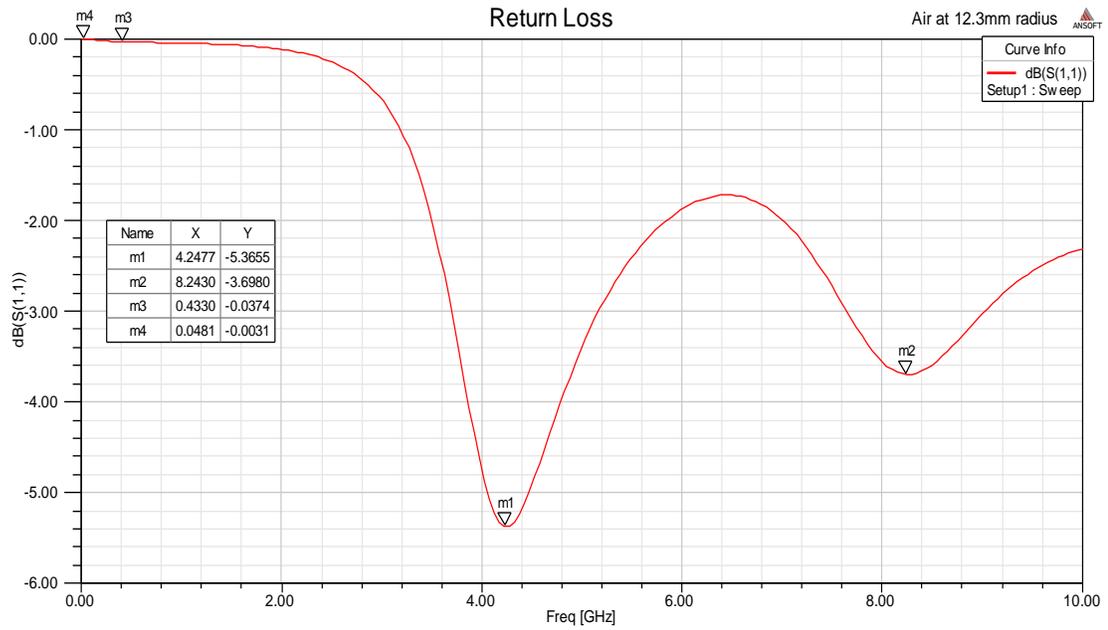
Figure 56 Return loss of the 12.3mm radius loop antenna simulated in air

Name	Freq	Ang	Mag	RX
m1	4.2477	-42.0990	0.5391	1.4459 - 1.4733i
m2	8.2430	-64.3429	0.6533	0.6657 - 1.3678i
m3	0.4330	43.6606	0.9958	0.0153 + 2.4963i
m4	0.0481	173.7472	1.0000	0.0000 + 0.0546i
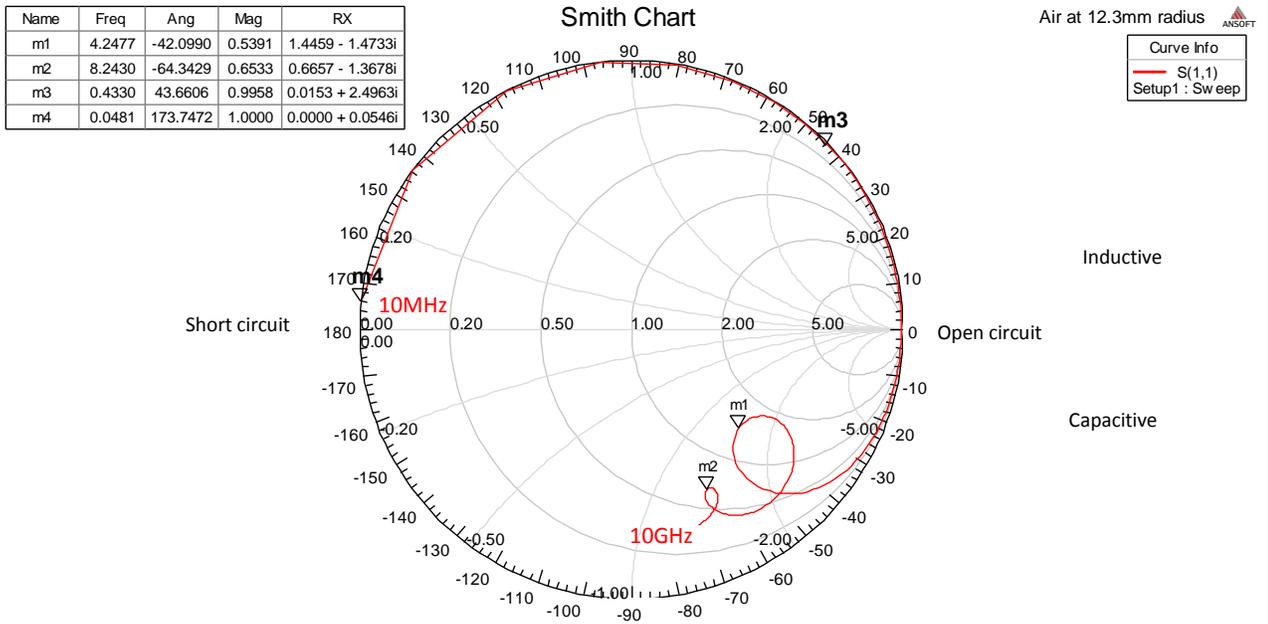
Figure 57 Smith chart of the impedance of the 12.3mm radius loop antenna simulated in air

119

Ahmed Abdallah Abdou
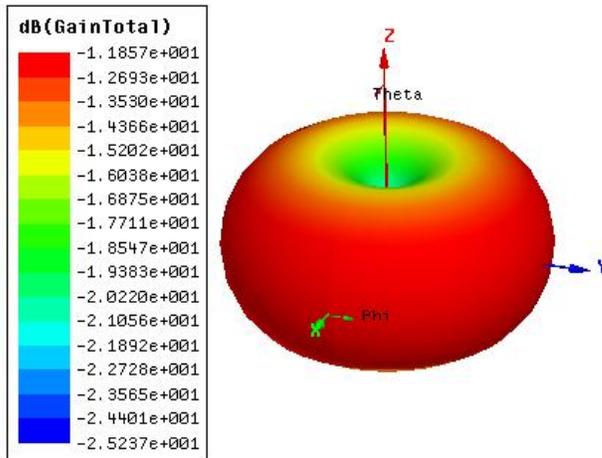
Figure 58 3D radiation plot of the gain of the 12.3mm radius loop antenna simulated in air
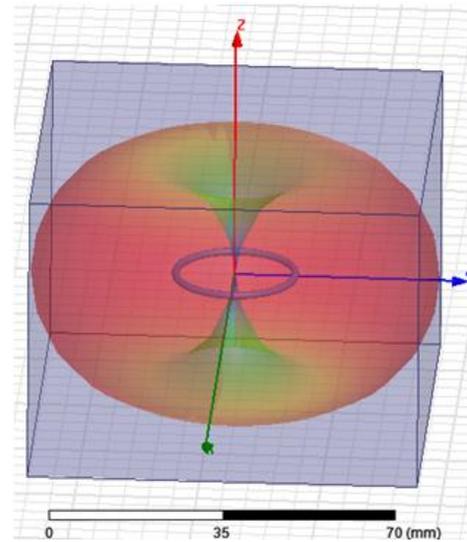
Figure 59 3D radiation field of the 12.3mm radius loop antenna simulated in air with respect to its position

Keeping the original radius of 12.3mm calculated for water and modelling the antenna in air shows in Figure 56 that the antenna does not resonate any more on the 433MHz but at 4.2GHz. This water to air frequency shift of approximately 9 times bigger is the inverse of the reduction factor 1/9 applied in Table 4 for air to water and used to construct the antennas in section 4.3. This validates the methodology used in constructing an antenna to operate in water taking into account the reduction factor due to water. However the antenna exhibited a gain up to -11.9dB in Figure 58 which means that the antenna designed for water is not appropriate in an air environment. The radiation of the loop antenna in Figure 59 has changed to omnidirectional on the XY plane with nulls along the Z axis. This phenomenon is due to the reduced size of the wavelength from air to water and further explained in [2].

120

Ahmed Abdallah Abdou

4.4.5. Results and discussion of loop antenna modelled from wavelength calculation in air

The loop antenna is modelled in air. The radius is calculated from the wavelength in air in Table 4 as 693mm and using equation (22) and yields a radius of 110mm. The simulation is run in air and the resonance is at 457MHz. The loop radius is iterated to make it resonate at 433MHz and the return loss and impedance are then displayed.
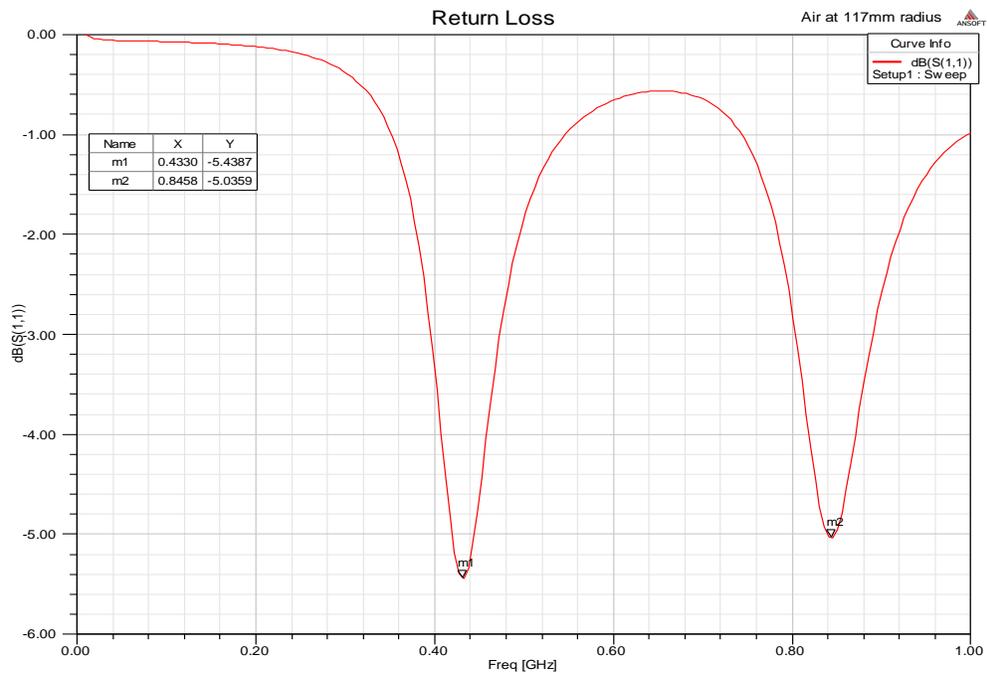
Figure 60 Return loss of the 117mm radius loop antenna simulated in air

Ahmed Abdallah Abdou

Name	Freq	Ang	Mag	RX
m1	0.4330	-4.8144	0.5345	3.2398 - 0.4069i
m2	0.8458	-5.7090	0.5600	3.4468 - 0.5595i
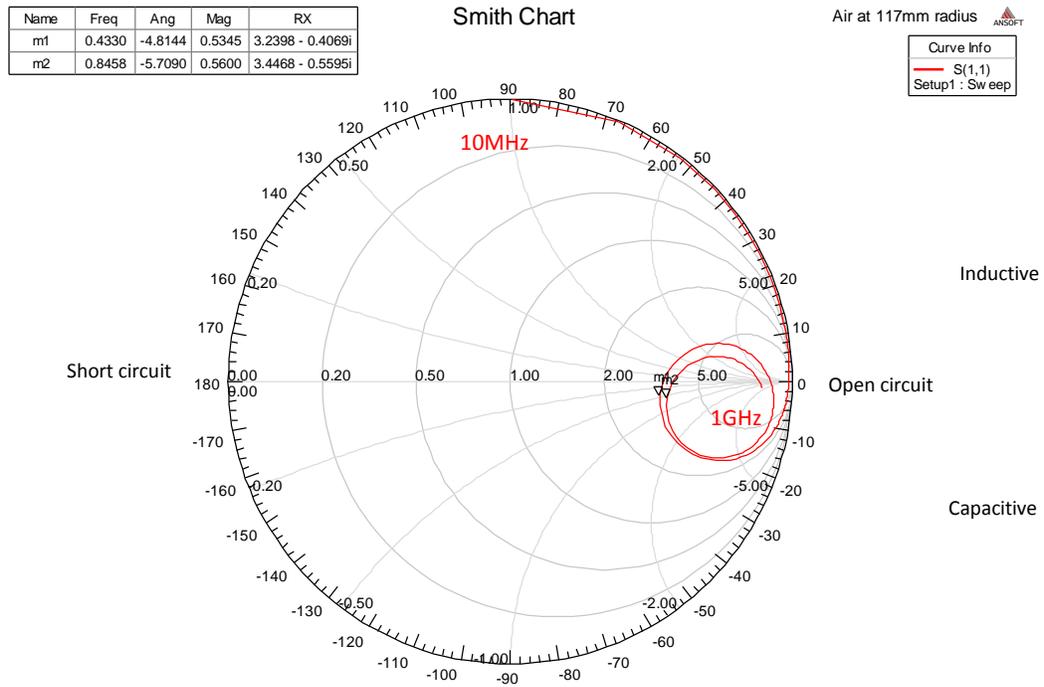
Figure 61 Smith chart of the impedance of the 117mm radius loop antenna simulated in air

Making a loop that resonates in air at 433MHz frequency from theoretical calculation, showed in the result of the modelling, a shift of 24MHz in the resonance frequency. However iterating the radius up to 117mm provided a resonance in the frequency of interest with a return loss of 5.38dB as shown in Figure 60. In neither resonance, does the return loss reach the required 10dB. Figure 61 shows that the impedance of the loop antenna modelled from theoretical calculation of the wavelength in air approximates to 150ohms and refers to an impedance mismatch in air. This confirms the statement in [2], that for mobile radio communications, the loop is often used in pagers but hardly used in mobile transceivers which may be due to its high resistance and reactance that makes it difficult to match to standard 50ohms transmission lines over moderate bandwidth.

Ahmed Abdallah Abdou

Loop antennas were used in water in [61] [60] and were found to be strongly responding to magnetic fields which makes them more advantageous for seawater. The antenna must be matched in this particular water with its particular salinity and temperature properties. However any change of these conditions will result in a mismatch of the antenna impedance. This can significantly reduce the communication range. The radiation of the loop in water is another factor making this type of antenna not suitable for our application.

4.5. Summary

Experiments in this chapter proved that underwater communication in the 433MHz ISM band is possible at least up to a metre and validates the theoretical predictions in the previous chapter. Although the loop antenna outperformed the other traditional antennas experimentally, the modelling shows that even with an optimised size, the antenna impedance in water and in air was mismatched. There was not any bandwidth available for the antenna in any of the two modelling environments. Without means of matching, the communication range required for the wireless sensor network would not be achieved. The radiation and directivity of the loop antenna is not the same in air and in water and the omnidirectional aspect of the antenna which cannot be maintained is another problem. The loop antenna and other traditional narrowband antennas are unsuitable without matching means and therefore bespoke antenna design with appropriate properties to suit underwater applications is sought.

123

Ahmed Abdallah Abdou

Chapter 5. Bow-tie antenna

5.1. Introduction

In the previous chapter, simulations and experiments demonstrated the unsuitability of using conventional and narrowband antennas for underwater communication without impedance matching due to the high dielectric property of water compared to air. However antennas utilising a matching circuit (RF transformers, balun, etc) may suffer from complete signal loss if any changes in temperature and salinity occur in the water. As the antenna in question is to be used in a wireless sensor network, another important aspect is the radiation of the antennas which is to be taken into account to ensure movement of the sensors in the water without complete signal loss. To select an antenna for wireless sensor network that could work in air as well as in water, the focus will be on selecting an antenna that has a broad bandwidth, an omnidirectional radiation pattern but also an antenna that can be prototyped for practical validation tests. The antenna will be modelled in air and in water in HFSS. If proven successful, the antenna will be prototyped for underwater tests in the laboratory tank.

5.2. Antenna selection and background

To find an antenna that could work in air and in water and to resolve impedance matching hurdles in air designed antennas for underwater applications, we propose the bandwidth technique. This means that the antenna has to have a broad bandwidth to accommodate the change in such a heavy dielectric medium (water). Balanis suggested in [100] that a simple configuration that can be used to achieve broadband characteristics is the biconical antenna

Ahmed Abdallah Abdou

formed by placing two cones of infinite extent together. However as it is not possible to manufacture an infinitely long biconical antenna, a geometrical approximation leads to the bowtie antenna fabricated from metal sheet. This relates to the third antenna selection criterion which is as crucial as the others. The ease of prototyping the antenna will help in validating it, from selection to design and implementation for real life underwater tests. In [102], the bowtie is defined as a planar version of the finite biconical antenna, which can be printed on a dielectric substrate. Therefore the antenna could be fabricated on a PCB. The bowtie has other advantages amongst other broadband antennas including biconical. The antenna could be massively produced for the many nodes that will form the WSN. Also as the antenna has to be used in water, the printed bowtie on PCB could be layered with waterproof material (glue or plastic).

With regards to the second antenna selection criterion, the author states in [102], that the radiation of the bowtie is a dipole-type radiation pattern, i.e. omnidirectional in the plane perpendicular to that of the antenna.

In [99], an actual biconical with a full cone angle of 120° has an omnidirectional pattern and nearly constant 50ohms input impedance (power reflection less than 1 percent) over a 6 to 1 bandwidth with cone diameter D=λ at the lowest frequency. In [103], the bandwidth of the bowtie antenna depends on the length of the plate. The flare angle and the length of the plate define the lower frequency. A biconical and a bowtie antenna are depicted in Figure 62.

Bowtie antennas have been used in many Ultra Wideband (UWB) applications [104] including ground penetrating radars [105] [106] and in mobile communication systems [107].

125

Ahmed Abdallah Abdou
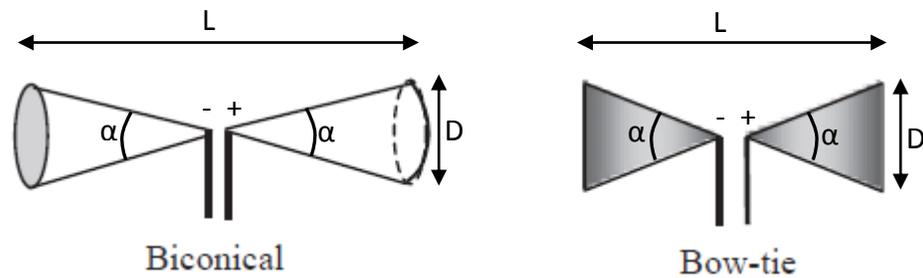
Figure 62 Diagrams of a Biconical and a Bow-tie antenna with flare angle α, cone diameter or outer width D, plate length L

In 2012, Elrashidi et al presented a study in [75] on underwater wireless sensor network communication using electromagnetic waves at resonance frequency 2.4GHz with a Bowtie antenna. The work is purely based on simulations at a frequency of 2.4GHz which we have already verified theoretically in section 3.5 and considered it as a highly attenuated band underwater. We have also demonstrated experimentally in section 3.6 and in our 2011 publications in [63] that at 2.4GHz, common low power transceivers could communicate only up to a very short range of 200mm. We have suggested that this band could be used for proximity sensing underwater and not for UWSN. This has been confirmed by Lloret et al. in their experimental work in 2012 [76] where they obtain 170mm communication range between two transceivers operating at 2.4GHz. Furthermore Elrashidi at al. claim using a bowtie in water whereas all their simulations are run in air. They have designed a bowtie antenna in FEKO software to resonate at 2.4GHz ISM in air with a RL of -14dB. There is no sign of simulation in water environment however the authors concluded with the results obtained in air that the antenna gain of -30dB is a very high value for underwater wireless

126

communication to overcome the high path loss due to attenuation. This (-30dB) value is a negative gain exhibited at 90˚ theta in air and therefore their antenna should be considered as a very lossy antenna which radiates poorly at 90˚ theta in air. Their maximum positive gain is only 1.5dB at 0˚ and 180˚ theta in air.

The selection of the bowtie antenna to operate efficiently in an underwater wireless sensor network is based on the three criteria set above which consist of an antenna with a broad bandwidth to be able to work in air as well as in water in case of water level variations, an omnidirectional radiation pattern to maintain signal strength as sensor nodes may be moved with water current and an ease of prototyping the antenna for practical validation tests. Also the bowtie antenna has to operate at lower than the 2.4GHz ISM band which is the 433MHz band theoretically and experimentally demonstrated useful in chapter 3. As a consequence a 433MHz bowtie antenna will be modelled in air and in water in HFSS then prototyped for underwater tests in the laboratory tank.

5.3. Modelling the Bow-tie antenna in air and in water

5.3.1. Design and simulations

The geometry of the bowtie antenna was created with the help of the HFSS Antenna Design Kit (ADK). This is a GUI-based wizard tool that automates geometry creation, solution setup, and post processing reports for 50 common antenna elements. The ADK then automatically generates physical dimensions for desired frequency [108]. A bowtie antenna is chosen and the desired frequency of operation at 433MHz is input. Then based on general design

Ahmed Abdallah Abdou

guidelines [109] the kit returns the parameters and dimensions needed as in Figure 63 and the antenna is created in HFSS with variables.
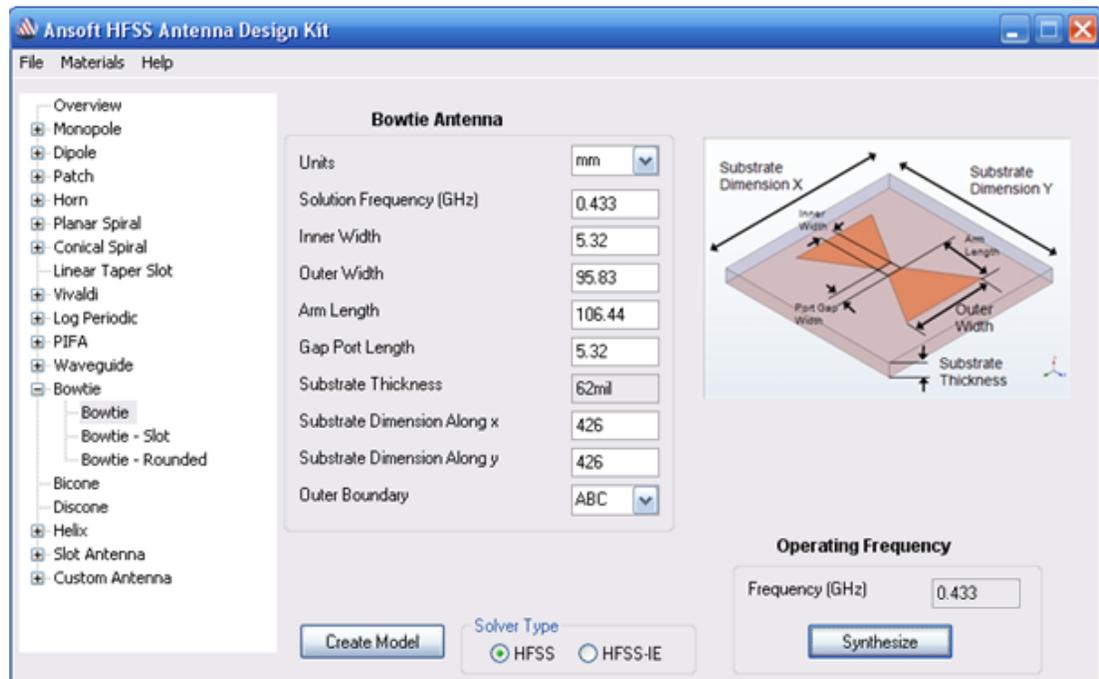
Figure 63 Screen shot of the Bowtie antenna created in HFSS's ADK and its parameters for

the 433MHz desired operating frequency

However for prototyping the antenna using the routing machine available in the Sensors laboratory within the Built Environment and Sustainable Technologies research institute within Liverpool John Moores University, some considerations had to be taken into account. The size of the levelling board required the restriction of the antenna board to a maximum length of 210mm and a width of 120mm. Therefore in HFSS, the two substrate dimensions variables of 426mm each were altered to the restricted size of the levelling board. However these two variables did not have an influence on the size of the radiating antenna and they act

128

Ahmed Abdallah Abdou

as a support for the copper sheet. The arm length given by the ADK is bigger than the length of the board and therefore in HFSS its size was changed from 106.44mm to 101.6mm. This makes the outer width smaller at 91.5mm instead of the original 95.8mm. The inner width and the port gap became 5.1mm. The new dimensions of the bowtie antenna were displayed in Table 5.

Table 5 New dimensions of the bowtie antenna

Solution frequency	0.433 GHz
Inner width	5.1mm
Outer width	91.5mm
Arm length	101.6mm
Gap port length	5.1mm
Substrate thickness	1.57mm
Substrate Dimensions Along x	120mm
Substrate Dimensions Along y	210mm

Also the kit uses a substrate of 62mil thickness and creates the antenna on a 2.2 relative permittivity. The standard single sided Printed Circuit Board that was used in the prototyping stage is made of 0.0356mm thick copper sheet and FR4 glass-reinforced epoxy laminate sheet. The PCB has a thickness of 1.6mm and a relative permittivity value of 4.4. Therefore in HFSS, the substrate permittivity is changed to 4.4.

Ahmed Abdallah Abdou

The antenna is modelled to resonate at 433MHz in an absorbing boundary condition with air material properties to mimic free space environment. Then to predict the behaviour of the bowtie antenna in water, the antenna is modelled in an absorbing boundary condition with water of 0.02S/m conductivity. The angle-view of the bow-tie antenna and the radiation bounds is shown in Figure 64.
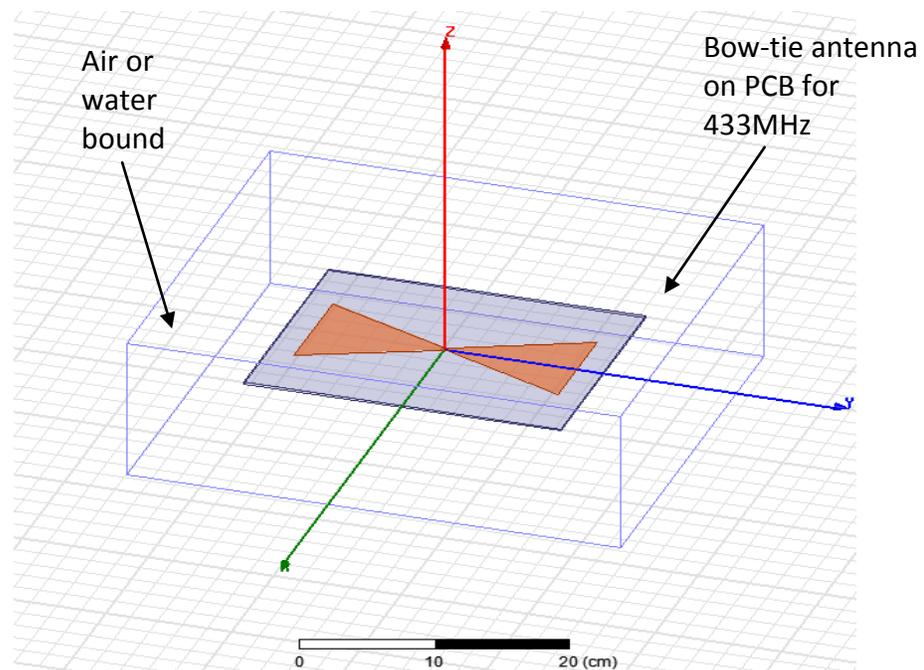
Figure 64 Modelling of the 433MHz bow-tie antenna within a radiation box in HFSS

In HFSS, the bowtie antenna was modelled both in air and water to obtain the following reports. Return losses of the antenna in air and in water were examined to observe where the maximum power transfer of the antenna occurs. The input impedances of the antenna in air and in water is presented in the Smith chart in order to visualize how well matched the

130

impedance of the antenna is in these two distinct environments. The direction of the antenna's radiation in air and water is shown in three dimension diagrams.

5.3.2. Results and discussion

The return losses of the antenna in air and in water are respectively represented in Figure 65 and Figure 66. The input impedances of the antenna in air and in water are respectively represented in the Smith chart in Figure 67 and Figure 68. Three dimension diagrams of the antenna radiation pattern simulation in air and in water are displayed respectively in Figure 69 and Figure 70.
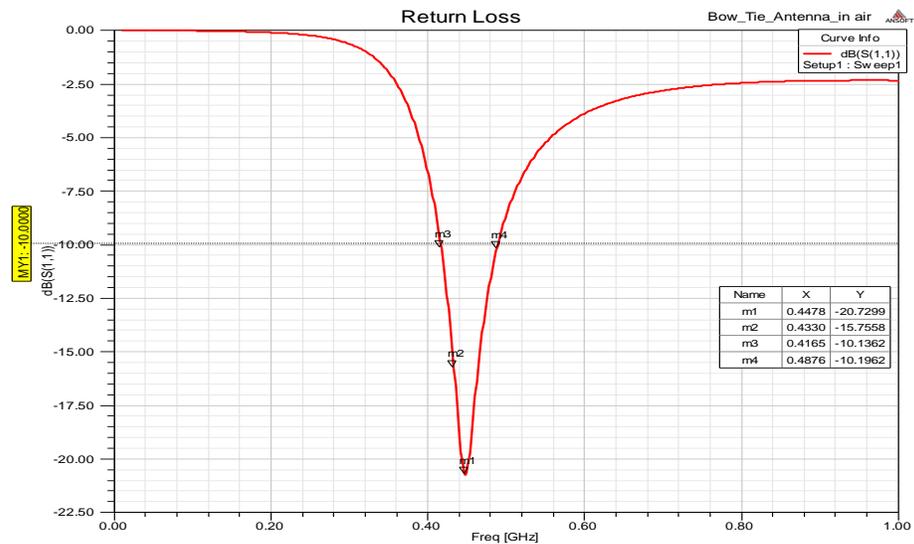
Figure 65 Return loss of the simulated 433MHz Bow-tie antenna in air

Ahmed Abdallah Abdou
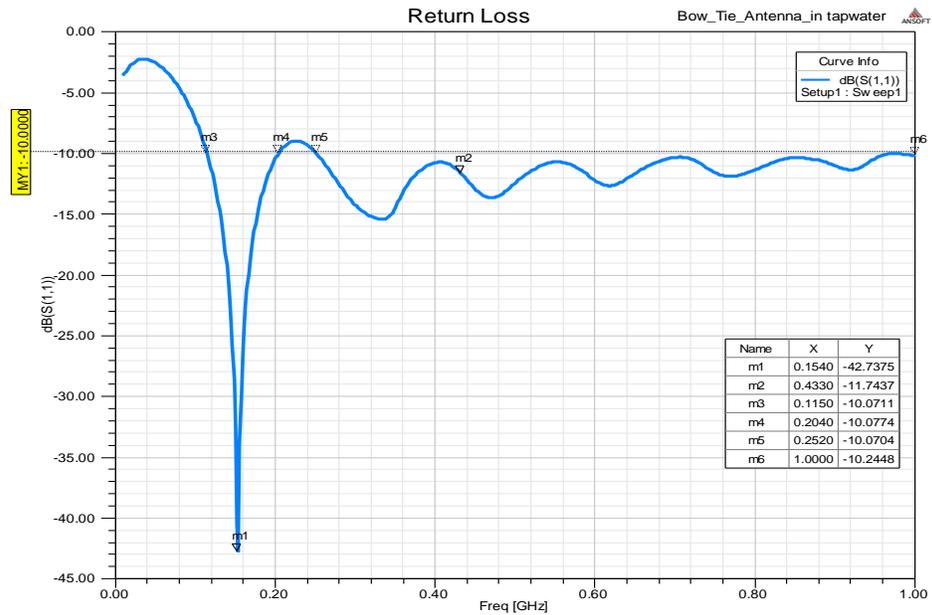
Figure 66 Return loss of the simulated 433MHz Bow-tie antenna in water

At first, the Bow-tie antenna is surrounded by air and the maximum power transfer occurs at 447MHz of frequency with a return loss of 20.7dB. At 433MHz, RL is 15.7dB as shown in Figure 65 . This value exceeds largely the aimed RL value of 10dB and is equivalent to 97% of energy transfer. The bandwidth of the antenna in air can be calculated as 71MHz. The bandwidth of the bowtie antenna is not as good as a biconical antenna and is limited by the truncation of the antenna as stated in [102]. However when the antenna is enclosed with water, the maximum power transfer occurs around 154MHz with a RL of 42dB and a bandwidth of 89MHz. More important, is the behaviour of that antenna from 252MHz up to 1GHz shown as a ripple region in Figure 66. In this region the antenna's bandwidth is very wide (748MHz) with at least 10dB RL. The 433MHz is included in this region and its RL is 11dBin water. This value exceeds the aimed RL value of 10dB and corresponds to 92% of power successfully transmitted.

132

Ahmed Abdallah Abdou
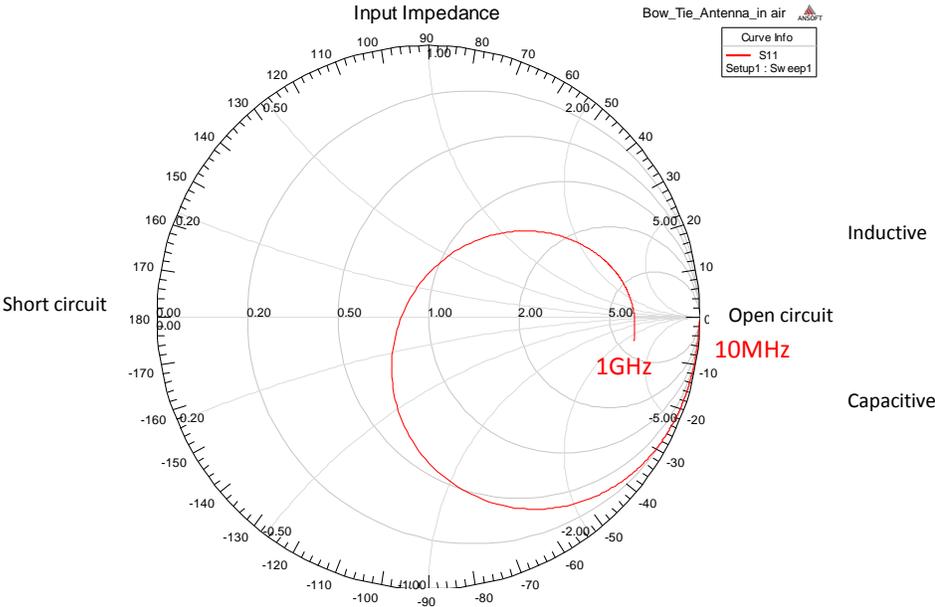
Figure 67 Smith Chart of the Input impedance for the simulated Bow-tie antenna in air
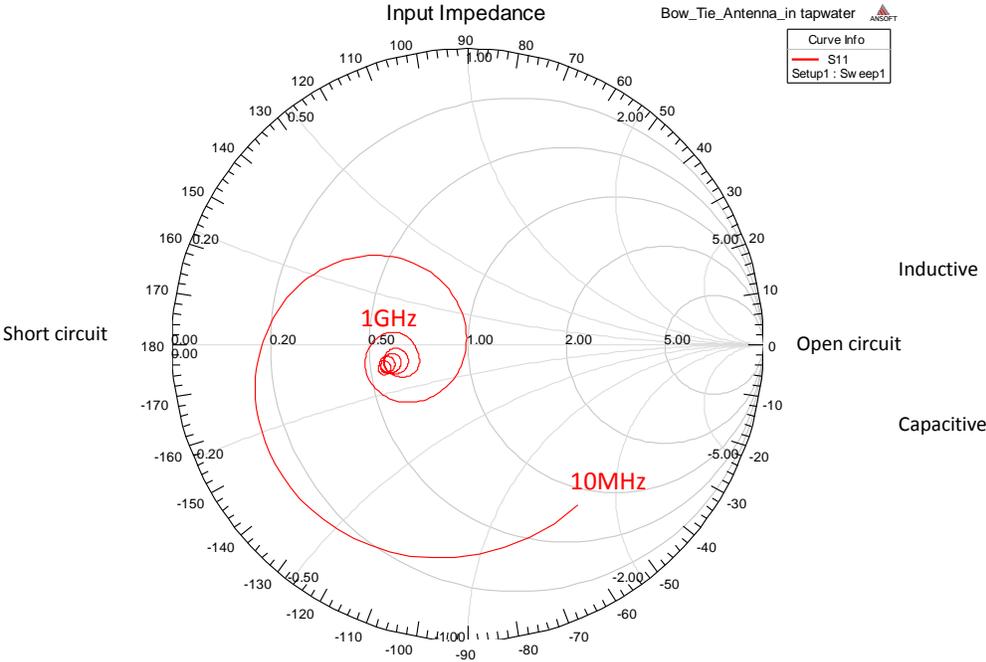
Figure 68 Smith Chart of the Input impedance for the simulated Bow-tie antenna in water

Ahmed Abdallah Abdou

In Figure 67, it can be seen that the line representing the input impedance of the modelled Bow-tie antenna in air starts for 10MHz frequency at where the resistive impedance is the highest. The antenna is acting as an open circuit (at 0). The line is situated in the lower half of the Smith chart and indicates that the antenna is capacitive. It then passes around the centre (near 1) for frequencies 400 to 500MHz where the antenna is resistive and better matched to radiate the most of its energy. The line finally finishes for frequencies above 500MHz towards the open circuit. Whereas in Figure 68, the input impedance line of the Bow-tie antenna in water starts at 10MHz, not as an open circuit, neither as a short circuit in the middle lower half of the chart which shows the capacitive behaviour. The line then goes to the upper half of the chart where it becomes inductive and then passes through the centre (at 1) around 150MHz for purely resistive behaviour where the antenna radiates most of its energy. Then for frequencies up to 1GHz the line rotates around a place not far from the centre to show that the antenna is behaving better in the remaining frequencies range.
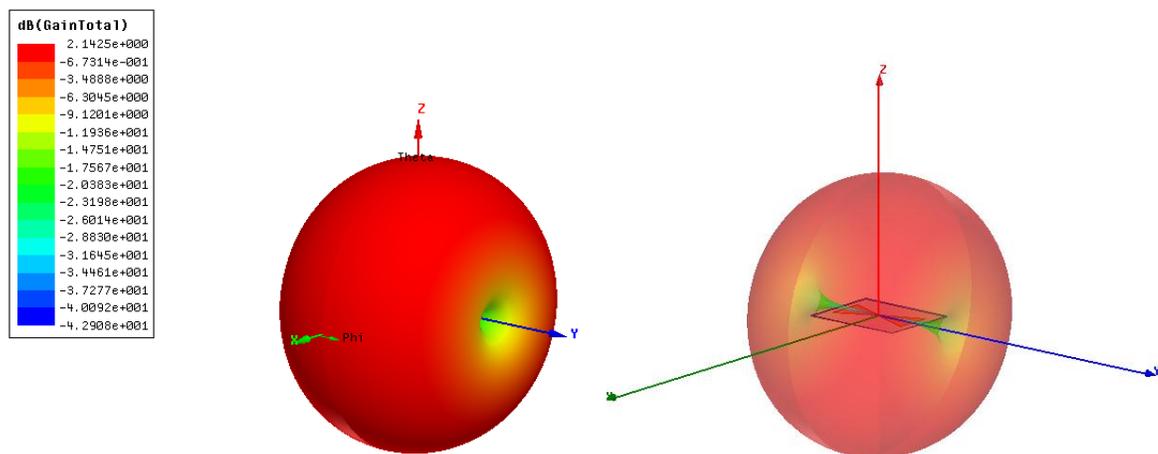
Figure 69 3D radiation pattern of the simulated Bow-tie antenna in air

Ahmed Abdallah Abdou
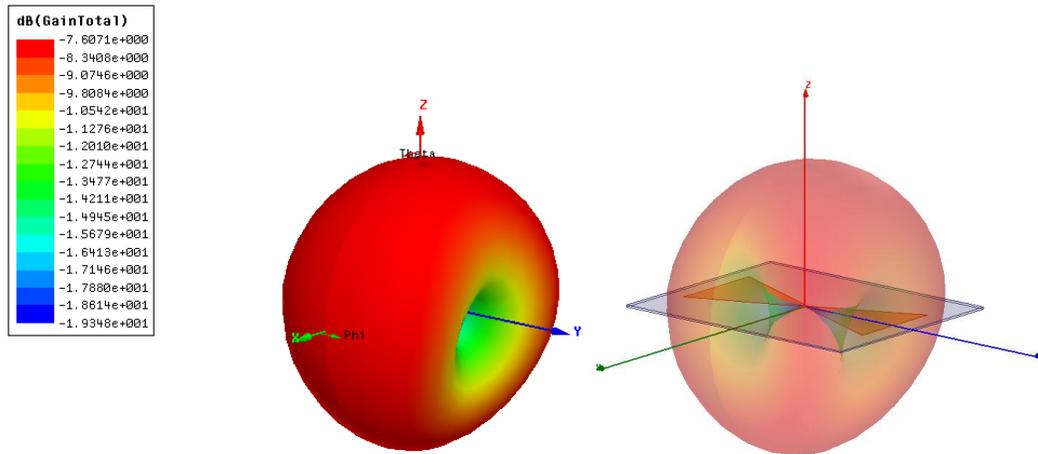
Figure 70 3D radiation pattern of the simulated Bow-tie antenna in water

In Figure 69, the far field radiation of the antenna in air is represented in a 3D graph. The radiation of the Bow-tie is a horn torus shape. The antenna radiates equally in all directions, it can be called an omnidirectional antenna except for the arms where there are nulls. Whereas in in water in Figure 70, the radiation pattern is smaller than for air, and has bigger nulls at the arms of the antenna.

Overall the simulation results in air and water envisaged the bow-tie antenna to be a good candidate for underwater wireless sensor networks.

5.4.   Construction of the antenna

To construct the Bow-tie antenna on a printed circuit board, two main steps have been followed. It consists of designing the antenna board on a specific software and then to etch the copper with a routing machine.

Ahmed Abdallah Abdou

5.4.1. EAGLE PCB design software

In the First step, a PCB design software EAGLE (Easily Applicable Graphical Layout Editor) is used. The package made by CadSoft consists of a schematics editor, a PCB editor and an auto-router module. This software is used to design an electronic schematic and lay out a printed circuit board (PCB). It comes with an extensive library of components, a library editor is also available to design new parts or modify existing ones. As there are no electrical schematics to design, only the PCB Layout editor is used to draw the copper traces of the antenna and the two holes for the connector as in Figure 71.
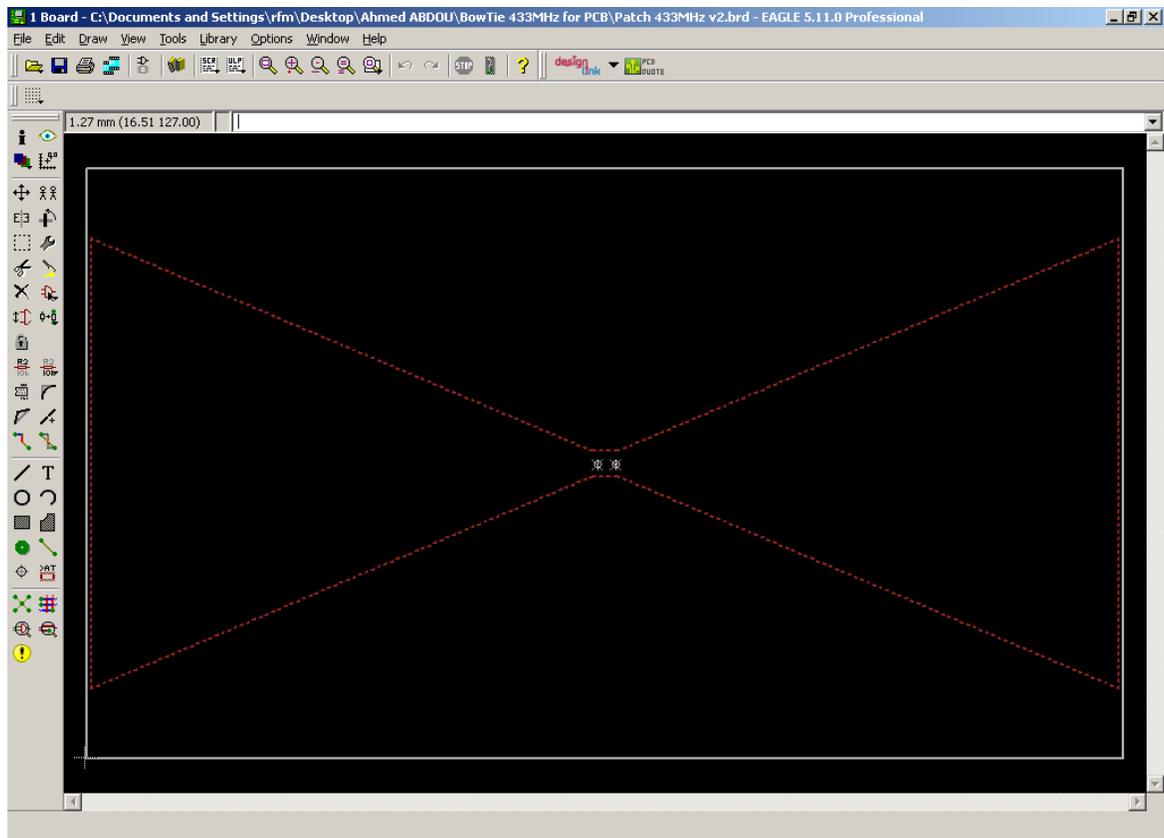
Figure 71 PCB layout of the Bow-tie antenna in EAGLE software

Ahmed Abdallah Abdou

5.4.2. CNC routing machine

The second step consists of loading the board layout drawn in EAGLE to produce the antenna board with the Computer Numerical Control routing machine Bungard CCD2 (Figure 72). To load the layout into the machine, it was necessary to convert the board layout to the Hewlett-Packard Graphical Language format by running the 'mil-outlines.ulp' in the Eagle software. However Eagle software was not able to open the HPGL file and software 'ABViewer7' was used as in Figure 73. Two files were produced to include the drilling and the routing. These files were then loaded consecutively in CCD-control software RoutePro 2000 (Figure 74) to produce the Bow-tie antenna on a single sided PCB as in Figure 75.
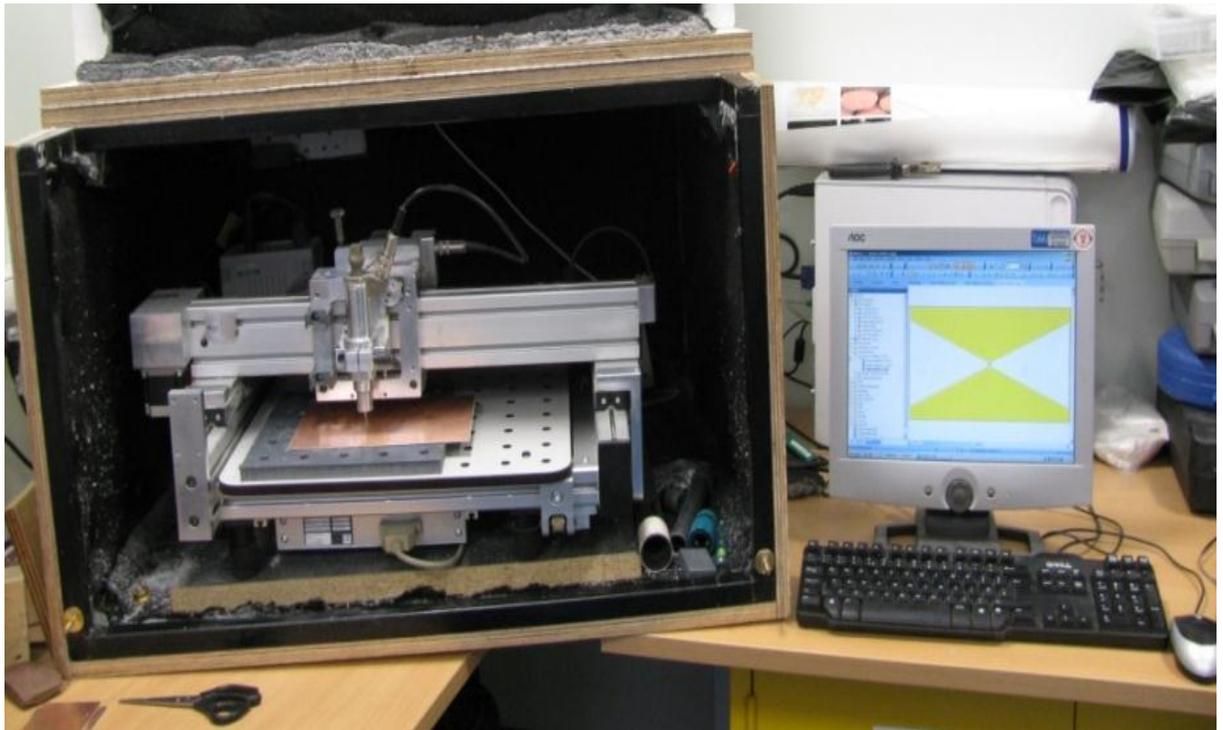
Figure 72 CNC Routing machine connected to a PC in the LJMU Sensors laboratory

Ahmed Abdallah Abdou
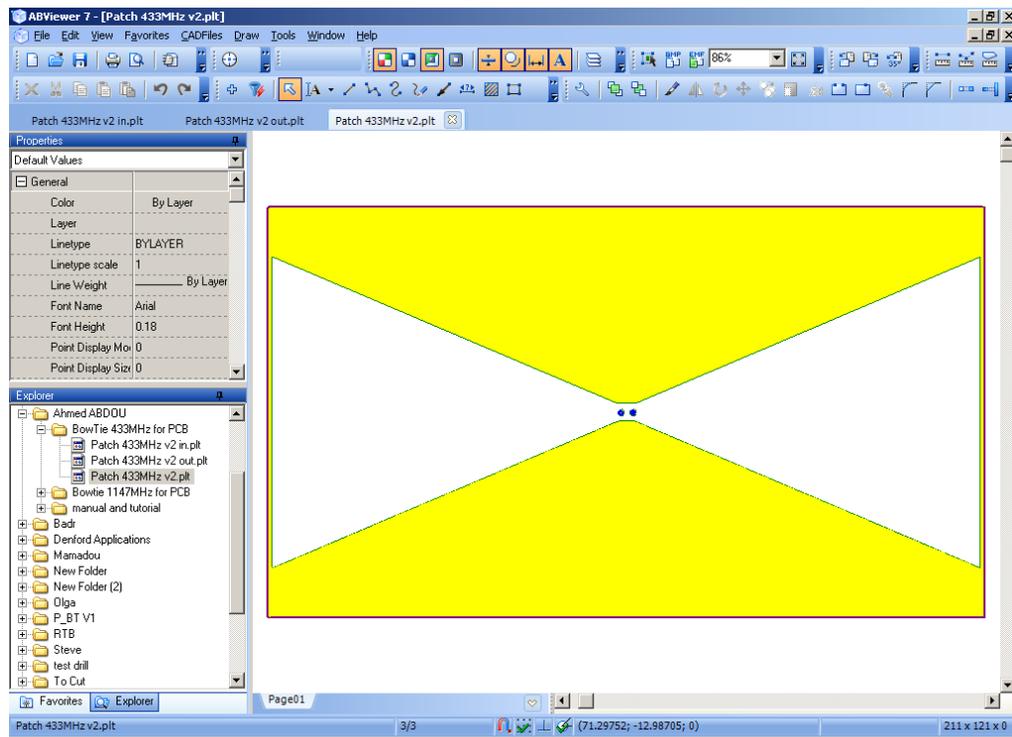
Figure 73 HPGL format of the Bow-tie antenna in ABViewer7 software
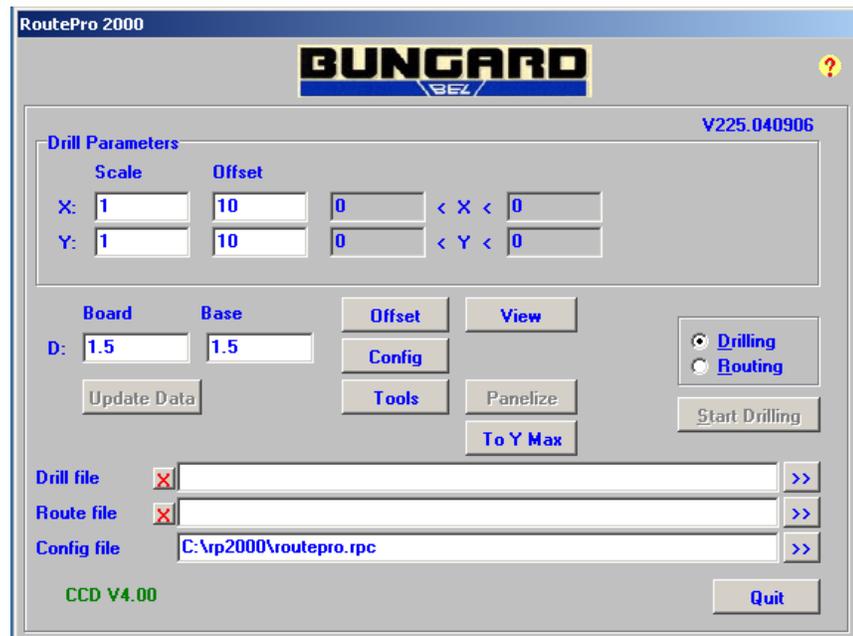
Figure 74 CCD-control software RoutePro 2000

Ahmed Abdallah Abdou
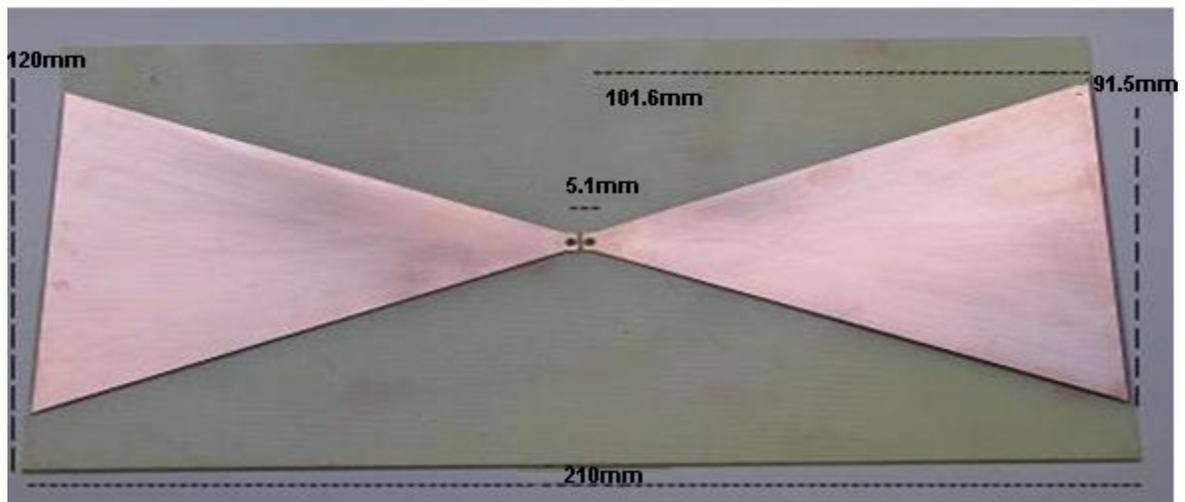
Figure 75 Angle view of the Bow-tie antenna fabricated with the CNC Routing machine

5.5. Waterproofing the PCB antenna for s11 tests

In order for the fabricated antenna to be tested underwater, the copper trace and the SMA connector have to be isolated from water. Therefore the copper on the front side of the antenna is fully covered with waterproof glue stick melted and poured carefully to form a 2mm waterproof layer. The cap of a 50ml polypropylene centrifuge tube is also holed and glued to the back side of the antenna so that its SMA connector can be joined to the RF cable. The bottom of the centrifuge tube is removed and the tube is passed through a hole made in the centre of an off-the shelf container lid. The RF cable is run through the container which an air tight 1.4 litre food container made from polypropylene and measuring 120×140mm. A watertight connector coupled with a 700mm long hose provided isolation of the RF cable from water into the container. The cable had an N type end. The setup is displayed in Figure 76.

Ahmed Abdallah Abdou
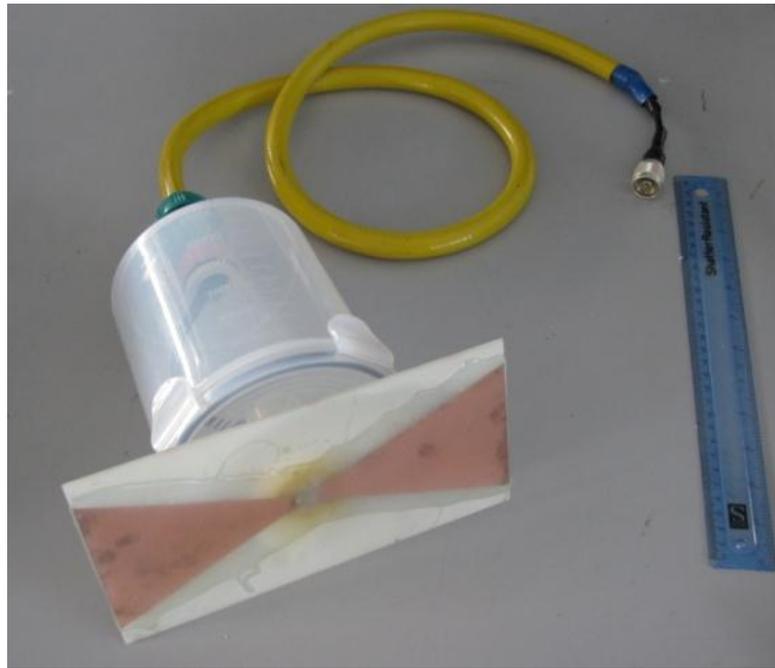
Figure 76 PCB Bow-tie antenna waterproofed with glue with its isolated RF cable

5.6. Experimental setup of bow-tie antenna's S11 in air and in water

The bow-tie antenna designed, constructed and waterproofed in the previous sections was tested in air and then tested in a plastic tank filled with 1200 litres of potable water with conductivity of 0.035S/m and temperature of 15°C. The fully waterproofed set is connected to a MS2024A Anritsu Network Analyser to collect S11 antenna parameters in air and in water as in Figure 77 for comparison. The position of the antenna is similar in both cases.

Ahmed Abdallah Abdou
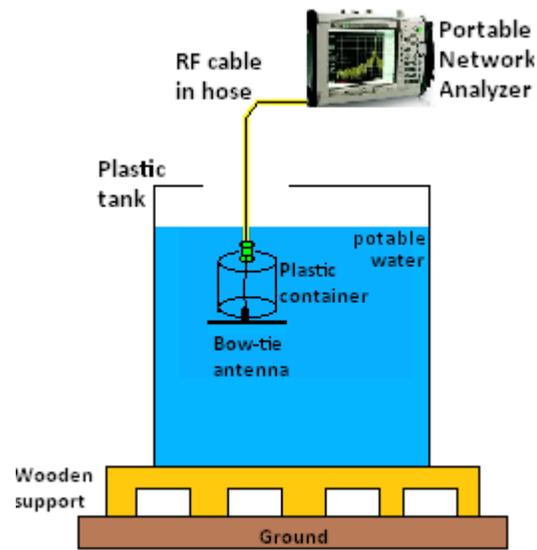
Figure 77 Experiment setup for S11 Return Loss in water

This experimental setup with the results obtained are published in [110].

5.7. Experiment results in air and in water for S11

The S11 data of the bow-tie antenna were collected during the experiments in air and in water and plotted respectively in Figure 78 and Figure 79. The graph in Figure 80 regroups all the S11 results for visual comparison.

141

Ahmed Abdallah Abdou
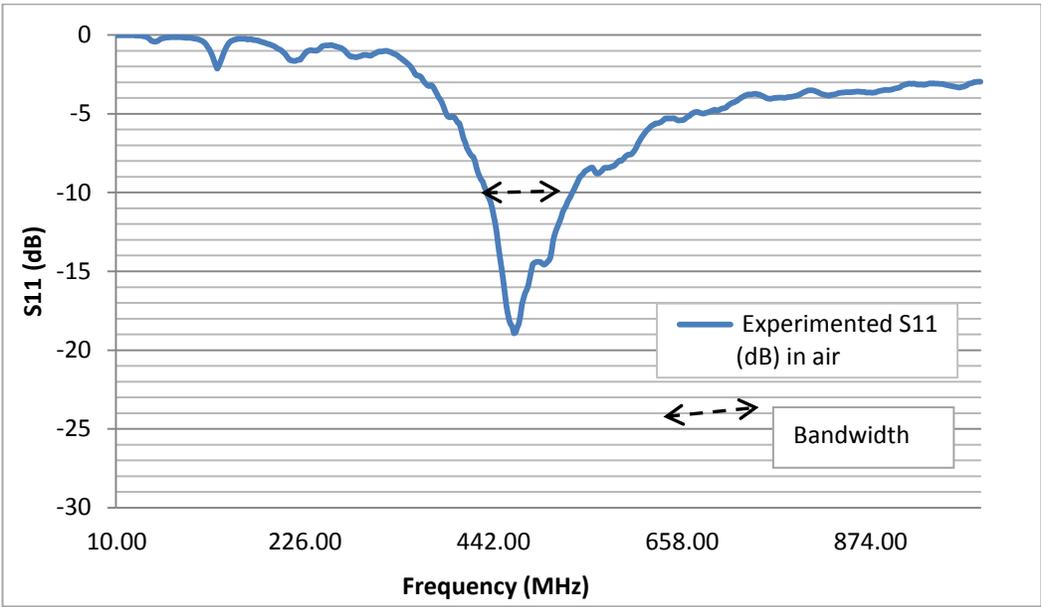
Figure 78 S11 Experimental results in air of the constructed Bow-tie antenna
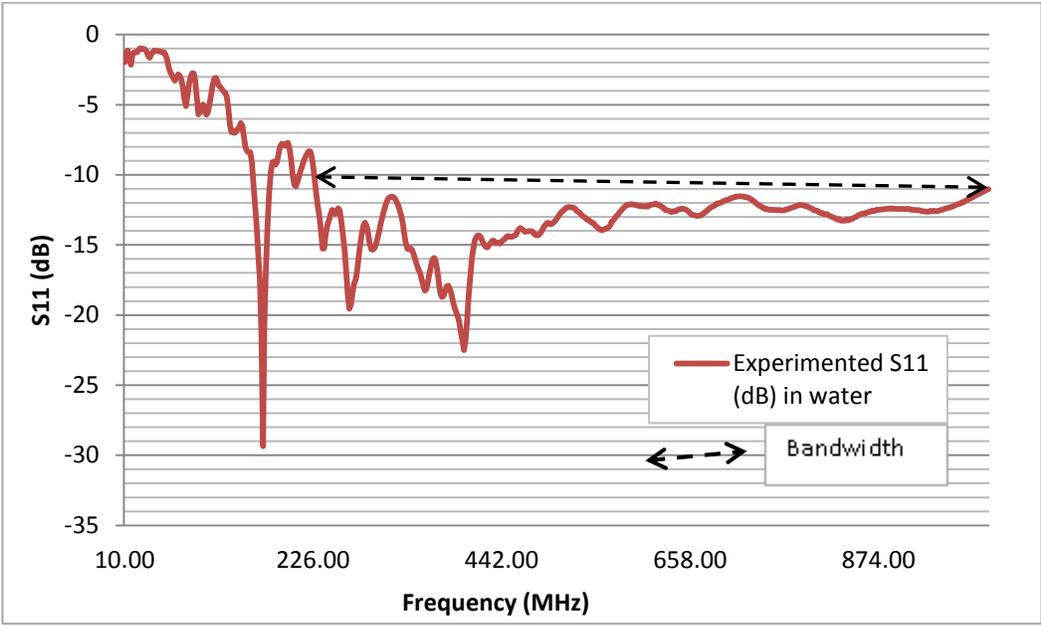
Figure 79 S11 Experimental results in water of the constructed Bow-tie antenna

Ahmed Abdallah Abdou
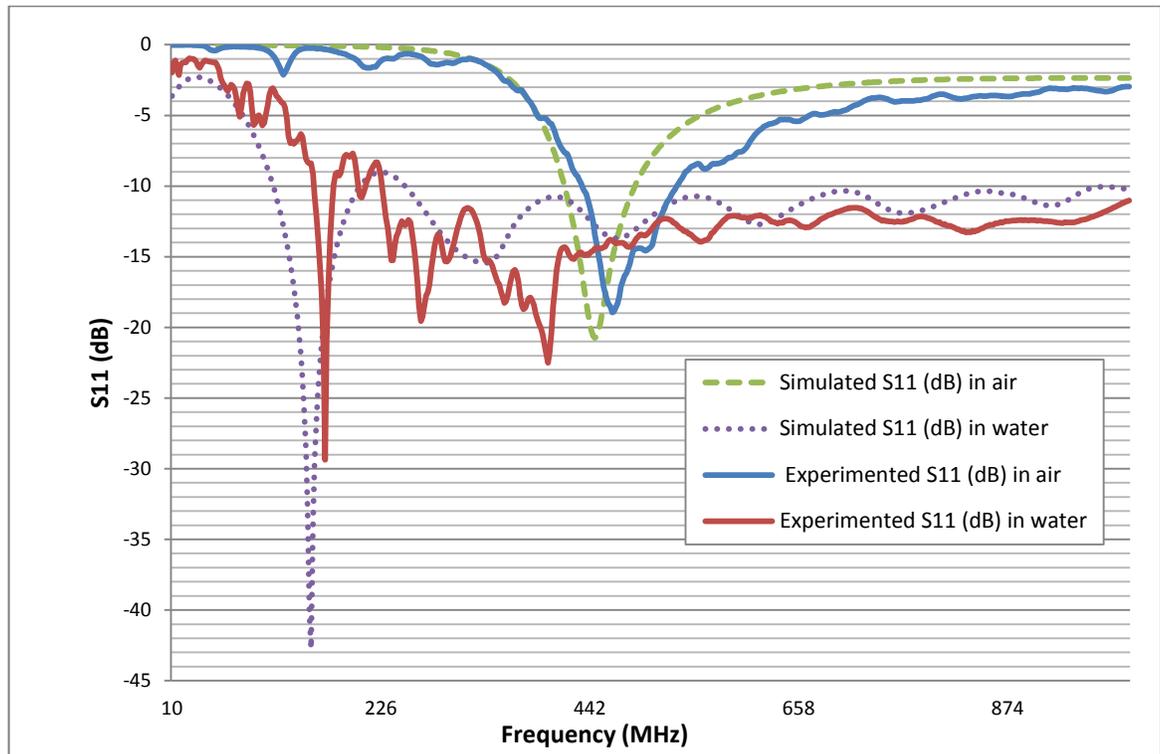
Figure 80 Simulated and experimented S11 (dB) of a bow-tie antenna in air and in water

5.8. Discussion

From Figure 80 experimental results in air with comparison to simulation results in air show a slight shift of 18MHz in the resonance frequency and a higher bandwidth of 20MHz as in Figure 78. The slight difference which is acceptable can be associated to many factors including the real life experiment and software simulations but also the layer of glue added on the constructed PCB antenna to waterproof it. However in the experiment at 433MHz the RL is 10dB and lies within the targeted RL for the antenna to be able to transmit more than 90% of its power. Overall the experimented curve follows the simulated one in air.

143

In Figure 80 experimental results in water, in comparison with simulation results in water show that there has been a slight shift of 14MHz in the resonance frequency with smaller amplitude. The bandwidth of this valley was only 18MHz which is 82MHz smaller than the simulated antenna in water. At 433MHz the RL is 15dB which allows the antenna to transfer more than 96% of its power. More importantly, is the behaviour of the antenna from 226MHz up to 1GHz shown as a ripple region in Figure 79. In this region the antenna becomes broadband with at least 12dB of RL. The experimental results follow the overall shape of the simulated curve and the ripple region shows the broadband aspect of the antenna. From Figure 80 the broadband aspect in water of the experimented curve is clearly situated under the simulated one giving more assurance that this important aspect can be maintained in the transition from simulation to the physical construction of the antenna. The Bow-tie antenna has shown from simulations and experiments that it is suitable for underwater communication.

5.9.   Further experimental investigation on the bow-tie antenna: the temperature change effects in water

5.9.1. Experiment setup

To experiment with the effects of temperature on the bow-tie antenna behaviour, a trial was set up as shown in Figure 81. It involved a network analyser taking S11 readings of the waterproofed antenna placed in a bucket of potable water (σ= 0.017 S/m at 15°C). The experiment was then repeated with water that was cooled to almost 0°C, and then again by water at 30°C.

Ahmed Abdallah Abdou
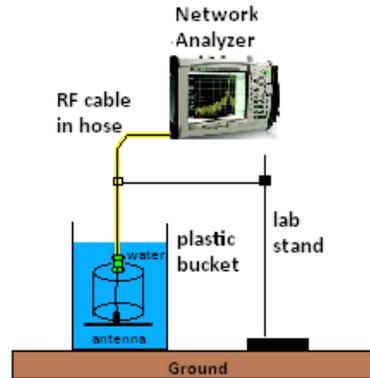
Figure 81 Experimental setup for temperature change effects on the antenna

5.9.2. Results and discussion

The S11 return loss data of the antenna at different temperatures in water are graphically represented in Figure 82 for comparison. The data of the antenna in air are also plotted for references in air.
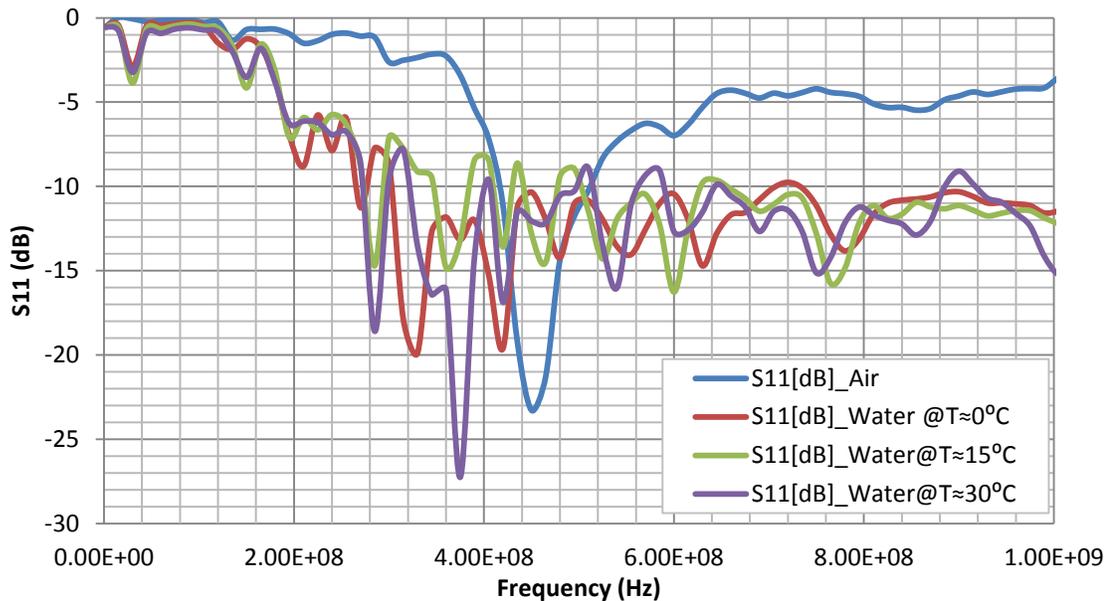
Figure 82 S11 return loss data of the antenna at different temperatures in water

Ahmed Abdallah Abdou

When the antenna is in air, because of the position of the antenna (facing the ground at 700mm distance) the resonance frequency is at 450MHz with a RL of 23dB. At 433MHz, it is 14dB.

In water at approximately 360MHz, the RL is approximately 10dB all the way to 1GHz giving a wideband bandwidth of 640MHz. This means that at any frequency within that region, a transmission of approximately 90% is achieved. However the increase of temperature does not result in a consistent change of the RL. In comparison with the air, there is no resonance frequency and therefore a temperature change can increase the communication distance or decrease it but only after reaching the distance achieved at 90% transmission.

Furthermore, the S11 reflected coefficient Γ real and imaginary data of the antenna at different temperatures in water are graphically represented in Figure 83 for the frequency range of interest lying in the 400-500MHz region only. The data from the antenna in air before the experiment and after the experiment are also plotted for reference. The 400-500MHz frequency ranges in different water temperature is close to the centre ($\Gamma=0$). Although after graphical reading on the Smith chart, the next step is to match for 50ohm impedance ($\Gamma =0$) but this is more appropriate for narrow band antenna at a given frequency. Maintaining a wide bandwidth to accommodate signal fluctuations in the water is a requirement as long as the antenna return loss is more than 10dB (90% of transmission).

Ahmed Abdallah Abdou
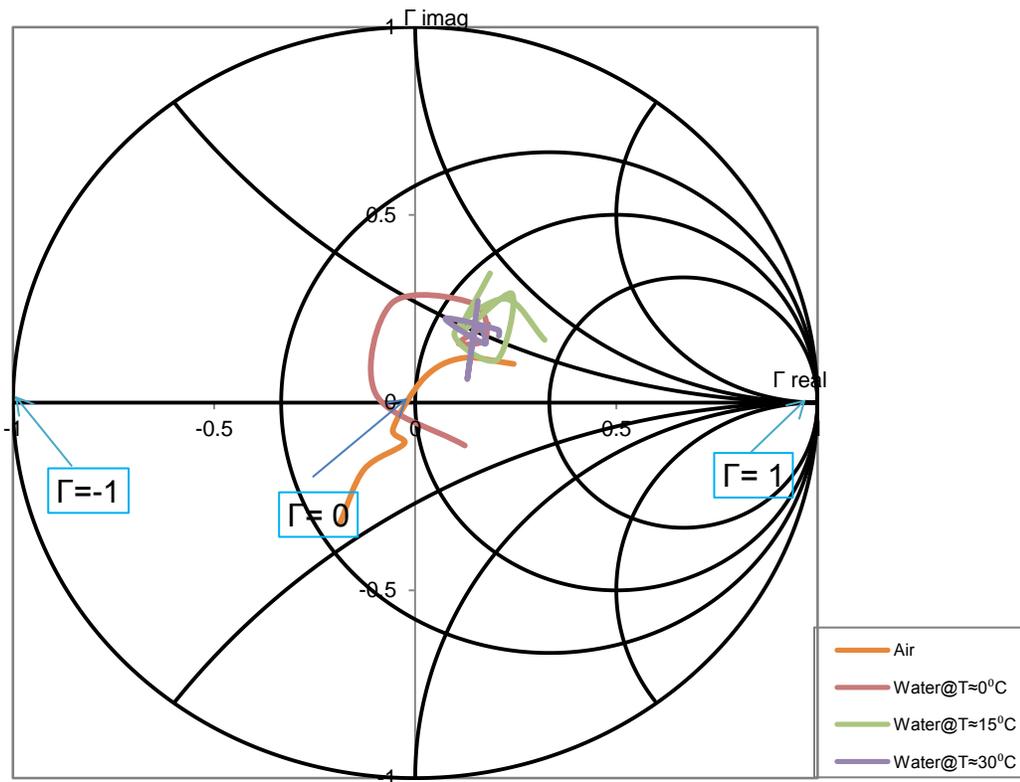
Figure 83 Smith chart of S11 reflected coefficient Γ real and imaginary data of the

antenna in water at different temperatures within the 400-500MHz region

The RL values at the 433MHz frequency of interest are graphically represented with the

change of temperature in Figure 84. The values are changing inconsistently with the increase

of the temperature which may be due to the fact that temperature and conductivity are

interdependent factors that affect attenuation of radio signals in water. Furthermore, the

difficulty in the experiment of not maintaining the fixed conductivity, due to the absence of a

special conductivity meter (without any automatic temperature compensation) may have

affected the results. However the worst scenario is at 15°C where the antenna RL is 9dB

147

Ahmed Abdallah Abdou

which corresponds to approximately 88% energy transmission. At other temperatures, there are at least 92%.
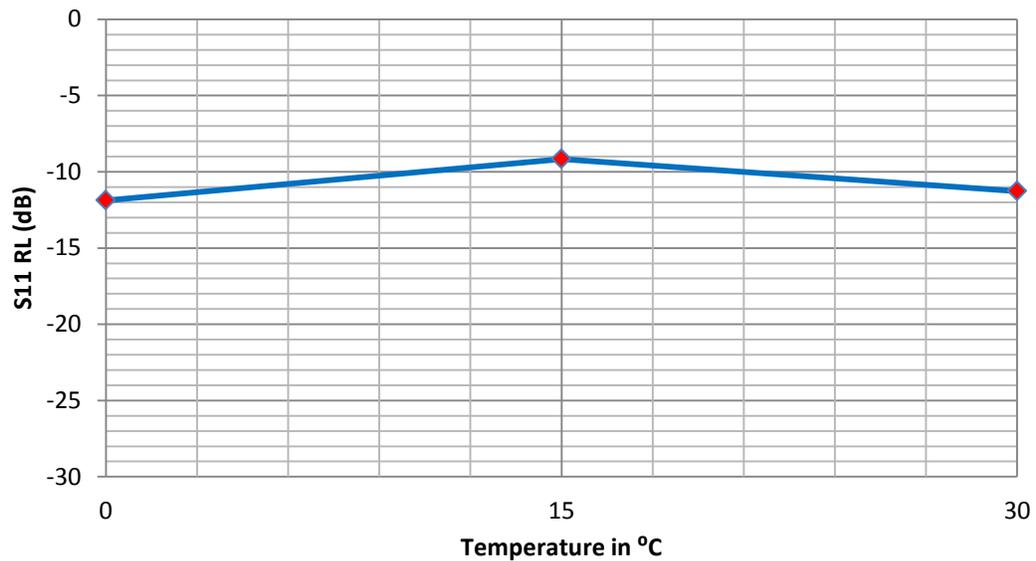
Figure 84 S11 return loss at 433MHz of the antenna at different temperatures in water

Narrowband antennas and traditional loop utilising matching circuit for a specific frequency in water can see their resonance frequency or amplitude shifting consistently with the increase of temperature but the experiment of the broadband bow-tie antenna in potable water have demonstrated immunity with the temperature change above the targeted RL of 10dB.

5.10.   Summary

With narrowband and traditional loop antennas suffering from impedance matching which results in signal losses in water, the bandwidth technique was proposed to accommodate the change in such a heavy dielectric medium. The planar version of finite biconical broadband antennas was investigated. The Bow-tie antenna was modelled to operate at 433MHz in air.

148

Although the simulation results in air shown a limited bandwidth, in water it showed an ultra-broadband behaviour. The antenna was successfully prototyped on PCB and waterproofed for underwater tests. The S11 results of the experiments demonstrated that the Bow-tie antenna that is designed and constructed for air could be used in water without any matching circuit. Further experiments have shown its immunity towards temperature change in water.

Ahmed Abdallah Abdou

Chapter 6. Wireless transmitter

6.1. Introduction

Most of underwater RF experiments in the literature review [111] utilise on the transmitting side a signal generator to create the signal to the antenna through a RG58 RF cable. Trials with this type of setup have shown in chapter 4 that the RF cable acts as an antenna and consequently may result in erroneous data received from crosstalk. In this chapter, a transmitter that generates a carrier signal at 433MHz is built from an electronic circuit and is powered by battery. It is then waterproofed for complete submersion in the laboratory tank for underwater tests with no RF cable floating in air/water to eliminate airborne transmission.

6.2. Electronics

In order to generate a carrier signal, a voltage control oscillator (VCO) was used. This is an electronic oscillator whose oscillation is controlled by an input voltage. A coaxial ZX95-535-S+ VCO that covers the 433MHz ISM frequency was acquired from Minicircuits. To experiment on the creation of the carrier in the laboratory a Tektronix PS280 DC Power Supply was used to provide power to the VCO and a Hameg HMS 3000 Spectrum Analyser was used to monitor the signal produced by the VCO. A fixed 12V input was supplied on the V_{cc} port of the VCO and a variable voltage was applied on the V_{Tune} port to oscillate at different frequencies. From the datasheet available in [112], a voltage of approximately 9V gives a frequency of 426.3MHz. Tuning the voltage to 9.5V created a carrier signal at 433MHz with a power output of +6dBm as visible on the spectrum in Figure 85.
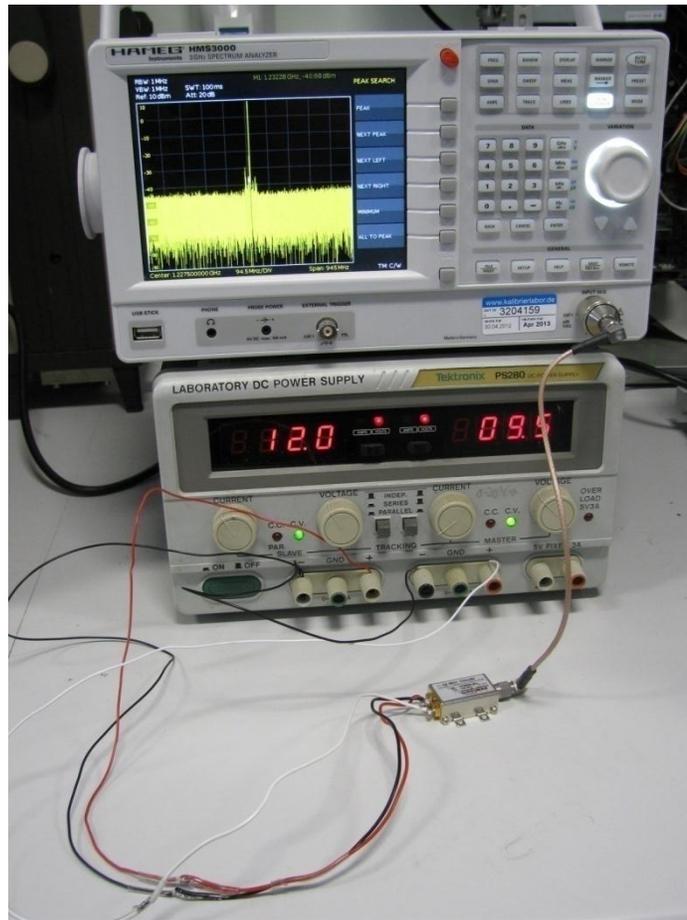
Figure 85 Carrier signal creation using DC power supply

To design a wireless transmitter the fixed part of the power supply is substituted with batteries and the variable part with a potentiometer. A Voltage Regulator is used to step down the voltage from the batteries. The Block diagram in Figure 86 illustrates the design of the transmitter's carrier generator.

151

Antenna

RF OUT

Voltage Controlled Oscillator

ZX95-535-S+

V tune

V In

Ground

Potentiometer

Voltage Regulator

Output

Input

Ground
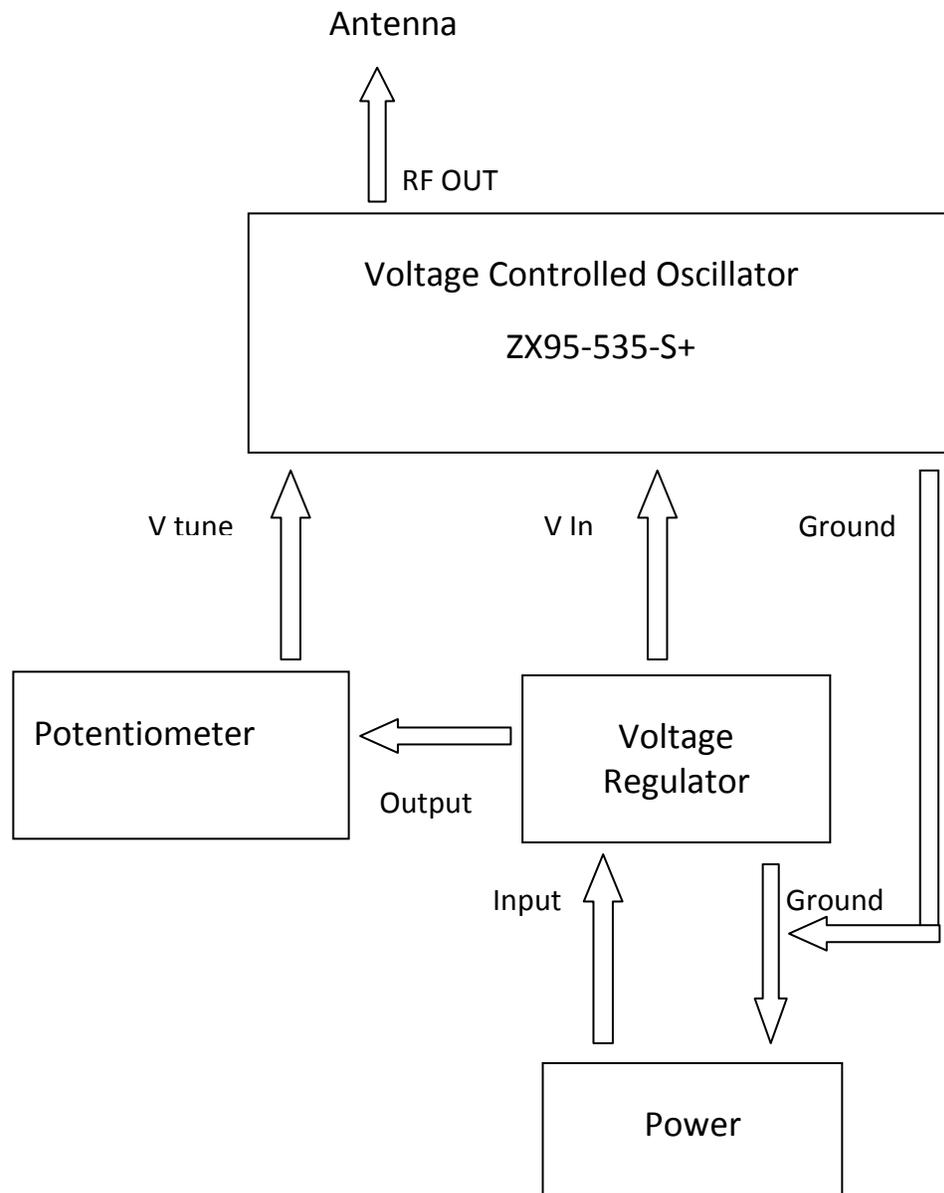
Power

Figure 86 Block diagram of the transmitter's carrier generator

The VCO runs on 12V fixed therefore a Voltage Regulator is needed to adjust the excess of voltage from the batteries. To supply enough power to the L7812 Voltage Regulator requiring 19V as in the datasheet available in [113], 16 AA 1.5V Energizer batteries are connected in

Ahmed Abdallah Abdou

series to deliver 24V. Two battery holders taking 8 batteries each were used to accommodate the 16 batteries that have a service time of approximately 65 hours as explained in the datasheet available in [114]. The 10kΩ potentiometer available in [115] is tuned to 9.5V to output a 433MHz carrier signal ready to be transmitted via an antenna. A jumper is added to the circuit for connecting the power on and off. The heat sink provides cooling to the voltage regulator. The setup is attached to a piece of hard bound board. Wooden legs were made so the batteries sit at the back. The setup weighing 525gram and measuring 100×100mm was designed to fit in a plastic container measuring 120×140mm. Figure 87 shows the battery powered transmitter's carrier generator.
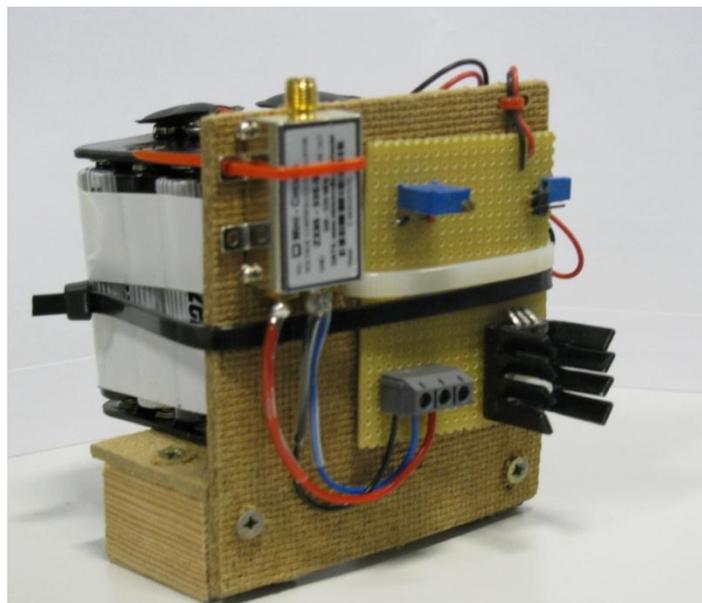
Figure 87 Battery powered transmitter's carrier generator set

153

The device was then connected to the spectrum analyser through an RG316 RF cable with SMA connectors on both ends, to test the carrier signal. Figure 88 shows the battery powered set generating the 433MHz carrier signal at +6dBm power output on the spectrum analyser.
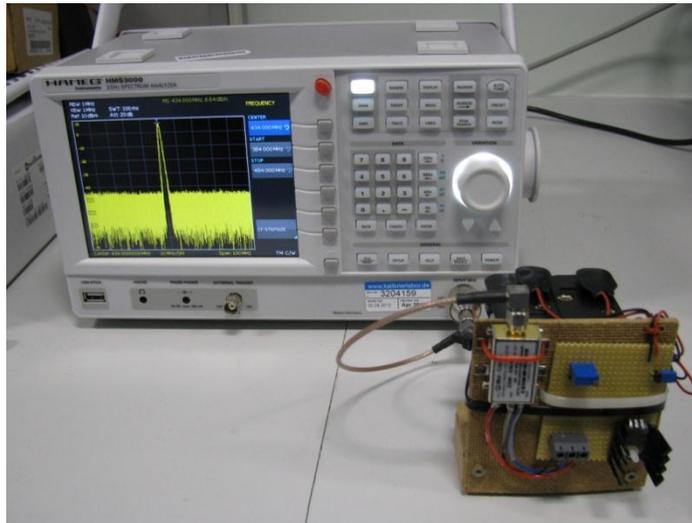
Figure 88 433MHz carrier signal test on spectrum analyser

6.3. Waterproofing the wireless transmitter

An off-the shelf, air tight 1.4litre polypropylene food container measuring 120×140mm was used to fit the 100×100mm electronics set. The lid of the plastic container was modified to run the RF cable. The bottom of a 50ml polypropylene centrifuge tube was removed and the tube is passed through a hole made in the centre of the container's lid and then glued by melting waterproof plastic glue stick. The cap of the centrifuge tube was also holed and glued to the back side of the antenna so that its SMA connector could be joined to the RF cable as in Figure 89. The front side of the antenna was fully covered with glue to make it waterproof. The antenna cap was closed on the tube, and the lid was clipped with the container comprising

154

the electronics set. This whole unit was pushed into another container with a weight for ballast as shown in Figure 90.

Figure 89 Opened up polypropylene waterproof set
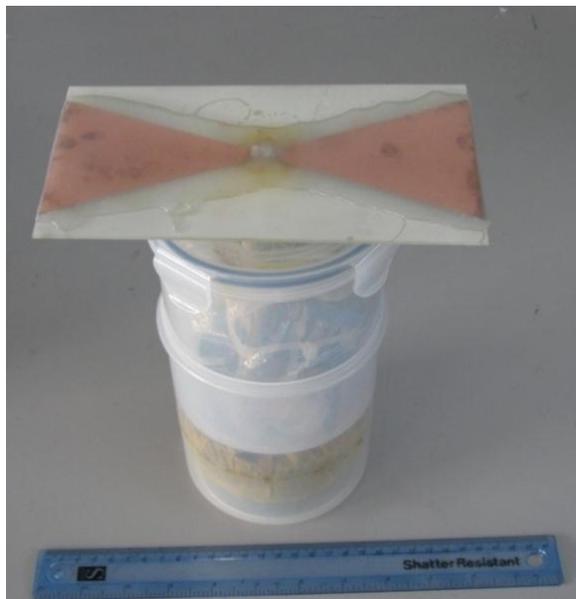
Figure 90 Closed up polypropylene waterproof set

Ahmed Abdallah Abdou

6.4. Experimental setup for S21 with off-the-shelve PP containers in laboratory

6.4.1. Transmission in air and in water at vertical separation

In order to experiment on the transmission of the carrier signal in air, a setup was prepared taking into account that the following experiment will be in the tank with water. In air the setup comprises the wireless transmitter positioned on a wooden chair at the same level as the bottom of the tank. The carrier signal is generated and transmitted through the antenna. On the receiver side a vertically moveable waterproofed bow-tie and plastic container were connected to a Hewlett Packard 8594E Spectrum Analyser through an RG58 cable in the hose, supported by a PVC tube. The receiver was positioned vertically above the transmitter with both sides' antennas facing each other. Then the receiver was moved upward with the PVC tube at an increment of 10mm to record the signal strength on the spectrum analyser (Figure 91). A temperature of 13.8℃ ±0.5 was recorded.

Figure 91 Experimental setup for S21 transmission in air

Ahmed Abdallah Abdou

The wireless transmitter containing the electronics was lowered into the tank. The PVC tube which the receiver and its antenna are attached to, was pushed down to align with the wireless transmitter's antenna. Then the tube was pulled at an increment of 10mm to move the receiver away the transmitter and record the signal strength on the spectrum analyser as shown in Figure 92. In water, the temperature was 14.7˚C ±0.5 and the conductivity was 0.035 S/m.
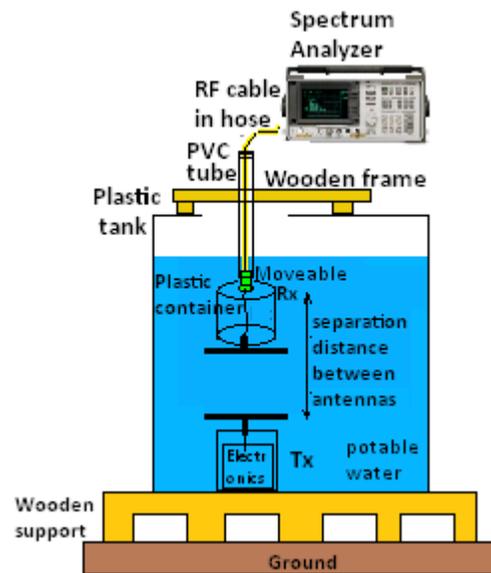
Figure 92 Experimental setup for S21 transmission in water

6.4.2. Radiation pattern in air and in water at vertical separation

The setup for the radiation pattern in air is the same as the transmission in air (Figure 91) but while in the previous setup the receiver is moved upward with the PVC tube, the receiver and the transmitter are instead fixed at a 100mm separation distance within the near field. Only the receiver tube is rotated to make the antenna turn at angles with increments of 10˚. The

157

experiment is repeated for a far field radiation pattern at a 500mm separation distance. The temperature was 13.8˚C ±0.5.

The setup for the radiation pattern in water was the same as the transmission in water (Figure 92) but while in the previous setup the receiver was moved upward with the PVC tube, the receiver and the transmitter were now fixed at a 100mm separation distance within the near field in water. Only the receiver tube was rotated to make the antenna turn at angles with increments of 10degrees. The experiment was repeated for a far field radiation pattern at a 500mm separation distance. The water temperature was 14.7˚C ±0.5 and the conductivity was 0.035 S/m.

6.4.3. Radiation pattern in water at horizontal separation

To collect signal strength data for the radiation patterns in water, while they are horizontally separated, the setup in Figure 93 was used. The receiver was connected to the Hewlett Packard 8594E spectrum analyser through the RF cable (in hose) and was kept at a fixed separation distance of 500mm. Readings were collected from the receiver while the wireless transmitter was rotated at angle increments of 10˚ up to 360˚. The experiment was repeated as the horizontal separation distance was increased to 1000mm.

Ahmed Abdallah Abdou
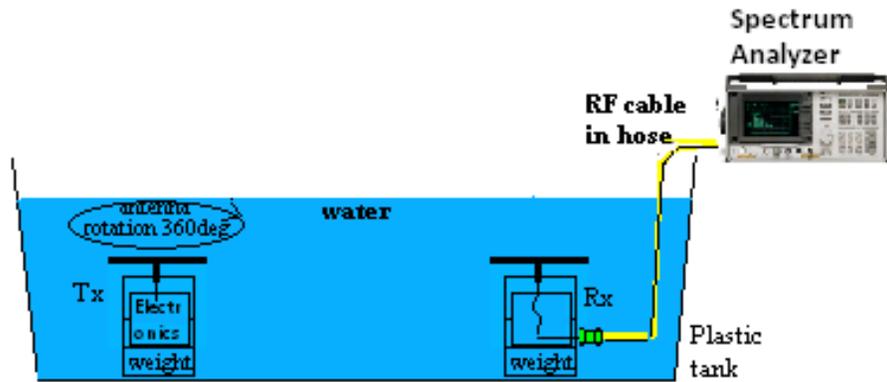
Figure 93 Experimental setup for radiation pattern at horizontal separation

6.5. Results for a S21 experiment with off-the-shelve PP containers in laboratory

6.5.1. Transmission at vertical separation distances in air and in water

Figure 94 displays signal strength (S21) experiment for the bow-tie antennas in air and in water in the tank over a distance of 450mm. The graph shows that in air the antenna signal strength dropped by 10dB over a separation distance of 450mm. However it seems that this is the maximum loss the antenna will suffer from in air. In water, at 10mm the signal loses 10dB compared to the air environment. This value added to the power of the VCO (6dB at 433MHz) is in agreement with the theoretical attenuation value of 16.6dB in Table 3. Two regions can be distinguished, the near-field region up to 300mm separation distance, and a far-field region onwards. The near field region includes the region where the signal drops more quickly. In the far field, the signal is around -40dB, and the signal amplitude drops at a lower rate.

Ahmed Abdallah Abdou
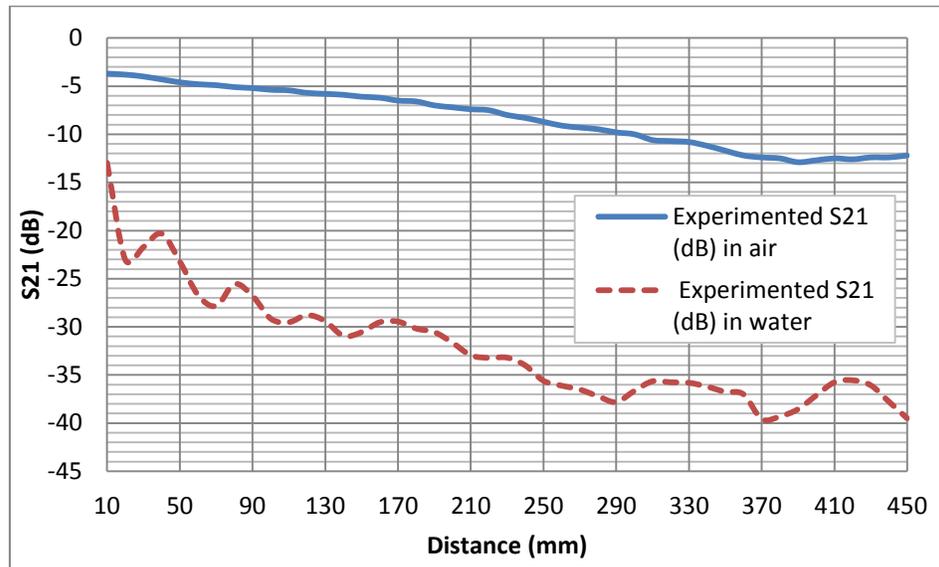
Figure 94 Comparison of bowtie antenna's signal strength (S21) experimented in air and in water over distance up to 450mm

6.5.2. Radiation pattern in air and in water at vertical separation

Figure 95 illustrates the radiation pattern of the bowtie antennas on a 360° plane, separated by 100mm, both in air and water. It can be seen that the highest signal occurred when the two antennas were 0° and 180° in line and the lowest signal, were at 90° and 270°. In water at 100mm separation distance, the overall shape is the same as in air but with a smaller signal and a small variation at the 90° angle.

Ahmed Abdallah Abdou
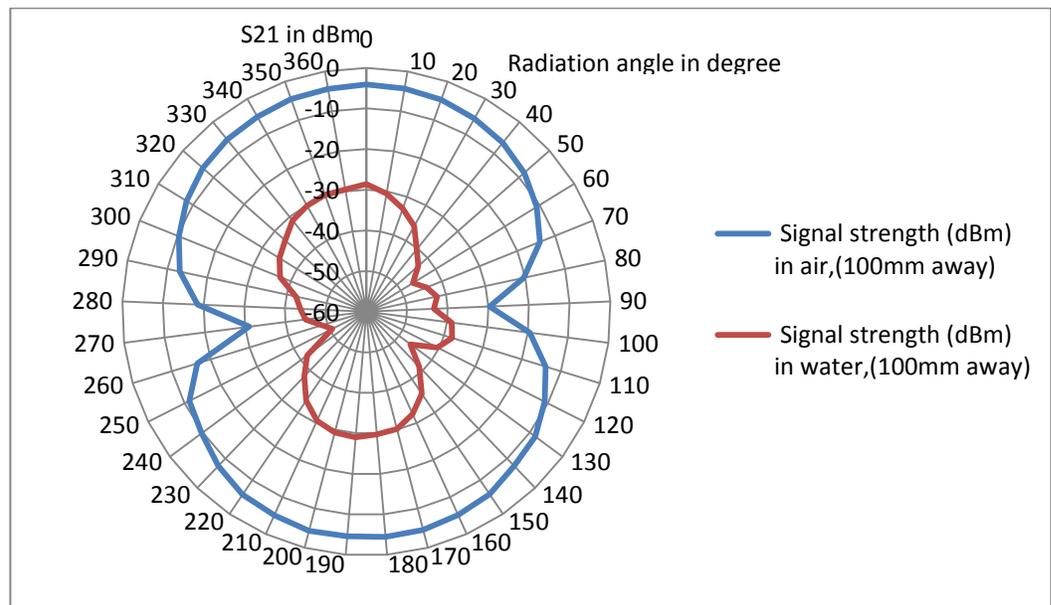
Figure 95 Comparison of bowtie antenna's signal strength radiation pattern (S21) over

radiation angles in air and in water at a vertical separation of 100mm

In Figure 96 the bowtie antennas were separated by 500mm vertically. The highest signals in air and in water still occurred at 0° and 180° with the lowest at 90° and 270°. In water the overall shape is the same with a smaller signal and an additional variation at 330°.

Ahmed Abdallah Abdou
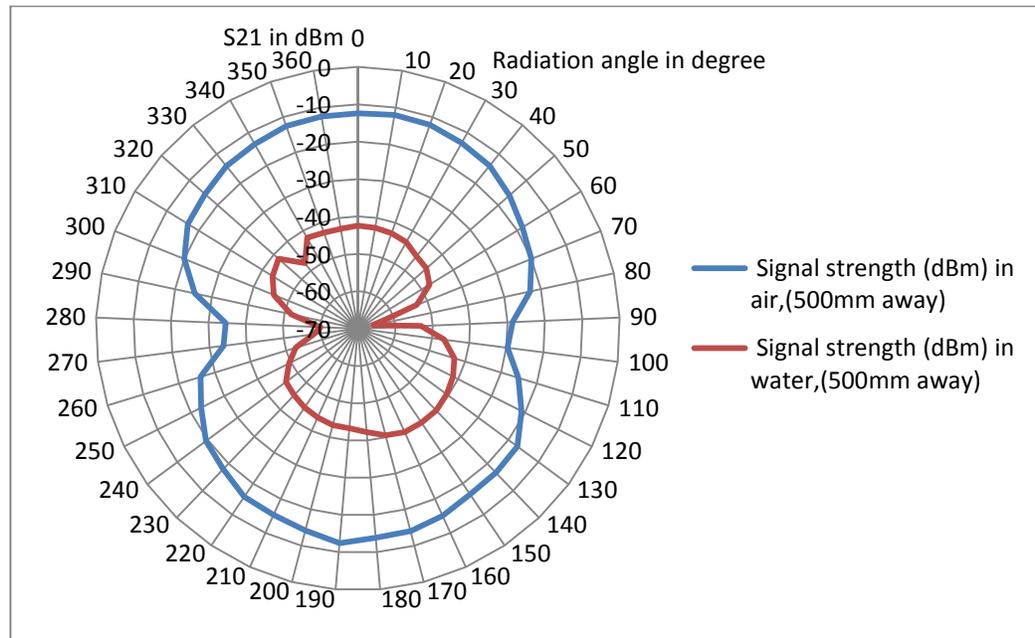
Figure 96 Comparison of bowtie antenna's signal strength radiation (S21) over radiation

angles in air and in water at a vertical separation of 500mm

At both separation distances, the signal strength of the bowtie antennas in water reduced because of the attenuation due to water. The small variations could be associated with reflections or errors. Also when the antennas were vertically separated, the radiation pattern in air was the same as in water.

6.5.3. Radiation pattern in water at horizontal separation

In Figure 97 the bowtie antennas were separated by 500mm then 1000mm horizontally in water over a radiation plane of 360˚. At a 500mm separation, the highest signals in water still occurred at 0˚ and 180˚ with the lowest at 90˚ and 270˚. At 1000mm the overall shape was the same with a smaller signal due to higher attenuation increased with distance and some

162

Ahmed Abdallah Abdou

variations at 330˚ may be associated with reflections or errors. However, the bowtie antennas

performed better in the water tank at horizontal separation when they were at 0˚ and 180˚.
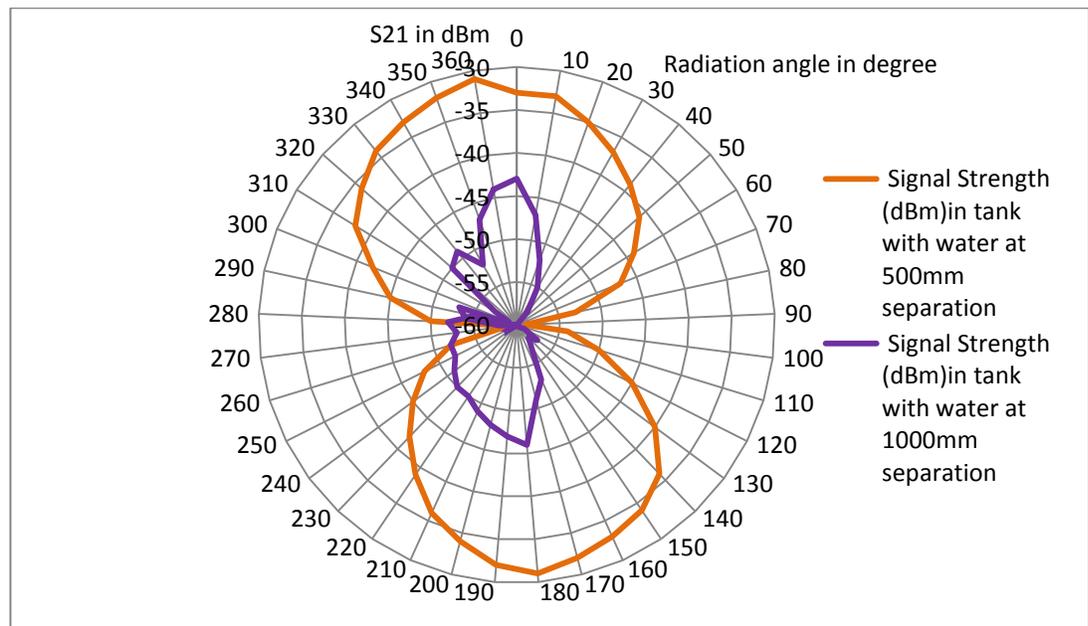
Figure 97 Comparison of bowtie antenna's signal strength radiation (S21) over radiation

angles in water at horizontal separation of 500mm and 1000mm

6.5.4. Comparing bowtie radiation pattern in water at vertical and horizontal separation

Figure 98 displays the radiation pattern on a 360˚ plane of the bowtie antennas in water at

vertical and horizontal separation of 500mm.The overall shapes are similar and in both cases

the antennas perform better at 0˚ and 180 ˚. The slight changes are related to the fact that the

dimensions of the tanks and the volume of water where vertical and horizontal tests have been

performed are not identical.

Ahmed Abdallah Abdou
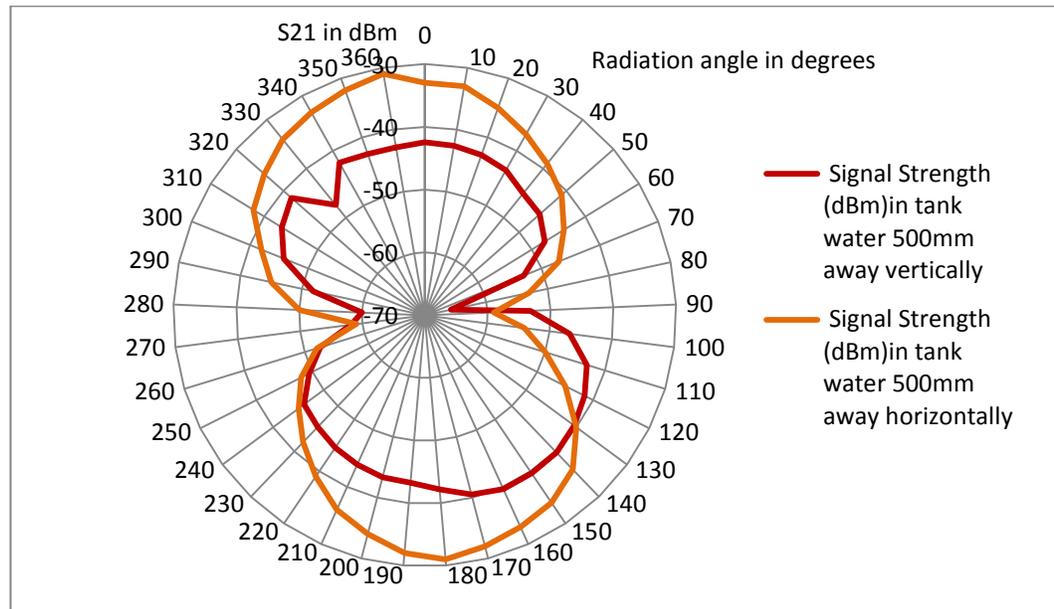
Figure 98 Comparison of bowtie antenna's signal strength radiation (S21) over radiation

angles in water at horizontal and vertical separation of 500mm

From the radiation pattern experiments, the maximum performance can be achieved when the

bow-tie antennas at 0˚ and 180˚. This performance is achieved in cases where the antennas'

separation is vertical (antenna facing each other) as shown in Figure 92 but also horizontal

(antennas symmetric) as shown in Figure 93.

Whether in air or in the water tank the same overall shape of the radiation pattern is repeated

in contrast with the loop antennas that give a maximum signal when at water. Therefore the

positioning of the antennas can be done in air and changes in water should not be expected.

6.6. Summary

To eliminate RF crosstalk, a battery powered wireless transmitter that generated a carrier signal at 433MHz was designed and prototyped. The set was waterproofed to run the S21 experiments. The carrier signal was transmitted and received wirelessly with success in tank with water up to a half metre separation distance. The far field result suggested that a detectable signal could be successfully received at much larger separation distances. The radiation pattern experiments confirmed that the same positioning of the bow-tie antennas in air can be maintained in water.

Ahmed Abdallah Abdou

Chapter 7. Real world tests in Liverpool Stanley canal

7.1. Introduction

In the previous chapter, wireless communication in the 433MHz ISM band between a battery powered transmitter and a receiver was successful in a tank full of potable water up to half metre distance. Distances were limited by the tank size. This chapter describes how the transceivers are now submerged in the Liverpool Stanley canal for maximum communication range. Experiments to collect S11 and S21 data were carried out.

7.2. Design and prototyping of a waterproof PVC enclosure

7.2.1. Transmitter's enclosure

For the transceivers to be submerged in open water, robust enclosures were designed. The transmitter's enclosure is shown in Figure 99. The container is mainly fabricated from polyvinyl chloride (PVC) to minimize reflections and the chance of the container acting as a cavity with comparison to stainless steel.

Stainless steel top support

Circular PVC top

Rubber sheet

PMMA antenna cover

Rubber sheet

PCB Bowtie antenna

PVC cover (antenna seat and cylinder cover)

O ring

Stainless steel support

PVC cylinder house of transceiver electronics

O ring

PVC cylinder bottom cover
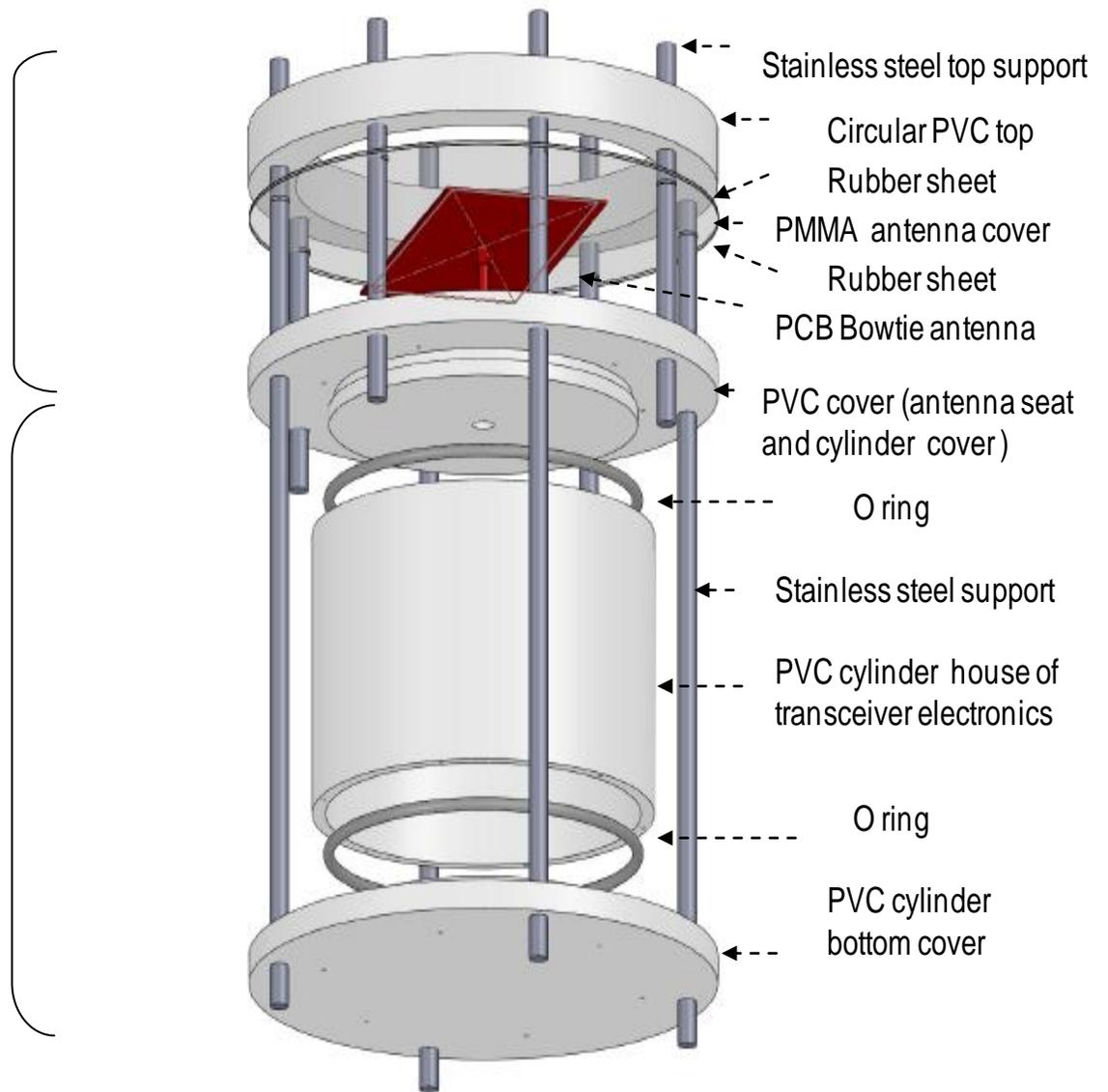
Figure 99 Exploded view of transmitter's enclosure designed in SolidWorks

7.2.1.1.   The top part of the enclosure

The top part involves the waterproofing of the antenna and the top sealing of the enclosure. The fact that the connectors are SMA type makes it susceptible to split especially considering that the transmitter is expected to be tested in a non-static environment (water). For the antenna to be in a fixed position, a thin layer of the plastic is removed in order to make it sit. This cover as shown in Figure 100 was used to protect and support the antenna but also to seal the cylinder of the enclosure. On the exploded view it is called PVC cover (antenna seat and cylinder cover)
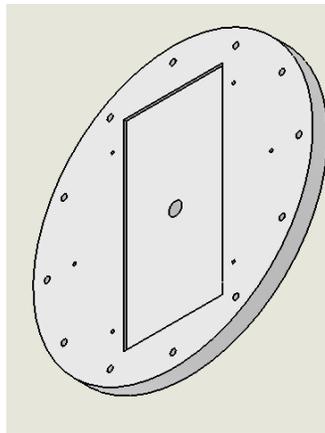
Figure 100 PVC cover

The polymethyl methacrylate (PMMA) part protects the top part of the antenna from water and is sealed to the PVC cover with a gasket and jointing compound. Figure 101 shows the PMMA antenna cover. The dielectric properties of this transparent material cause a small shift in the resonant frequency in air, however in water this shift is not visible as it happens under the target RL of 10dB because of the broadband behaviour of the bowtie antenna.

Ahmed Abdallah Abdou
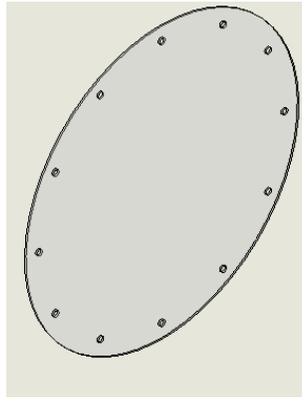
Figure 101 PMMA

A thin layer of rubber gasket covered in non-setting gasket jointing compound by Hylomar provided a water tight seal. 8 Stainless steel bars 70mm long with a diameter of 5.4mm are used with nuts to mechanically seal the layers forming the top part of the enclosure. In the exploded view they are called Stainless steel top support.

The circular PVC top shown in the exploded view is used to completely close the top with the stainless steel bars. The shape as shown in Figure 102 is made to provide tight sealing but also to minimise signal disturbance of the antenna in the middle.
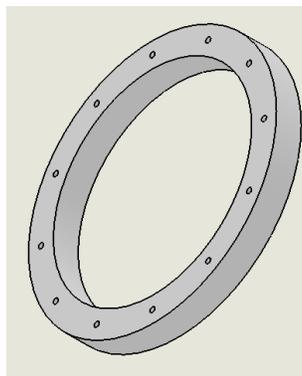
Figure 102 PVC Cover

Ahmed Abdallah Abdou

7.2.1.2. *The bottom part of the enclosure*

The bottom part housed the electronics. This PVC cylinder contained the transceiver electronics. (Figure 103)
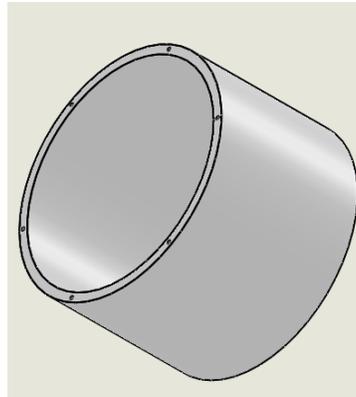
Figure 103 Cylinder

Plastic O rings as shown in Figure 104 on each side of the cylinder were used to aim for complete water tightness.
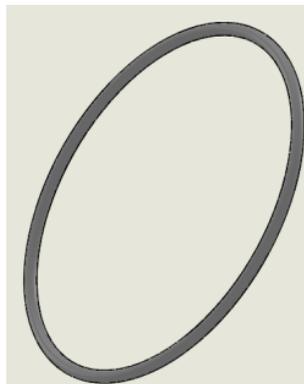
Figure 104 O Ring for cylinder

Ahmed Abdallah Abdou

The PVC cylinder Bottom cover in Figure 105 was used to close the bottom of the container with an O Ring.
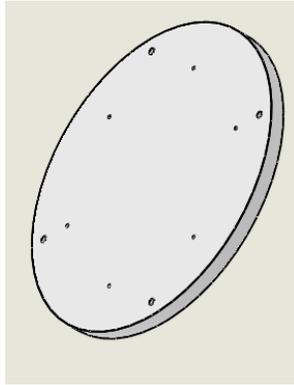
Figure 105 PVC cylinder Bottom cover

Four stainless steel threaded bars give a mechanically strong seal when tightened with nuts but also facilitate dismantling of the container after tests. In the exploded view they are named as Stainless steel support.

The complete transmitter's enclosure was assembled without the antenna (Figure 106) and tested in the tank of the laboratory. At first, the container has shown small leakage. Then after using the non-setting gasket jointing compound by Hylomar in a few trials, the leakage has stopped. The container was subjected to a five hour submersion and did not suffer any leaks either in the antenna seat or in the electronics house.

Ahmed Abdallah Abdou
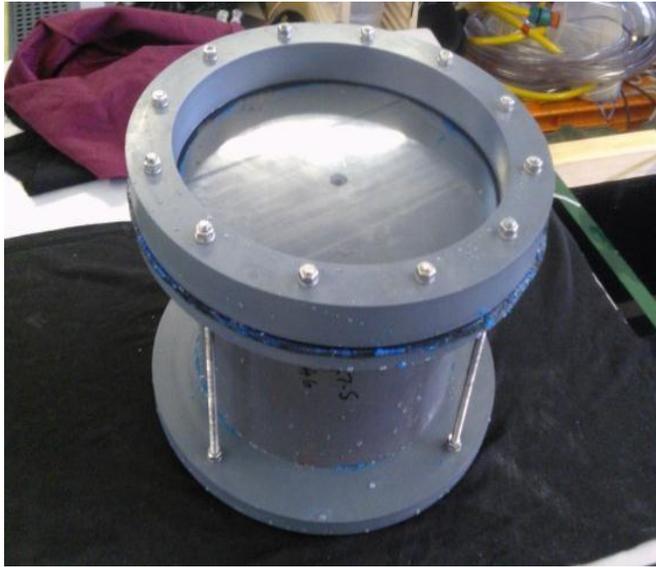
Figure 106 Transmitter's enclosure

Figure 107 shows the underwater transmitter assembled with the antenna and the electronics after being tested in the tank.

Figure 107 Underwater transmitter

172

7.2.2. Receiver's enclosure

The receiver enclosure differs from the transmitter, it's only the top part (as it does not include any electronics) and its antenna is connected directly to a RG58 RF cable. A hose was cut to length to cover the cable and a hose connector provides waterproofing. (Figure 108)
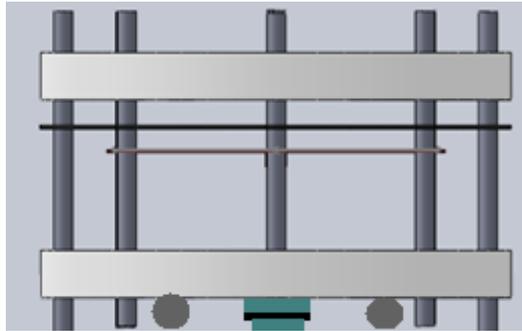
Figure 108 Receiver's enclosure designed in SolidWorks

The complete receiver's enclosure is assembled with the antenna (Figure 109) and tested in the tank. The container, submerged for five hours, did not show any leaks in the antenna seat or from the hose connector.

Figure 109 Underwater receiver

173

7.3. Effect of the fabricated PVC enclosure on the transmission

Upgrading from an off the shelf PP container to a more robust PVC enclosure to house the electronics of the transceivers was successful in terms of waterproofing. However as electromagnetic waves are susceptible to their surroundings, the change of enclosure may affect the transmitted and received signals and therefore requires a close look. An experiment in the laboratory water tank was carried out with the wireless transmitter in the PVC enclosure tested for S21 transmission. The results are displayed in Figure 110. The new signal followed the same pattern as the previous but with less loss which meant that greater distance will be achieved.
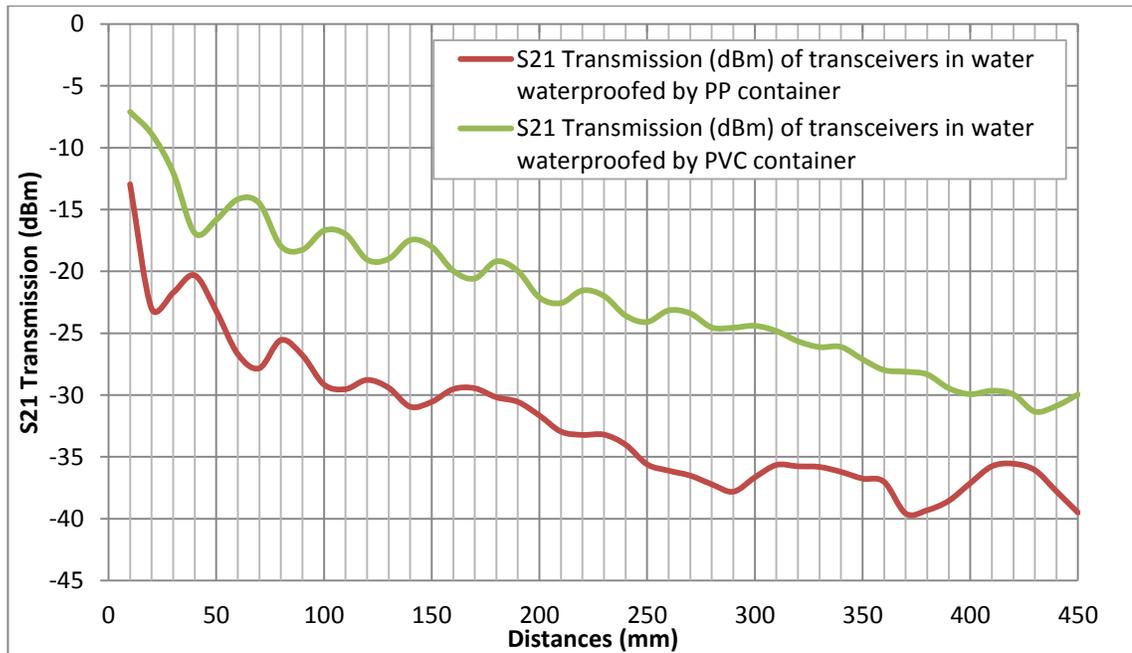
Figure 110 Effects of the fabricated PVC enclosure on the transmission

Ahmed Abdallah Abdou

7.4. Experimental method for S11 and S21 with the fabricated PVC enclosures in the canal

Previous experiments in water took place in laboratory tanks with limited distances. Also the absence of water current in the tank is not giving a close match to a real-life water environment. In Liverpool L5, United Kingdom, the Stanley canal (Figure 111) was identified as a suitable site for long distance communication and immersion of transceivers. Permission was sought from the Canal and River Trust North West body. After assessing the risks involved and fulfilling all the Health and Safety requirements, the trials were approved.
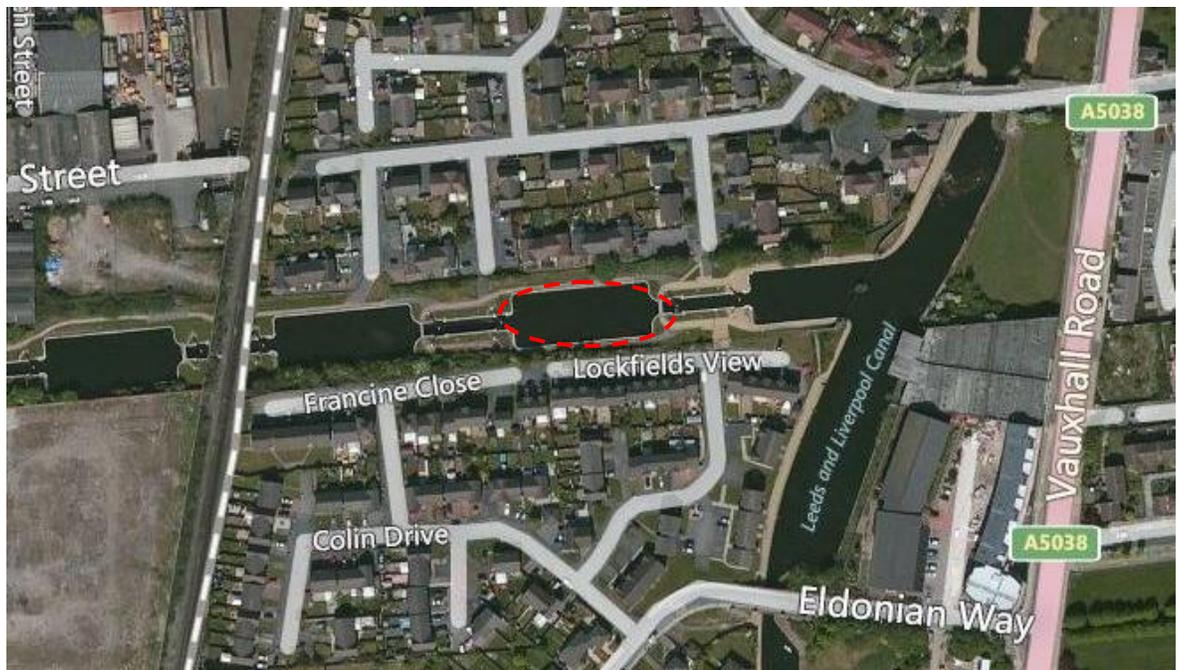
Figure 111 Bing maps, top view of the Stanley canal locks and their surroundings [116]

(in circle: Top Lock Footbridge)

Ahmed Abdallah Abdou

In the canal, the conductivity and temperature of the water were measured. Using the conductivity meter HI33000, readings were taken at three different locations, and were found to be 606±3μS/cm. A K type thermocouple attached to a TM-902C thermometer was used to record the water temperature during the test, this was 16.3±0.4˚C. The electrical equipment that was used for the experiment is listed below:

The Anritsu MS2711D Handheld Spectrum Analyser for 100 kHz to 3GHz (Figure 112) connected to the receiver recorded the signal strength of the transmitted carrier signal (433MHz).

Figure 112 Anritsu MS2711D Handheld Spectrum Analyser

The R&S ZVL Vector Network Analyser 9 kHz to 3GHz (Figure 113) was used to measure the impedance of the antenna in this water environment.

Ahmed Abdallah Abdou

Figure 113 R&S ZVL Vector Network Analyser 9kHz to 3GHz

To supply enough power for the above analysers, a Halfords portable powerpack 200 (Figure 114) was used generating 230-240V mains power with a 20Ah battery and inverters.

Figure 114 Halfords portable powerpack 200

177

Other equipment that was used for the experiments is pictured in Figure 115.

Heavy duty nylon rope

Lifebuoy

50N Buoyancy aid $\times$ 3

Shackle and pulley

Conductivity meter

Temperature meter

Tape measure
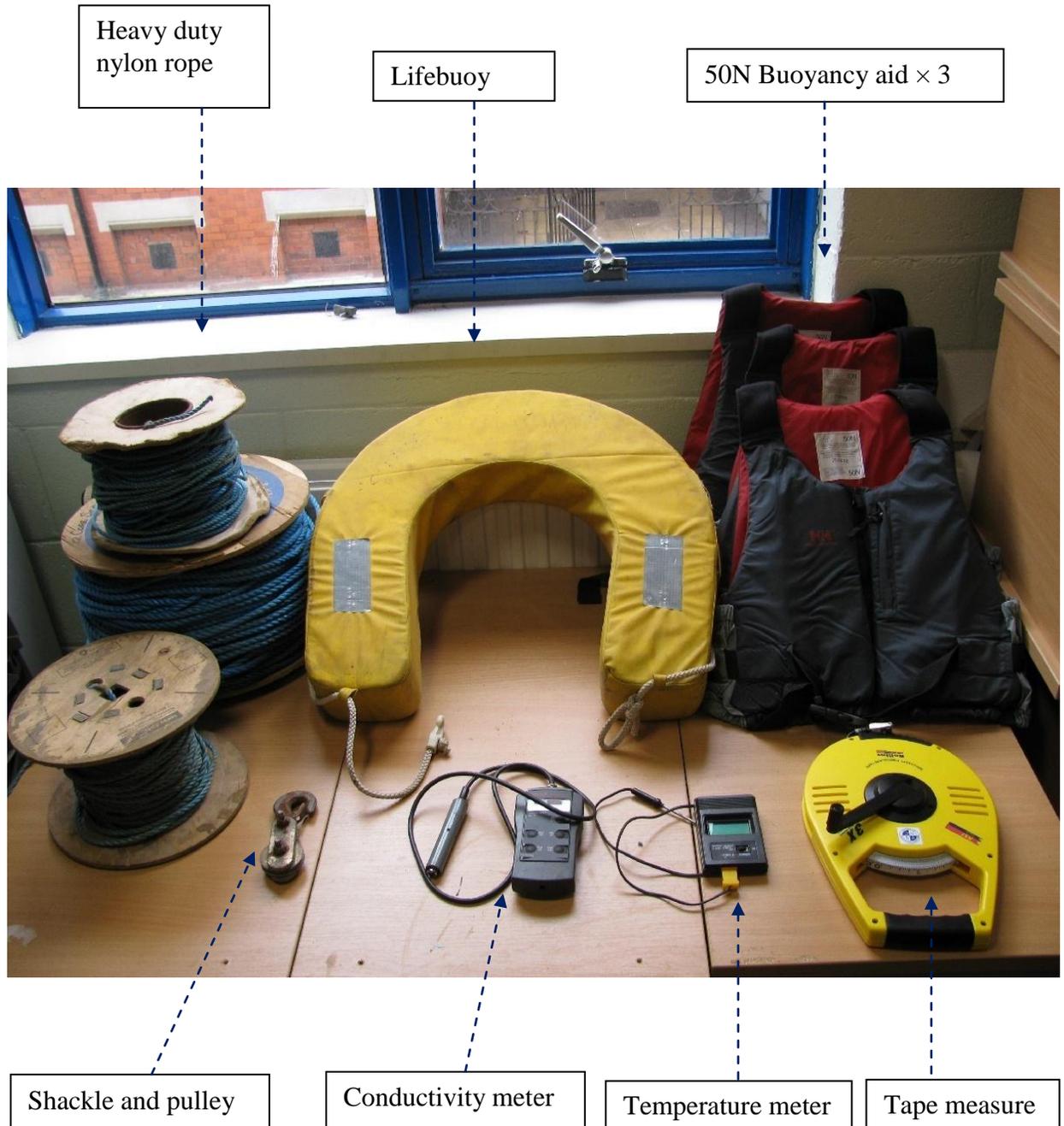
Figure 115 Other equipment used for the canal experiments

Ahmed Abdallah Abdou

7.4.1. S11 Reflection coefficient for Smith Chart

The experiment was run in the Top Lock (Lock No 1) Footbridge to measure the changes of the antenna's behaviour in the canal. This test recorded the real and imaginary values of the reflection coefficient Γ. These were then displayed in the Smith chart for analysis.
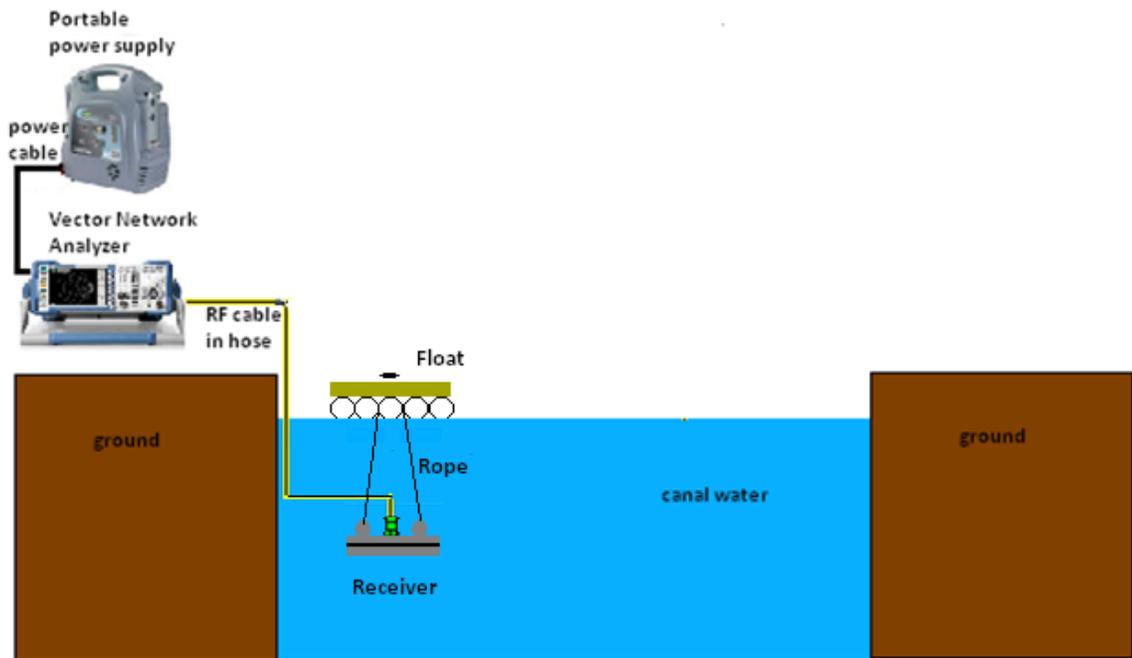
Figure 116 S11 of receiver in Stanley Top Lock (Lock No 1) Footbridge

7.4.2. S11 Return loss

Reflection coefficient data experimented in Figure 116 was also converted to Return Loss values in order to be graphically represented.

Ahmed Abdallah Abdou

7.4.3. S21 Transmission at horizontal separation

The transmitter (Tx) and receiver (Rx) were then attached to floats made of 5×2L empty bottles (Figure 118) to stay in the middle of the water, at 1metre depth as in Figure 119. Their antennas were facing upward. The wireless transmitter attached to one side of the rope that goes through the eyelet is moved away by pulling one end of the nylon rope which is marked for separation increments. Some weight is hung in the air on the guard rails to maintain balance when pulling. The receiver attached to the other side of the rope that goes through the eyelet is held fixed near the shore and records signal strength on the spectrum analyser. On both ends, for quick release, shackles are attached to nylon rope and pulleys giving flexibility for the transceivers' movement.

Figure 117 S21 Horizontal test for signal strength of transceivers against distance in Stanley

Top Lock (Lock No 1) Footbridge
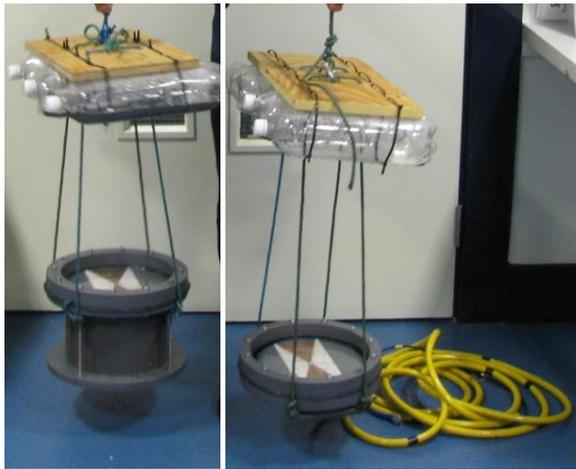
Figure 118 Floats attached to transmitter and

receiver in air in laboratory
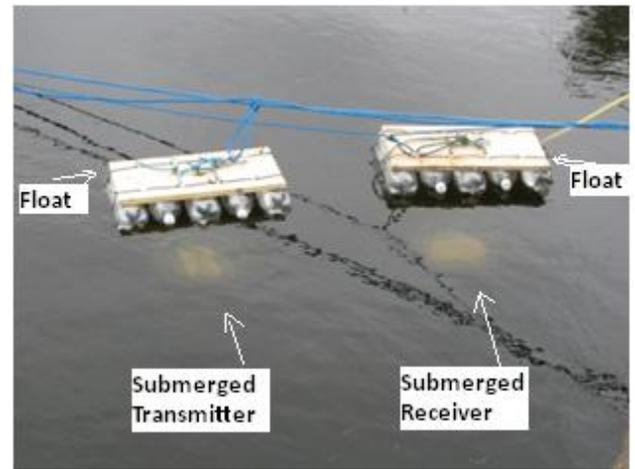
Figure 119 Floats attached to submerged

transmitter and receiver in the canal

7.4.4. S21 Radiation pattern at horizontal separation

The transceivers signal strength data were recorded for radiation pattern in water while they are horizontally separated, the setup in Figure 120 was used. The receiver was connected to the spectrum analyser through the RF cable in hose and was kept near the shore. The wireless transmitter was positioned at a fixed separation distance of 3metres. The first reading was taken then the transmitter attached to a rope was rotated at angles increments of 10˚ up to approximately 90˚ to record the signals strengths on the receiver. Due to limited access to the site and the health and safety restrictions only a quarter of the full plane was assessed.

Ahmed Abdallah Abdou
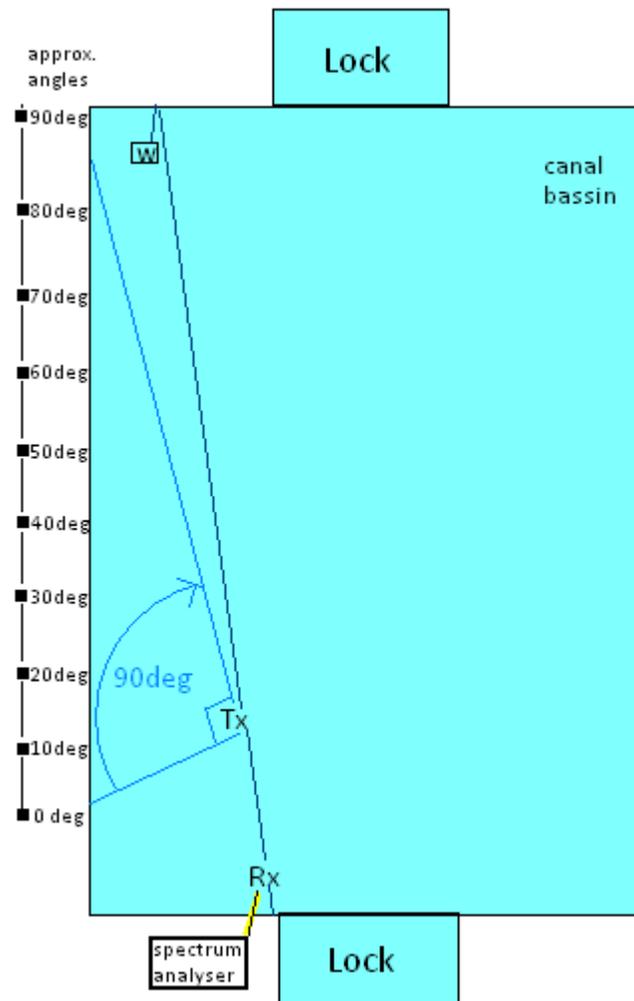
Figure 120 S21 Radiation pattern experiment at horizontal separation in Stanley canal

7.5. Results and discussion

7.5.1. S11 Reflection coefficient in Smith chart

The real parts and Imaginary parts of the antenna's reflection coefficient while in the water of the canal were collected from the VNA for frequencies between 100MHz and 800MHz.

182

Ahmed Abdallah Abdou

However because the 433MHz frequency of interest was in the 400-500MHz region, this region only was displayed in Figure 121.
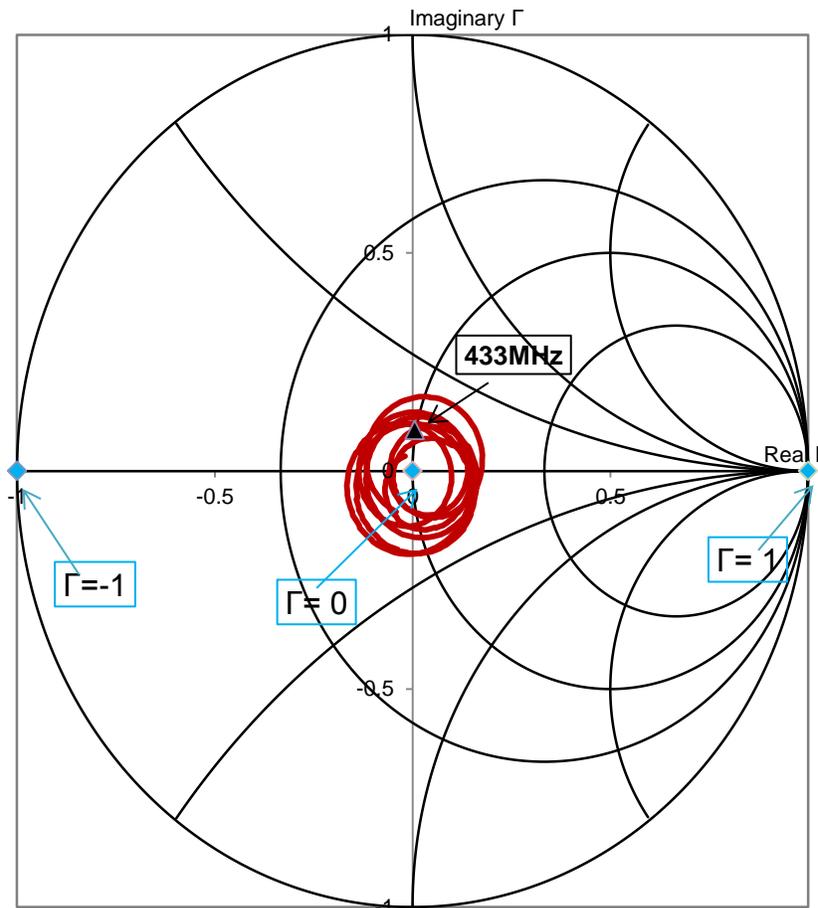
Figure 121 Smith chart for the receiver's antenna in Stanley canal for frequencies

400-500MHz

The 400-500MHz frequency range is close to the centre and the 433MHz marker was one of the closest on this range. Although after graphical reading on the Smith chart, the next step is to match for 50ohm impedance (Γ=0), however this is more appropriate for narrow band

Ahmed Abdallah Abdou

antenna at a given frequency. Maintaining a wide bandwidth to accommodate signal fluctuations in the water is a requirement as long as the antenna return loss is more than 10dB (90% of transmission).

7.5.2. Return Loss
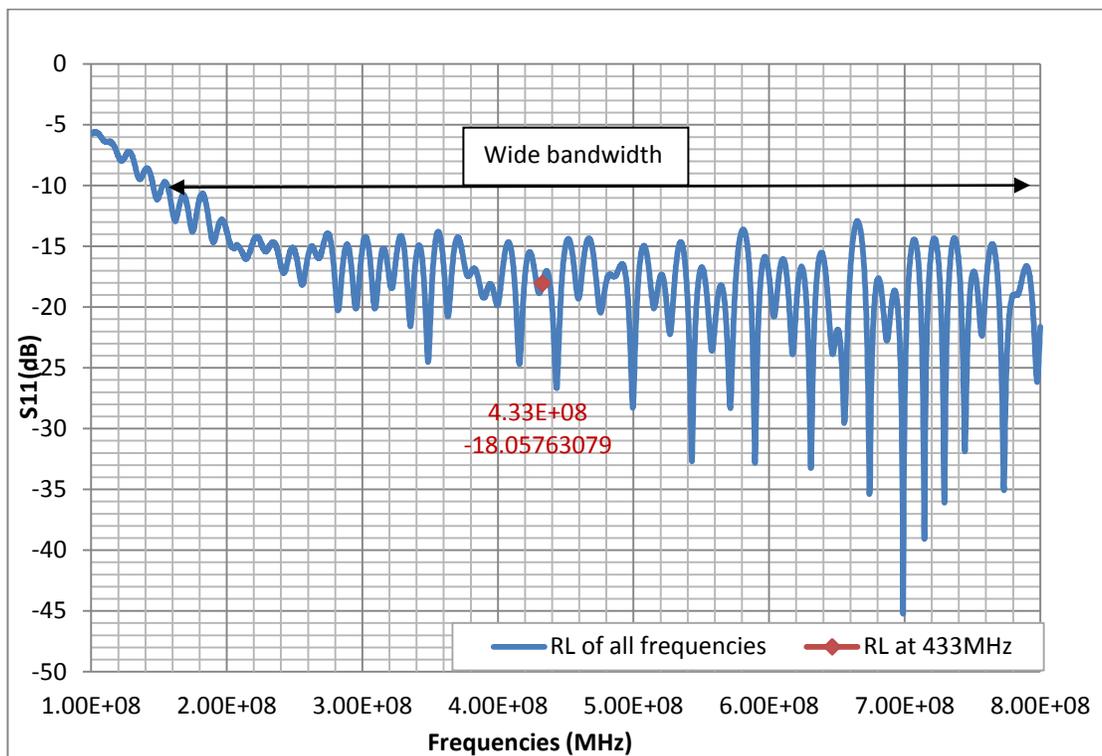
Figure 122 S11 Return loss of the receiver's antenna in Stanley canal

The converted values of real and imaginary reflection coefficient to return loss were plotted in Figure 122. From this graph a wide bandwidth with a minimum of 10dB RL was seen from approximately 150MHz up to 800MHz. At 433MHz the RL was -18.05dB and was equivalent to 98.42% transmission.

Ahmed Abdallah Abdou

7.5.3. S21 Transmission at horizontal separation

The transceivers were separated every metre for the first 10metres then every 2metres until 30metres. Ten signal strengths readings were collected in microvolts (µV) and averaged by the spectrum. Those values were then converted in dBm and plotted in Figure 123. At 12m separation between the transmitter and the receiver, the locks were opened consecutively for boats passage. This created waves which made the attached transceivers fluctuate. This phenomenon depicted a real world application where transceivers could be moved from their original position and therefore the signal strength before and after the opening of the locks was important.
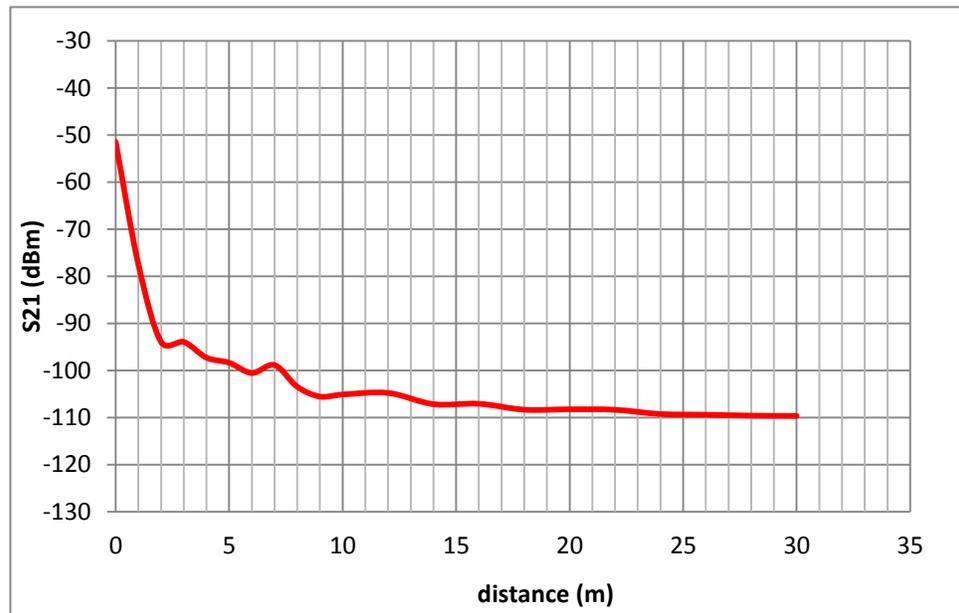
Figure 123 S21 Transmission of transceivers separated horizontally in the canal water

Figure 123 displays signal strength (S21) experimented for the bow-tie antennas in water in the canal over a distance of 35m. Two regions were observed, a near-field region up to

Ahmed Abdallah Abdou

approximately 2m separation distance and a far-field region onwards up to 30m. After that the signal was recovered any more. In the near-field region, the signal lost 43dB. The far field losses were expected to attenuate approximately 20dB/m according to the theoretical calculations in Table 3 for a 433MHz plane wave in water referred to as freshwater. However in this experiment, the losses were 15dB for 28 metres. This could be explained that the low signal reached the noise level because of the spectrum analyser sensitivity or the signal had to travel in lower permittivity material (ground and air) before reaching the submerged antenna. In the first case, the signal was in the -110dB the far field loss region and transceivers operating at 433MHz that have sensitivity down to -122dBm could be used to detect such small signals at such big distances in the water with the bow-tie antenna. In the second case it would not matter if the signal found other paths than water to reach the receiver as long as it could be recovered.

With regards to the opening of the locks, the signal changed only 1%. The fact that the transceivers resisted the waves created by the opening of the locks in the canal provided some confidence for usage even in windy periods.

7.5.4. S21 Radiation pattern at horizontal separation in Stanley canal

Figure 124 displays the signal strength as radiation pattern on a 360˚ plane of the transceivers separated horizontally 3metres in the canal. Only up to 90˚ of data was recorded and represented graphically.

Ahmed Abdallah Abdou
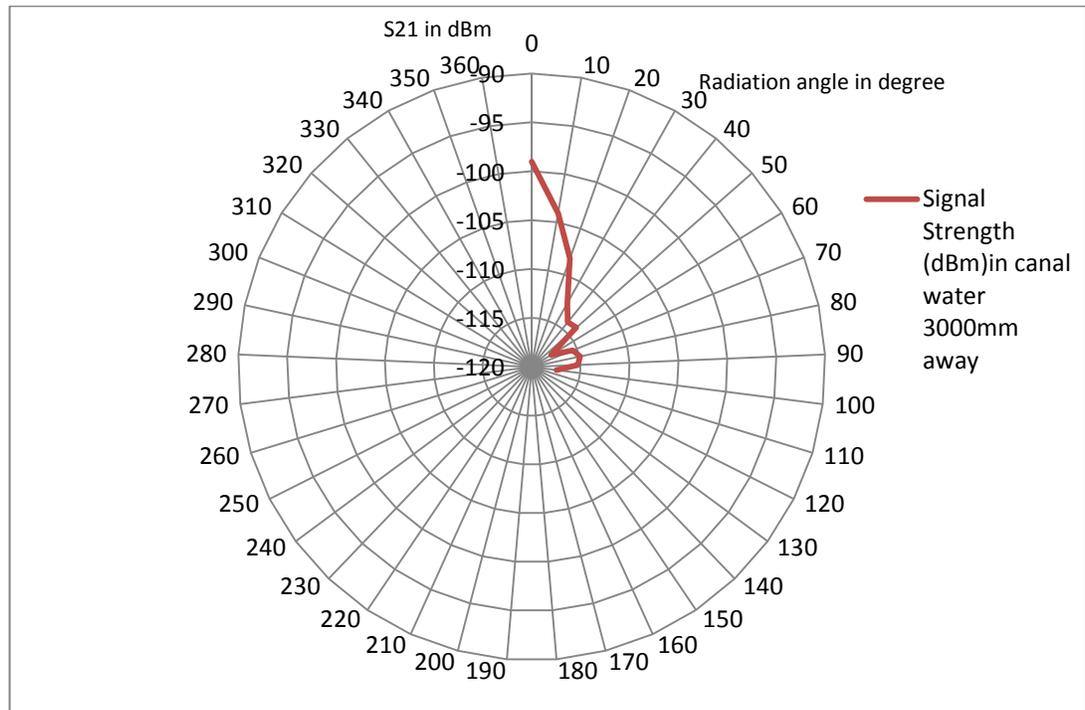
Figure 124 S21 radiation pattern (up to approximately 90˚) at horizontal separation in Stanley canal

From the quarter plane represented in Figure 124, the highest signal occurred at 0˚ and the lowest at 90˚. This is in agreement with all the radiation experiment resulted both in air and water. The shape in between the 0˚ and 90˚ angles followed the shape of the first quarter of radiation of transceivers in the tank of water at 1000mm separation in Figure 97. Therefore the radiation patterns of the remaining 3 quarters in the canal were predicted as in Figure 125.

Ahmed Abdallah Abdou
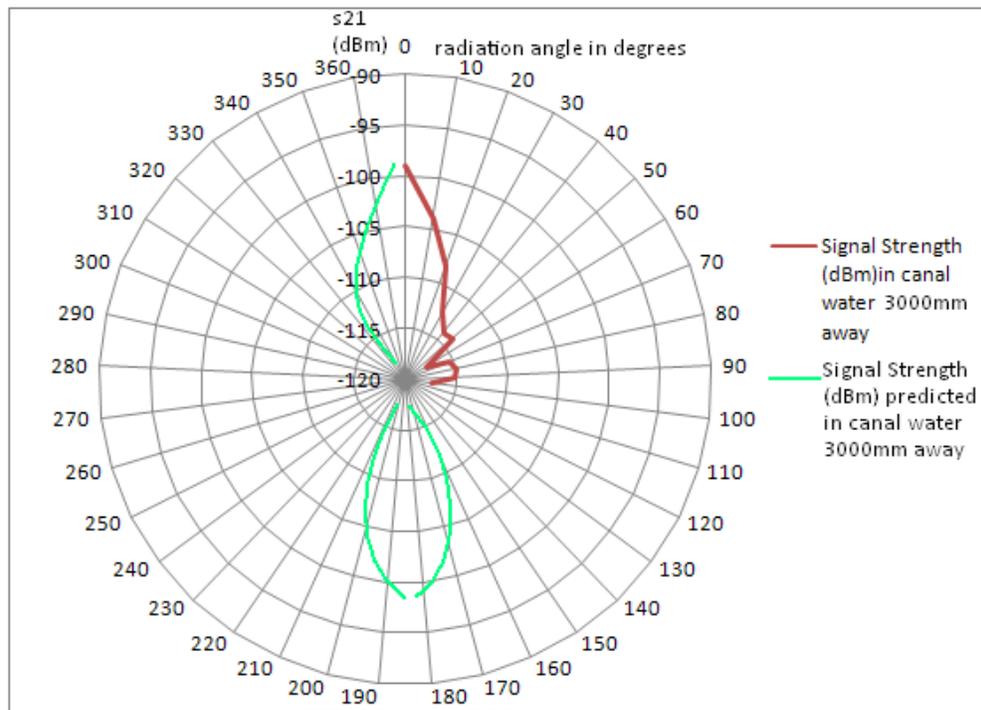
Figure 125 S21 Radiation pattern and predicted at horizontal separation in Stanley canal

The best positioning of the transceivers for communicating under the water of the canal was when the antennas were 0˚ and 180˚ in line. The worst positioning was at approximately 90˚ and 270˚ with signal strength that gone smaller up to -117dBm.

7.6. Summary

In this chapter, robust waterproof enclosures were designed and prototyped for the transceivers to be experimented in a real world trial in Liverpool Stanley Canal freshwater. S11 results shown that the 433MHz air designed and constructed Bow-tie antennas behaved well even in freshwater. S21 transmissions results proved thriving communication range up to 30metres. This can be used in many applications that apply two way communications. In

Ahmed Abdallah Abdou

Wireless Sensor Networks where an omnidirectional pattern of the sensors is required, a separation of 5 to 10metres with such low power signal can be realistic to cover a wide area.

Ahmed Abdallah Abdou

Chapter 8. Further Modelling with the Bowtie antenna

8.1. Introduction

In chapter 5, the Bowtie antenna modelled to operate at 433MHz in air taking into account the restrictions of the levelling board of the PCB machine proved its usefulness in water without matching circuit and therefore the immediate focus was not on optimizing the size of the antenna. Instead in chapter 6, the focus was more on how to eliminate or reduce the chance of RF crosstalk from the cables that may act as antennas and could results in false readings in a two way communication system that was planned for a real life test in the Liverpool Stanley Canal freshwater as in chapter 7. In this chapter, we altered the bowtie antenna sizes and modelled the antenna in water with the same conditions as chapter 5. Therefore the arm length of the antenna was changed while keeping the outer width of the antenna fixed to 91.5mm. In [103], it is stated that the bandwidth of the bowtie antenna depends on the length of the plate and that the flare angle and the length of the plate define the lower frequency. Therefore we monitored the starting low frequency with a minimum of 10dB return loss and the bandwidth available. In practice, this will allow us to see whether the antenna prototyped in chapter 5 could be optimised and prototyped again in our laboratory or elsewhere. For these, we had two cases:

- Case 1: The levelling board of the PCB machine restricted the size of the antenna board to a maximum of 210mm length and 120mmwidth. Therefore the maximum arm length of 101.6mm was reduced in 20mm steps down to 20mm.

Ahmed Abdallah Abdou

- Case2: There were possibilities to prototype the antenna on a PCB machine with an antenna board of 350mm length and 120mm width. Therefore the minimum arm length here was 101.6mm and was increased in 20mm steps up to 160mm.

8.2. Case 1: restricted to an antenna board of 210mm length and 120mm width

8.2.1. Bowtie antenna design alteration and modelling

This first case was a reality because the antenna board size was restricted by the levelling board of the PCB machine to 210mm length and 120mm width. Therefore we reduced the bowtie maximum arm length of 101.6mm by approximately 20mm down to 20mm as sketched in Figure 126. The dimensions of the bowtie antenna after alterations were measured in HFSS and displayed in Table 6. Reducing the arm length increased the flare angle.
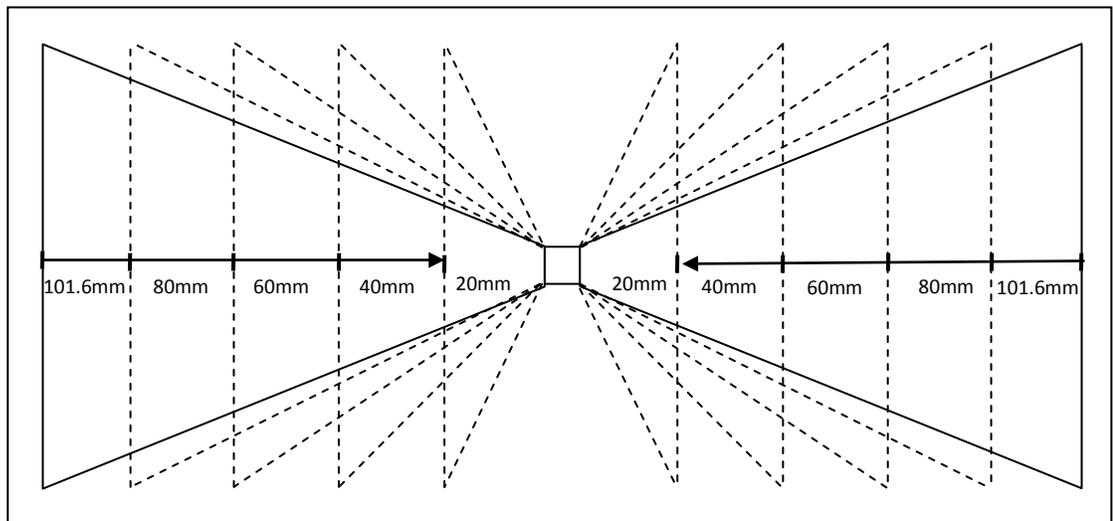
Figure 126 Schematic of Bowtie antenna with reduced arm length from 101.6mm to 20mm

on a 210mm×120mm antenna board

Ahmed Abdallah Abdou

Table 6 Measured dimensions in HFSS of the Bowtie with reduced arm length from 101.6mm

to 20mm

Board width Sub x(mm)	Board length Sub y(mm)	Outer width(mm)	Hypotenuse (mm)	Angle in degrees	Arm length (mm)
120	210	91.5	110.4	46.07	101.6
120	210	91.5	90.9	56.74	80
120	210	91.5	73.9	71.5	60
120	210	91.5	58.87	94.4	40
120	210	91.5	47.6	130.31	20

8.2.2. Results and discussion
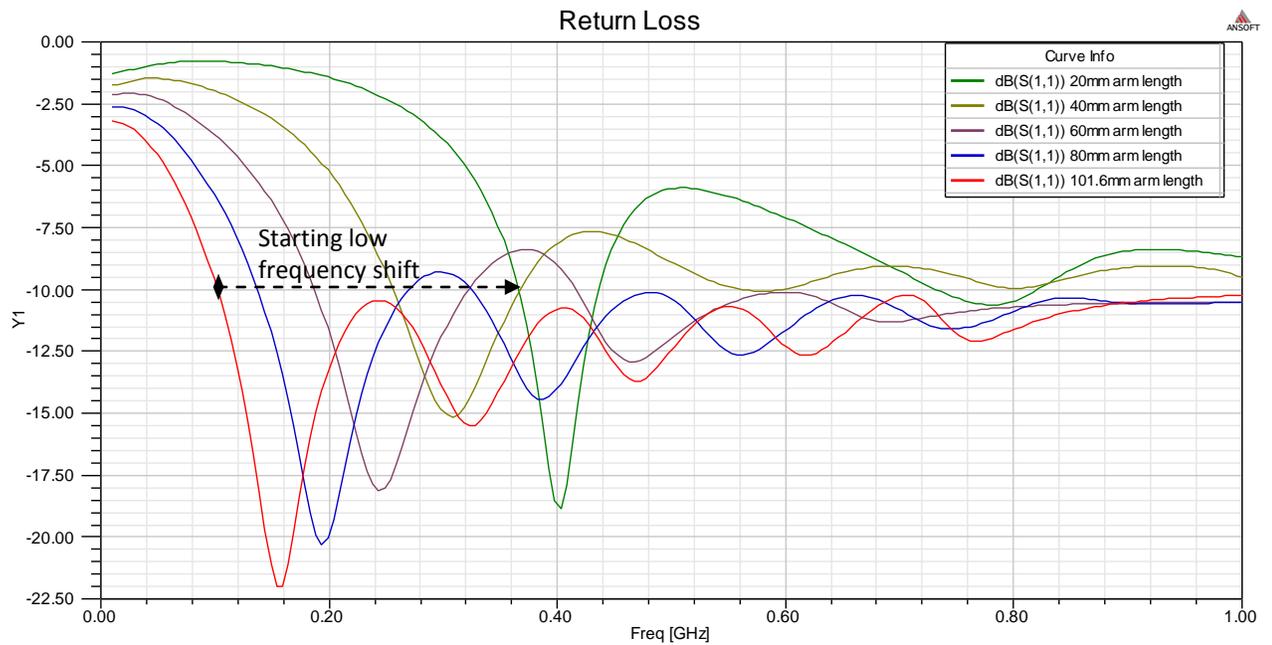
Figure 127 Return Loss (dB) of the Bowtie antenna modelled in water with reduced arm

length from 101.6mm to 20mm

Ahmed Abdallah Abdou

Table 7 Consequences of reduced arm length from 101.6mm to 20mm of the Bowtie antenna

modelled in water

Arm length (mm)	Starting low frequency (GHz)	Bandwidth (GHz)
101.6	0.104	0.9
80	0.139	0.13, 0.67
60	0.189	0.13, 0.18, 0.4
40	0.258	0.11
20	0.368	0.06, 0.09

From Figure 127 and Table 7, reducing the arm length pushed the starting low frequency with at least 10dB of return loss to higher frequencies. E.g. the bowtie antenna with arm length 101.6mm had a starting low frequency of 104MHz, but when the arm length was reduced to 20mm then the starting low frequency was 368MHz.

As the arm length is reduced, the bandwidth available in water was reduced too. E.g. there was a large bandwidth (0.9 GHz) available when the arm length was 101.6mm whereas when the arm length was reduced to 20mm the bandwidth available was divided in two very small ones (0.06 and 0.09GHz).

In this case 1, reducing the arm length (increasing the flare angle) with fixed outer width deteriorated the large bandwidth needed in water to cover the frequency shift from air to water. This will make the antenna not resonating in air at 433MHz and neither in potable nor in fresh water. Also changes (e.g. temperature, salinity) within the water environment may result in signal loss. Therefore the reference size was the ideal compared to the others in case 1

Ahmed Abdallah Abdou

in potable and freshwater. For saline water, where low frequency was needed to operate in, the reduction of the arm length did not help.

8.3. Case 2: not restricted to the levelling board length, arm length size could be increased

8.3.1. Bowtie antenna design optimisation and modelling

The second assumption was that there were possibilities to prototype the antenna on a PCB machine with approximately double the length of levelling board up to 350mm but keeping the 120mm width unchanged. Therefore the minimum arm length of the bowtie antenna was 101.6mm and was increased in approximately 20mm steps up to 160mm as sketched in Figure 128. The dimensions of the bowtie antenna after alterations were measured in HFSS and displayed in Table 8. Increasing the arm length reduced the flare angle.
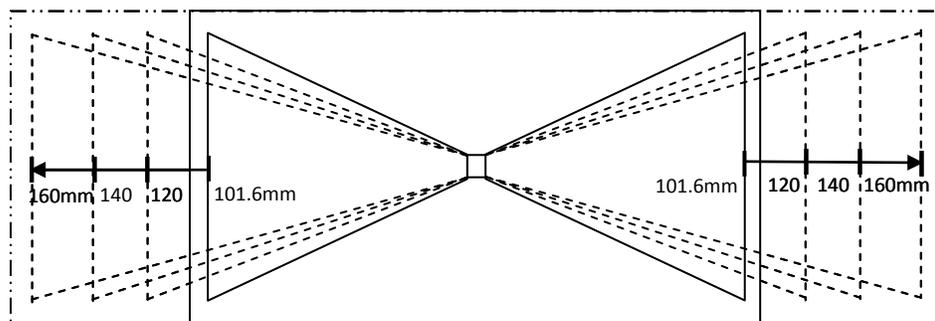
Figure 128 Schematic of Bowtie antenna with increased arm length from 101.6mm to 160mm

on a 350×120mm antenna board

Ahmed Abdallah Abdou

Table 8 Measured dimensions in HFSS of the Bowtie antenna with increased arm length from

101.6mm to 160mm

Board width Sub x(mm)	Board length Sub y(mm)	Outer width(mm)	Hypotenuse (mm)	Angle in degrees	Arm length (mm)
120	350	91.5	165.7	30.22	160
120	300	91.5	146.5	34.29	140
120	250	91.5	127.5	39.59	120
120	210	91.5	110.4	46.07	101.6

8.3.2. Results and discussion
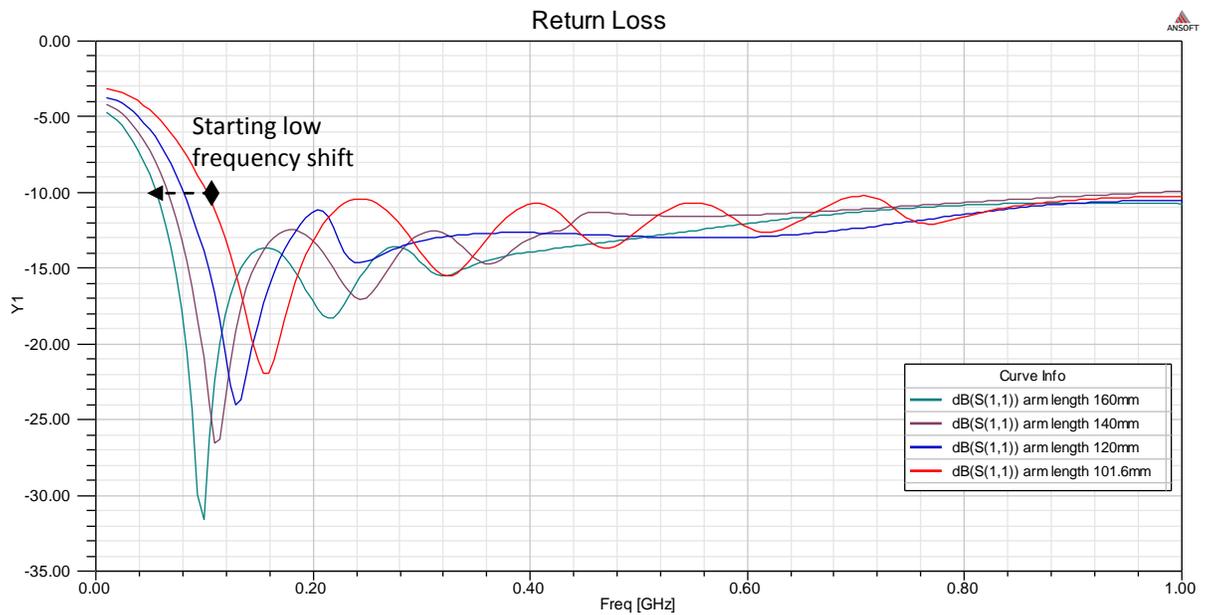
Figure 129 Return Loss (dB) of the Bowtie antenna modelled in water with increased arm

length from 101.6mm to 160mm

195

Table 9 Consequences of increased arm length from 101.6mm to 180mm of the Bowtie

antenna modelled in water

Arm length (mm)	Starting low frequency (GHz)	Bandwidth (GHz)
160	0.056	0.94
140	0.067	0.85
120	0.082	0.9
101.6	0.104	0.9

From Figure 129 and Table 9, increasing the arm length pushed the starting low frequency with at least 10dB of return loss to lower frequencies. E.g. the bowtie antenna with arm length 101.6mm had a starting low frequency of 104MHz, but when the arm length was increased to 160mm then the starting low frequency was 56MHz.

The large bandwidth (≈0.9GHz) obtained with 101.6mm arm length was maintained at every increased arm length.

In this case 2, increasing the arm length (reducing the flare angle) with fixed outer width maintained the large bandwidth needed in water to cover the frequency shift from air to water. This is making the antenna resonates in air at 433MHz as well as in potable and fresh water. Also changes (e.g. temperature, salinity) within environments will not affect the signal. Therefore the reference size was ideal compared to the others in case 2 only in potable and fresh water. For saline water, where low frequency was needed to operate in, the increase of the arm length could help.

Ahmed Abdallah Abdou

In all cases, as from the theory of the Bowtie antenna referenced earlier, the bandwidth of the bowtie antenna is dependent on the length of the antenna board. The flare angle and the length of the antenna board defined the starting lower frequency.

8.4. Summary

In this chapter, the Bowtie antenna prototyped in chapter 5 and tested in the canal in chapter 7 was subjected to further modelling in water. This consisted of altering the sizes of the antenna. Two cases were presented. On the first case, the length of the antenna board was restricted to the length of the PCB levelling board. By changing the size of the antenna in this case, the modelling resulted on a reduction of the large bandwidth and a shift of the starting low frequency to higher frequencies which are both unwanted. The sizes of our prototyped antenna have shown that the antenna is optimised in potable and freshwater. However when the length of the antenna board was extended, the modelling resulted in a large bandwidth maintained and the shift of the starting low frequency to lower frequencies which predicted that the antenna will also be able to operate in high salinity water (seawater).

Ahmed Abdallah Abdou

Chapter 9. Conclusion

Although the challenges in water environment are becoming more alarming, industrial and environmental bodies are still relying on traditional and periodic methods in assessing water health. As technology is evolving, it is providing solutions to many problems. Only some of the environmental agencies and water industries in developed countries have made use of technology with the revolution of sensors technology and real time systems. In countries with financial resource shortage, the cost of these systems makes it almost impossible to acquire them. Therefore globally there has been a huge need for scientists and technologists to find new and cheap alternatives capable of replacing conventional and costly ways for assessing water environment in real time. We have explored State of the art water communications and found that in many applications, acoustic and optical traditional ways of communicating underwater between sensor nodes have underperformed and were found unreliable. We have proposed a breakthrough in underwater communication. This is by using wireless sensor network communicating through radio and microwaves, a technology that has excelled in over-the-air applications. This has driven us to aim to investigate short range Electromagnetic wave communication utilising a sensor network platform. In order to achieve this aim we have set objectives. The first objective consists of investigating the feasibility of radio frequency and microwaves communication underwater using the unlicensed ISM band. The second objective consists of testing the feasibility of using commercial over the air transceivers in water to sense its health. The third objective is to design, simulate and test an antenna to operate efficiently in water. The fourth objective is about investigating the feasibility of

Ahmed Abdallah Abdou

forming a WSN to operate in the water column. The first three objectives are the most critical as the frequency and the antenna are interrelated and the fact that this has to be in water makes them very challenging however tests with commercial over-the-air wireless transceivers in water can give a preliminary experimental validation to the first objective. Unlocking these objectives will answer most of the research and will lead to the last objective set, because the suitable antenna for the appropriate frequency is key to successful transfer of modulated carrier signal between the sensor nodes forming the WSN especially in a medium like water.

In order to predict the appropriate frequency to operate in water, it was vital to understand how electromagnetic waves propagate. So a review of the theory of electromagnetic wave propagation was undertaken. A study of the effects of the permittivity and the salinity of water on absorption was carried out. This showed that lower frequencies suffered less absorption. For potable and freshwater, however the losses up to around 600MHz, still allowed realistic transmission up to a few metres, and suggested 433MHz and 6.7MHz for communication. For saline water, the absorption is considerably higher but it was concluded that the 6.7 MHz ISM band might still be practical. This covered the first objective, which consisted of investigating the feasibility of radio frequency and microwaves communication underwater using the unlicensed ISM band. With most commercial transceivers for sensor nodes operating at 2.4GHz ISM, it was necessary, through experimentation, to show the limitations of this frequency. The theoretical model predicted high attenuation in the 2.4GHz ISM band and this has been validated in the laboratory tank experiments using a commercial low powered wireless transceiver with the loss of temperature sensing signal at 200mm in section 3.6.1.1. This covered the second objective consisting of testing the feasibility of using commercially

Ahmed Abdallah Abdou

available over-the-air wireless transceivers in water to sense its health. The communication range achieved was limited because of the highly attenuated 2.4GHz frequency of the transceiver and the unsuitable antenna for water. Therefore this band that provides many advantages including high data rate, availability in complete kits, was recommended more favourable in proximity communications for applications requiring a higher data rate (i.e. Automated Underwater Vehicles collecting data from an underwater node where acoustic and optical are not viable options) than in UWSN. Further Experiments in the tank validated that the 433MHz and 6.7MHz could travel further in potable water and the antenna has a crucial role in signal transmission and reception which require further investigation. Apart from the theoretical prediction of the usefulness of 433MHz in potable and freshwater, we have operated in this band because it offers many advantages over the 6.7MHz including the higher data rate needed for more frequent data sampling and fast data download, off the shelf transceiver availability and smaller wavelength size to construct an antenna. The choice of the 433MHz frequency for our sensor node which resulted from detailed theoretical and experimental investigation provided in chapter 3, covers the first two objectives and makes way to the third objective to design and simulate an antenna to operate efficiently in water. However the size of the tank limited the experimental verification of this frequency to communicate up to its maximum distance for sensor nodes separation that will form the network.

In chapter 4, we have recalled the theory to construct an antenna to operate in air or in water. Traditional antennas made of copper wire were made for the approved 433MHz frequency and tested in the tank of the laboratory. The popular loop antenna outperformed and therefore was

Ahmed Abdallah Abdou

subjected to a modelling stage. This consisted of designing and analysing the antenna behaviour in HFSS in water and air environment. Analyses examined include the return loss and the bandwidth available, the impedance and the radiation pattern of the antenna. This has shown that the antenna does not have any bandwidth in air or in water even when the size is optimised. Although the size of the loop to operate in water has been determined from the theory to take into account the water reduction factor, the impedance of the antenna in water and in air is mismatched even when its size is optimised for resonance. This meant that without matching circuit, communication range required for the UWSN would not be achieved if we choose any traditional narrowband antenna including the loop and therefore bespoke antenna must be sought in order to meet the objective. However antenna with matching circuit will suffer from reduction of signal strength or complete signal loss in varying underwater parameters including salinity and temperature. Although this chapter does not meet the second objective set, it has allowed us to specify in chapter 5 the criteria needed on the antenna in order to operate in water efficiently without any matching means. To select an antenna for wireless sensor network that could work in air as well as in water, the focus has been on selecting an antenna that has a broad bandwidth, an omnidirectional radiation pattern but also an antenna that can be prototyped for practical validation tests. The planar version of the broadband finite biconical antenna is the Bowtie which can be printed on a dielectric substrate, and this is selected and investigated. The antenna is modelled in air at 433MHz and in 0.02S/m water in HFSS. Although the simulation results in air shown a limited bandwidth, in water they show an ultra-broadband behaviour that is needed. The impedance has shown that the matched antenna in air was close to a matched antenna in potable and freshwater. The

Ahmed Abdallah Abdou

antenna has an omnidirectional radiation pattern in air and maintains it in water. This validates the first two selection criteria and proceeds to the third criteria referring to ease of prototyping for practical validation of the antenna in water. The antenna is then successfully prototyped on PCB and waterproofed for underwater tests. The S11 results of the experiments demonstrate that the Bow-tie antenna that is designed and constructed for air can be used in water without a matching circuit. It is understood that this is first time that an antenna designed to operate in air at 433MHz has been shown to operate in water without any matching. The S11 results of the simulated 433MHz Bowtie antenna in air and in water were in good agreement with experimented ones. This implies a recommendation for HFSS in modelling the behaviour of the antenna in liquids including water. However there has been a limitation on analysing the signal transmission S21 between two antennas in an open water environment. Further experiments have shown the Bowtie antenna immunity towards temperature change. This attribute is linked to its broadband characteristic in water and is needed. Designing, simulating and testing the 433MHz Bowtie antenna which resulted in its efficient operation in water has led to demonstrate for the first time the application of bowtie antenna and specifically our 433MHz bowtie antenna in potable and freshwater. This covers the third objective which has been the crucial part of the research and consisted of designing, simulating and testing an antenna to operate efficiently in water. The first and the third objectives form the communication device which is an important component out of the five main components of the sensor nodes explained in section 2.4.3.1. The remaining four components could be off-the-shelf components connected to our communication device.

As this sensor node is going to operate in a network, our communication device had to be able to generate its own carrier signal for transmission to form the physical layer of the network. Also to validate the first and the third objectives against erroneous results that may arise from RF cables crosstalk during experiments in water, the carrier signal had to be generated from a wireless battery powered RF source. We have therefore designed and prototyped a battery and low powered 433MHz carrier signal generator. The electronic set is waterproofed and tested in a laboratory tank with the Bowtie antenna for S21 signal transmission. Experimental results confirm the suitability of the bowtie antenna in a true wireless sensor node and successful reception of the 433MHz carrier signal transmitted through the antenna for up to half a meter. This distance was limited because of the tank size however analysis of the signal showed a far field region predicting higher communication range. The fourth objective consisted of investigating the feasibility of forming a WSN to operate in the water column. In order to form a network, sensor nodes had to be able to communicate at least for a distance of 3 to 5metres, as mentioned in the design specification. Therefore we have subjected our communication device to an experiment in Liverpool Stanley Canal Freshwater. For this we have designed robust waterproof enclosures for the transceivers in SolidWorks and prototyped. The S11 results have shown that our bowtie antenna behave well even in freshwater. The S21 transmissions results have proved a thriving communication range up to 30metres. This range has broadened the applications of our communication device with the Bowtie antenna for two way communication systems operating in potable and freshwaters. In WSN, an omnidirectional pattern of the sensors is required; therefore we recommend a separation of 5 to 10metres with such low power signal to cover a wide area. The fourth objective is therefore

Ahmed Abdallah Abdou

met in chapter 7 and the findings confirm that our communication system combined with the remaining 3 off the shelf components (memory, controller, water health sensor) will form a wireless sensor node. Duplicating this node will constitute the WSN needed to cover and monitor the health of a wide underwater zone.

The contribution to knowledge is the experimental demonstration of reliable communication at 433MHz using a broadband antenna which unlocks the potential of underwater WSN applications, including applications in water quality measurement, using radio communication.

Further modelling in water on the 433MHz Bowtie antenna prototyped and tested in the canal is done. This consisted of altering the sizes of the antenna. Two cases were presented. On the first case, the length of the antenna board was restricted to the length of the PCB levelling board. By changing the size of the antenna in this case, the modelling resulted in a reduction of the large bandwidth and a shift of the starting low frequency to higher frequencies which are both unwanted for water communication. The sizes of our prototyped antenna have shown that the antenna was optimised in potable and freshwater. However when the length of the antenna board was extended, the modelling resulted in a large bandwidth maintained and shift of the starting low frequency to lower frequencies which predict that the antenna could also be able to operate in high salinity water (seawater). These findings are unique and open up a huge area of investigation which could be applied in a wide range of seawater applications including seawater environmental monitoring, commercial subsea applications, defence and military applications etc.

Ahmed Abdallah Abdou

Chapter 10. Future work

The Bowtie antenna could be attached to an off the shelf board transceiving at 433MHz which will replace the carrier signal generator and send a modulated signal. This will form the complete communication system. Different types of modulation could be studied in water.

Depending on the application, single or multi parameters sensor that can measure properties like pH, Dissolved Oxygen, turbidity, chlorophyll a, temperature, pressure, salinity, conductivity can be attached to the underwater communication system. Those related to the application will be studied; the condition and parameters, under which maximum reliability and sensitivity will occur, will be considered.

The communication system and the sensor could be duplicated to form a network of sensor nodes. This could monitor physical variables such as water temperature and pressure as well as variables such as conductivity, turbidity and certain pollutants. The network could track accidental release of pollutants flowing in water from land. It could monitor and model the behaviour of underwater ecosystems. The network could be used to identify or monitor in real time deliberate pollution or even potential terrorist attack to water reservoirs that could contaminate water supply and put in danger public health. A map of the water reservoir with areas of contamination could be generated for the authorities to take immediate action like stopping, the supply of contaminated water from getting to the public.

Ahmed Abdallah Abdou

The network of underwater sensor nodes could be modelled in platforms such as Opnet or Ns-2 where parameters of the network including power, quantity of service (throughput), quality of service (QoS), mobility, protocols, etc can be studied.

Further modelling on the Bowtie antennas could be done to find the optimised size to operate efficiently in saline water. This could then be prototyped and tested in seawater. The Bowtie antenna could be re-engineered to suit saline water applications.

Ahmed Abdallah Abdou

References

[1]   A. Al-Shammaa, A. Shaw, and S. Saman, "Propagation of Electromagnetic Waves at MHz Frequencies Through Seawater," *IEEE Transactions on Antennas and Propagation*, vol. 52, no. 11, pp. 2843–2849, Nov. 2004.

[2]   Y. Huang and K. Boyle, *Antennas from theory to practice*. John Wiley & Sons, Ltd, 2008.

[3]   T. Apps, "Apps Laboratories," *salinity*, 2012. [Online]. Available: http://www.appslabs.com.au/salinity.htm. [Accessed: 20-Jan-2012].

[4]   R. Weiner and R. Matthews, *Environmental Engineering*, Fourth Edi. 2003.

[5]   Environment Agency, "The unseen threat to water quality," 2007.

[6]   Betancourt, V. Hemmen, Greco, and Kenyon, "International Convention for the Prevention of Pollution of the Sea by Oil," *International Conventions*, 1954. [Online]. Available: http://www.admiraltylawguide.com/conven/oilpol1954.html. [Accessed: 05-Apr-2012].

[7]   F. Bernardini, "UNECE Convention on the Protection and Use of Transboundary Watercourses and International Lakes," 1992.

[8]   European Commission, "Urban Waste Water Directive Overview," *Environment*, 1991. [Online]. Available: http://ec.europa.eu/environment/water/water-urbanwaste/index_en.html. [Accessed: 05-Apr-2012].

[9]   European Commission, "Implementation of nitrates Directive 91/676/EEC," *Environment*, 1991. .

[10]   European Commission, "Drinking water directive 98/83/EC," *Drinking water legislation*, 1998. [Online]. Available: http://ec.europa.eu/environment/water/water-drink/legislation_en.html. [Accessed: 05-Apr-2012].

[11]   European Commission, "The EU Water Framework Directive," 2000. [Online]. Available: http://ec.europa.eu/environment/water/water-framework/index_en.html. [Accessed: 05-Apr-2012].

[12]   N. F. Gray, *Water technology: an introduction for environmental scientists and engineers*, Second edi. Dublin: Elsevier Butterworth-Heinemann, 2005, p. 127.

Ahmed Abdallah Abdou

[13]   European Commission, "Environmental liability," *Liability*, 2004. [Online]. Available: http://ec.europa.eu/environment/legal/liability/. [Accessed: 05-Apr-2012].

[14]   European Commission, "Bathing water directive 2006/7/EC," *Bathing water quality*, 2006. [Online]. Available: http://ec.europa.eu/environment/water/water-bathing/. [Accessed: 05-Apr-2012].

[15]   European Union, "DIRECTIVE 2008/56/EC OF THE EUROPEAN PARLIAMENT AND OF THE COUNCIL," *Official Journal of the European Union*, no. L 164 2008 EC, pp. 19–40, 2008.

[16]   HMSO, *The Water Resources Act 1991 (Amendment) (England and Wales) Regulations 2009 No. 3104*, vol. 1991, no. 3104. WATER RESOURCES , ENGLAND AND WALES, 2009.

[17]   HMSO, "Water Industry Act 1991," *Legislation*, 1991. [Online]. Available: http://www.legislation.gov.uk/ukpga/1991/56/contents. [Accessed: 05-Apr-2012].

[18]   Department for Environment Food and Rural Affairs, "The Environmental Damage (Prevention and Remediation) Regulations 2009," London, 2009.

[19]   HMSO, "Marine and Coastal Access Act 2009," *Legislation*, 2009. [Online]. Available: http://www.legislation.gov.uk/ukpga/2009/23/contents. [Accessed: 05-Apr-2012].

[20]   Environment Agency, "Managing and improving the water environment," 2011. .

[21]   Department for Environment Food and Rural Affairs, "The Natural Choice: securing the value of nature," London, 2011.

[22]   Department for Environment Food and Rural Affairs, "Water for Life," London, 2011.

[23]   Department for Environment Food and Rural Affairs, "Tackling water pollution from the urban environment Consultation on a strategy to address diffuse water pollution from the built environment," London, 2012.

[24]   Department for Environment Food and Rural Affairs, "Summary of responses to the consultation on ' Tackling water pollution from the urban environment '," London, 2013.

[25]   Government, "Improving water quality," *Policy*, 2014. [Online]. Available: https://www.gov.uk/government/policies/improving-water-quality.

Ahmed Abdallah Abdou

[26]   European Union, "Council Directive 98/83/EC of the 3rd November 1998 on the quality of water intended for human consumption," *Official Journal of the European Communities*, vol. L330/32, no. 5.12.98, 1998.

[27]   Environment Agency, "The Microbiology of Drinking Water (2002) - Part 1 - Water Quality and Public Health," 2002.

[28]   Environment Agency, "The Microbiology of Drinking Water (2010) - Part 2 – Practices and procedures for sampling Methods for the Examination of Waters and Associated Materials," 2010.

[29]   Wattera, "Water quality equipment," *Innovations in Water Monitoring*, 2013. [Online]. Available: http://www.waterra-in-situ.com/pages/category/water_quality.asp?gclid=CP6R1NGMursCFQHHtAodnW0Aaw . [Accessed: 18-Dec-2013].

[30]   EMS, "Environmental Monitoring Solutions," *Water quality*, 2013. [Online]. Available: http://www.em-solutions.co.uk/products/water_monitoring. [Accessed: 18-Dec-2013].

[31]   Cole-Parmer Instrument Company Limited, "Global Water Dissolved Oxygen," *Global Water DO Sensor*, 2013. [Online]. Available: http://www.coleparmer.co.uk/Product/Global_Water_Dissolved_Oxygen_Sensor/UY-99243-38?referred_id=3482&gclid=CJuos6ucursCFdLItAodyXEAKQ. [Accessed: 18-Dec-2013].

[32]   YSI/Xylem, "YSI Integrated Systems & Services," *Water Quality Monitoring System*, 2013. [Online]. Available: http://www.ysisystems.com/floating-platform-selector.php. [Accessed: 18-Dec-2013].

[33]   YSI, "Real-time Water Quality Data from Dubai Creek," *YSI Environmental*, 2013. [Online]. Available: http://www.ysi.com/media/pdfs/A526-Dubai-Municipality-Utilizes-Real-time-Water-Quality-Monitoring-Instruments.pdf. [Accessed: 18-Dec-2013].

[34]   YSI, "Water Quality Is Key To The Success Of Cardiff Bay," *Water Today*, pp. 12–15, 2011.

[35]   N. Mohamed, I. Jawhar, J. Al-Jaroodi, and L. Zhang, "Monitoring Underwater PIpelines Using Sensor Networks," *2010 IEEE 12th International Conference on High Performance Computing and Communications*, pp. 346–353, Sep. 2010.

Ahmed Abdallah Abdou

[36]   S.Sato, H.Yamamoto, and Y. Okuyama, "Pipeline built-in electric power generating set," 4740711, 1988.

[37]   N. Mohamed, I. Jawhar, J. Al-Jaroodi, and L. Zhang, "Sensor network architectures for monitoring underwater pipelines.," *Sensors (Basel, Switzerland)*, vol. 11, no. 11, pp. 10738–64, Jan. 2011.

[38]   I. F. Akyildiz, D. Pompili, and T. Melodia, "Underwater acoustic sensor networks: research challenges," *Ad Hoc Networks (Elsevier)*, vol. 3, no. 3, pp. 257–279, May 2005.

[39]   Teledyne RESON, "Hydrophones," 2012. [Online]. Available: www.teledyne-reson.com/products/hydrophones/. [Accessed: 05-Feb-2012].

[40]   University of Rhode Island, "Acoustic monitoring," *Discovery of Sound in the Sea*, 2012. [Online]. Available: http://www.dosits.org/animals/effectsofsound/howdoyoumeasureamarinemammalsreactiontosound/acousticmonitoring/. [Accessed: 05-Feb-2012].

[41]   W. Au, *The Sonar of Dolphins*. New York: Springer-Verlag, 1993.

[42]   M. Stojanovic, "On the relationship between capacity and distance in an underwater acoustic communication channel," *ACM SIGMOBILE Mobile Computing and Communications Review*, vol. 11, no. 4, p. 34, Oct. 2007.

[43]   L. Berkhovskikh and Y. Lysanov, *Fundamentals of Ocean Acoustics*. New York: Springer, 1982.

[44]   R. Coates, *Underwater Acoustic Systems*. New York: Wiley, 1989.

[45]   J. Krautkramer and H. Krautkramer, *Ultrasonic testing of materials*. Heidelberg, Germany: Springer, 1990.

[46]   I. Vasilescu, K. Kotay, D. Rus, M. Dundabin, and P. Corke, "Data collection, storage, and retrieval with an underwater sensor network," *Proceedings of the 3rd international conference on Embedded networked sensor systems - SenSys'05*. ACM Press, New York, New York, USA, p. 154, 2005.

[47]   Y. Tsuchida, N. Hama, and M. Takahata, "An optical telemetry system for underwater recording of electromyogram and neuronal activity from non-tethered crayfish.," *Journal of neuroscience methods*, vol. 137, no. 1, pp. 103–9, Aug. 2004.

Ahmed Abdallah Abdou

[48]   J. Smart., "Underwater optical communications systems part 1: variability of water optical parameters," in *IEEE Military Communications Conference. MILCOM*, 2005, pp. 1140–1146.

[49]   J. A. Simpson, "A 1 Mbps Underwater Communications System using LEDs and Photodiodes with Signal Processing Capability," North Carolina State University, Raleigh, NC, 2007.

[50]   M. Doniec, I. Vasilescu, M. Chitre, C. Detweiler, M. Hoffmann-kuhnt, and D. Rus, "AquaOptical : A Lightweight Device for High-rate Long-range Underwater Point-to-Point Communication," in *OCEANS 2009, MTS/IEEE Biloxi - Marine Technology for Our Future: Global and Local Challenges*, 2009, pp. 1–6.

[51]   W. Cox, "A 1 Mbps Underwater Communication System Using a 405 nm Laser Diode and Photomultiplier Tube," North Carolina State University, Raleigh, NC, NC, 2007.

[52]   SAPHOTONICS, "No Title," *Technologies*, 2012. [Online]. Available: http://www.saphotonics.com/high-bandwidth-optical-communications/underwater/. [Accessed: 04-Dec-2012].

[53]   F. Hanson and S. Radic, "High bandwidth underwater optical communication," *Applied Optics*, vol. 47, no. 2, pp. 277–283, 2008.

[54]   L. J. Johnson, R. J. Green, and M. S. Leeson, "Underwater optical wireless communications : depth dependent variations in attenuation," *Applied Optics*, vol. 52, no. 33, pp. 7867–7873, 2013.

[55]   M. A. A. Ali, "Analyzing of Short Range Underwater Optical Wireless Communications Link," *INTERNATIONAL JOURNAL OF ELECTRONICS & COMMUNICATION TECHNOLOGY*, vol. 4, no. 3, pp. 125–132, 2013.

[56]   B. E. A. Saleh and M. C. Teich, *Fundamentals of Photonics*, Second. Wiley Interscience, 2007.

[57]   J. R. Apel, *Principles of Ocean Physics*. Academic Press, 1987.

[58]   M. Lanzagorta, *Underwater Communications*, VirginiaTe. Virginia: Morgan & Claypool Publishers, 2013, pp. 32–42.

[59]   J. A. Willoughby and P. D. Lowell, "Development of loop aerial for submarine radio communication," *American Physics Society*, vol. 14, no. 2, p. 193, 1919.

Ahmed Abdallah Abdou

[60] A. Shaw, A. I. Al-Shammaa, S. R. Wylie, and D. Toal, "Experimental Investigations of Electromagnetic Wave Propagation in Seawater," in *2006 European Microwave Conference*, 2006, no. September, pp. 572–575.

[61] J. H. Goh, A. Shaw, and A. I. Al-Shammaa, "Underwater wireless communication system," *Journal of Physics: Conference Series*, vol. 178, p. 012029, Jul. 2009.

[62] A. A. Abdou, A. Shaw, J. Cullen, S. Wylie, A. Mason, and A. Al-Shamma, "A Review of Underwater EM Wave Propagation to Investigate the Development of a Through Water WSN," in *6th Built Environment And Natural Environment*, 2011, pp. 1–6.

[63] A. A. Abdou, A. Shaw, A. Mason, A. Al-Shamma, J. Cullen, and S. Wylie, "Electromagnetic (EM) Wave Propagation for the Development of an Underwater Wireless Sensor Network (WSN)," in *Sensors, 2011 IEEE*, 2011, no. 1, pp. 1571 – 1574.

[64] WFS Technologies Ltd, "Subsea Wireless Solutions," *Subsea Wireless Technologies*, 2013. [Online]. Available: http://www.wfs-tech.com. [Accessed: 05-Dec-2011].

[65] W. Merrill, K. Sohrabi, L. Girod, J. Elson, F. Newberg, and W. Kaiser, "Open Standard Development Platforms for Distributed Sensor Networks," in *Unattended Ground Sensor Technologies and Applications IV*, 2002, pp. pp.327–337.

[66] A. Mason, A. Shaw, and A. I. Al-Shammaa, "Inventory Management in the packaged Gas Industry Using Wireless Sensor Networks," in *Advances in Wireless Sensors and Sensor Networks*, S. C. Mukhopadhyay and H. Leung, Eds. Springer, 2010, pp. 75–100.

[67] L. E. Cordova-Lopez, A. Mason, J. D. Cullen, A. Shaw, and A. I. Al-Shammaa, "Online vehicle and atmospheric pollution monitoring using GIS and wireless sensor networks," *Journal of Physics: Conference Series*, vol. 76, p. 012019, Jul. 2007.

[68] E. Stuntebeck, D. Pompili, and T. Melodia, "Wireless underground sensor networks using commodity terrestrial motes," *2006 2nd IEEE Workshop on Wireless Mesh Networks*, pp. 112–114, 2006.

[69] S. Pandya, J. Engel, J. Chen, Z. Fan, and C. Liu, "CORAL: Miniature Acoustic Communication Subsystem Architecture for Underwater Wireless Sensor Networks," in *The 4th IEEE International Conference on Sensors*, 2005.

[70] T.-H. Won and S.-J. Park, "Design and implementation of an omni-directional underwater acoustic micro-modem based on a low-power micro-controller unit.," *Sensors (Basel, Switzerland)*, vol. 12, no. 2, pp. 2309–23, Jan. 2012.

Ahmed Abdallah Abdou

[71]   M. Dunbabin, P. Corke, I. Vasilescu, and D. Rus, "Data muling over underwater wireless sensor networks using an autonomous underwater vehicle," in *Proceedings of the 2006 IEEE International Conference on Robotics and Automation*, 2006, no. May, pp. 2091–2098.

[72]   D. Anguita, D. Brizzolara, and G. Parodi, "Building an Underwater Wireless Sensor Network Based on Optical: Communication: Research Challenges and Current Results," *2009 Third International Conference on Sensor Technologies and Applications*, pp. 476–479, Jun. 2009.

[73]   R. M. Hagem, D. V. Thiel, S. G. O'Keefe, and T. Fickenscher, "THE EFFECT OF AIR BUBBLES ON AN UNDERWATER OPTICAL COMMUNICATIONS SYSTEM FOR WIRELESS SENSOR NETWORK," *Microwave and Optical Technology Letters*, vol. 54, no. 3, pp. 729–732, 2012.

[74]   J. Lloret, "Underwater sensor nodes and networks.," *Sensors (Basel, Switzerland)*, vol. 13, no. 9, pp. 11782–96, Jan. 2013.

[75]   A. Elrashidi, A. Elleithy, M. Albogame, and K. Elleithy, "Underwater Wireless Sensor Network Communication Using Electromagnetic Waves at Resonance Frequency 2 . 4 GHz," in *CNS '12 Proceedings of the 15th Communications and Networking Simulation Symposium*, 2012.

[76]   J. Lloret, S. Sendra, M. Ardid, and J. J. P. C. Rodrigues, "Underwater wireless sensor communications in the 2.4 GHz ISM frequency band.," *Sensors (Basel, Switzerland)*, vol. 12, no. 4, pp. 4237–64, Jan. 2012.

[77]   H. Karl and A. Willing, *Protocols and Architectures for Wireless Sensor Networks*. John Wiley & Sons, Ltd, 2005, p. 18.

[78]   D. K. Cheng, *Field and Wave Electromagnetics*, Second. Addisson Wesley Publishing Company, 1989, p. 367.

[79]   S. J. Orfanidis, "Electromagnetic Waves and Antennas," 2008. [Online]. Available: http://www.ece.rutgers.edu/~orfanidi/ewa/. [Accessed: 09-Dec-2013].

[80]   Ofcom, "Spectrum," *The Communications Market 2005-Overview*, 2005. [Online]. Available: http://stakeholders.ofcom.org.uk/market-data-research/market-data/communications-market-reports/cm05/overview05/spectrum/. [Accessed: 06-Dec-2013].

Ahmed Abdallah Abdou

[81]   ITU, "Frequency allocations map," *Article 5 Frequency Allocation*, 2009. [Online]. Available: http://life.itu.int/radioclub/image/regmap.gif. [Accessed: 06-Dec-2013].

[82]   M. N. O. Sadiku, *Elements of Electromagnetics*, Third. Oxford University Press, 2001, pp. 417–422.

[83]   R. W. P. King and G. S. Smith, *Antennas in Matter*. Cambridge, MA: MIT Press, 1981.

[84]   D. Lide, *CRC Handbook of Chemistry and Physics*, 2010th ed. CRC Press/ Taylor and Francis, 2010.

[85]   P. Debye, *Polar Molecules*. New York: Chemical Catalog Company, 1929.

[86]   B. D. Thomas, T. G. Thomson, and C. L. Utterback, "The electrical conductivity of sea water," *Const. Int. Explor. Mer*, vol. 9, no. 1934, pp. 28–35, 1934.

[87]   R. A. Cox, "The physical properties of seawater," in *Chemical Oceanography*, vol. 1, J. P. Riley and G. Skirrow, Eds. New York: Academic Press, 1965.

[88]   L. A. Klein and C. . Swift, "An improved model for the dielectric constant of seawater at microwave frequencies," *IEEE J. Oceanic Eng.*, pp. 104–111, 1977.

[89]   C. Guillou, W. Elisson, L. Eymard, K. Lamkaouchi, C. Pringent, G. Delbos, G. Balana, and S. A. Boubakara, "Impact of new permittivity measurements on sea surface emissivity modelling microwaves," *Radio Science*, vol. 33, no. 3, pp. 649–667, 1998.

[90]   J. R. Wang, "A comparison of the MIR-E stimated and Model-Calculated fresh water surface emissivities at 89, 150 and 220 GHz," in *IEEE Transactions on Geoscience and Remote Sensing*, 2002, pp. 1356–1365.

[91]   T. Meissner and F. J. Wentz, "The complex dielectric constant of pure and sea water from microwave satellite observations," *IEEE Transactions on Geoscience and Remote Sensing*, vol. 42, no. 9, pp. 1836–1849, Sep. 2004.

[92]   A. P. Stogryn, H. T. Bull, K. Rubayi, and S. Iravanchy, "THE MICROWAVE DIELECTRIC PROPERTIES OF SEA AND FRESH WATER," Azusa, 1995.

[93]   Würth Elektronik eiSos GmbH & Co KG, "Chip-Antenna WE-MCA part no 7488910245," *Specification for release*, 2004. [Online]. Available: http://katalog.we-online.de/pbs/datasheet/7488910245.pdf. [Accessed: 25-Mar-2011].

Ahmed Abdallah Abdou

[94]   A. A. Abdou, A. Shaw, A. Mason, A. Al-Shamma, S. Wylie, and J. Cullen, "Wireless Sensor Network for Underwater Communication," in *Wireless Sensor Systems*, 2012, pp. 3–8.

[95]   Texas Instruments, "Wireless Sensor Monitor Using the eZ430-RF2500 (SLAA378D)," Dallas, 2011.

[96]   Texas Instruments, "Project collateral and source code (SLAC139)," 2007. [Online]. Available: http://www.ti.com/lit/zip/slac139. [Accessed: 10-Nov-2011].

[97]   Texas Instruments, "CC2500 datasheet (SWRS040C)," Dallas, 2007.

[98]   Futurlec, "Radio modules," *Boards*, 2012. [Online]. Available: http://www.futurlec.com/Radio-433MHZ.shtml. [Accessed: 02-Oct-2013].

[99]   J. D. Krauss and R. J. Marhefka, *Antennas for all applications*. New York: McGraw-Hill, 2002, p. 7.

[100] C. A. Balanis, *Antenna Theory: Analysis and Design*. New Jersey: John Wiley & Sons, Ltd, 2005.

[101] A. Sligar, "Antenna Modeling Considerations," *Ansys*, pp. 1–12, 2007.

[102] X. Begaud, *Ultra Wide Band Antennas*. London: ISTE, 2011.

[103] I. Oppermann, M. Hamalainen, and J. Linatti, *UWB: Theory and Applications*. Chichester: John Wiley & Sons, Ltd, 2004, pp. 134–135.

[104] K. H. Sayidmarie and Y. A. Fadhel, "A Planar Self-Complementary Bow-Tie Antenna For UWB Applications," *Progress In Electromagnetics Research C*, vol. 35, no. October 2012, pp. 253–267, 2013.

[105] Y. Nishioka and O. Maeshima, "FDTD Analysis of Resistor-Loaded Bow-Tie Antennas Covered with Ferrite-Coated Conducting Cavity for Subsurface Radar," vol. 47, no. 6, pp. 970–977, 1999.

[106] A. A. Lestari, A. G. Yarovoy, and L. P. Ligthart, "Adaptive Wire Bow-Tie Antenna for GPR Applications," *IEEE Transactions on Antennas and Propagation*, vol. 53, no. 5, pp. 1745–1754, 2005.

Ahmed Abdallah Abdou

[107] Y. Lin and S. Tsai, "Analysis And Design Of Broadside-coupled Striplines-fed Bow-tie Antennas," *IEEE Transactions on Antennas and Propagation*, vol. 46, no. 3, pp. 459–460, 1998.

[108] A. Sligar, "Ansoft HFSS Antenna Design Kit Overview of HFSS Antenna Design," *Ansys*, pp. 1–16, 2007.

[109] C. Balanis, "Wideband and Travelling-Wave Antennas," in *Modern Antenna Handbook*, New York: Wiley, 2008.

[110] A. A. Abdou, A. Shaw, A. Mason, A. Al-Shamma'a, J. Cullen, S. Wylie, and M. Diallo, "A matched Bow-tie antenna at 433MHz for use in underwater wireless sensor networks," *Journal of Physics: Conference Series*, vol. 450, p. 012048, Jun. 2013.

[111] K. P. Hunt, C. M. S. Hydraulics, J. J. Niemeier, A. Kruger, C. M. Stanley, H. C. Maxwell, and S. Hydraulics, "Short Paper : Antennas for Mussel-Based Underwater Biological Sensor Networks in Rivers," in *The fifth ACM International Workshop on Underwater Networks WUWNet '10*, 2010.

[112] Minicircuits, "Voltage Control Oscillator ZX95-535-S+," *Oscillators*, 2012. [Online]. Available: http://217.34.103.131/pdfs/ZX95-535.pdf. [Accessed: 13-Sep-2012].

[113] STMicroelectronics, "L7812CV Voltage Regulator," *L7800 SERIES Positive Voltage Regulators*, 2004. [Online]. Available: http://www.taydaelectronics.com/datasheets/A-207.pdf. [Accessed: 03-Sep-2012].

[114] Energizer, "AA Energizer E91," *Energizer Technical Information*, 2012. [Online]. Available: http://data.energizer.com/PDFs/E91.pdf. [Accessed: 13-Sep-2012].

[115] Farnell, "Square Trimpot Trimming Potentiometer 3296W-1-103LF," *Trimmer Potentiometers*, 2010. [Online]. Available: http://www.farnell.com/datasheets/684085.pdf. [Accessed: 13-Sep-2012].

[116] Microsoft corporation, "Bing maps," 2013. [Online]. Available: http://www.bing.com/maps/#Y3A9NTMuMzAyOTM0fi0yLjc5NTY4NSZsdmw9OSZzdHk9ciZlbz0w. [Accessed: 17-Feb-2013].

Ahmed Abdallah Abdou